

AERIAL ROPEWAYS

THE DESIGN AND APPLICATION
OF
AERIAL ROPEWAYS

By
WALTER G. BOOTH, B. ENG.

A Thesis
Submitted to the Faculty of Graduate Studies
in Partial Fulfilment of the Requirements
for the Degree
Master of Engineering

McMaster University

October 1965

MASTER OF ENGINEERING (1965)
(Mechanical)

McMASTER UNIVERSITY
Hamilton, Ontario

TITLE: The Design and Application of Aerial Ropeways

AUTHOR: Walter G. Booth, B. Eng. (McMaster University)

SUPERVISOR: Professor J. N. Siddall

NUMBER OF PAGES: xiv, 248

SCOPE AND CONTENTS: The history of aerial ropeways and cableways is reviewed. Aerial transport systems are classified according to their design differences. The construction and application of monocable and bicable ropeways are discussed. Cableways are separated into two systems -- the tautline and slackline cableway. Their design and use are reviewed.

The types of chair lift intermediate support tower are examined. Structural models of four types were built, strain gaged and tested. Experimental stresses are compared to theoretical prediction for each model subjected to external loads.

The engineering problems involved in locating the intermediate towers of a chair lift are discussed.

ACKNOWLEDGMENTS

The author sincerely appreciates the guidance and many helpful suggestions given by Professor J. N. Siddall of McMaster Univeristy.

The author also wishes to acknowledge the kind assistance of Mr. F. L. Edwards, Sales Engineer, and Mr. G. Geiling, Design Draftsman of The Timberland Ellicott Limited, Woodstock, Ontario.

TABLE OF CONTENTS

Chapter		Page
	List of Illustrations	ix
	List of Tables	xiii
1	Introduction	1
2	Historical	7
2.1	Aerial Ropeway History	7
2.2	Cableway History	11
3	Classification of Aerial Ropeways	14
3.1	Monocable Systems	14
3.1.1	Fixed Clip Monocable System	14
3.1.2	Detachable Clip Monocable System	18
3.2	Bicable Systems	19
3.2.1	Continuous Bicable System	19
3.2.2	Reversible (Jigback or To and Fro) Bicable System	22
4	Classification of Cableways	25
4.1	Tautline Cableways	25
4.1.1	Fixed Tautline Cableway	26
4.1.2	Radial Tautline Cableway	26
4.1.3	Movable Tautline Cableway	27
4.2	Slackline Cableways	27

Chapter		Page
5	Structural Design of a Chair Lift Intermediate Support Tower	30
5.1	External Loads Imposed on a Chair Lift Intermediate Support Tower	32
5.1.1	Calculation of the Maximum Chordload "R"	33
5.1.2	Calculation of the Loading due to Wind	35
5.2	Design of the Chair Lift Intermediate Support Tower Models	37
5.3	Design of the Chair Lift Lattice Tower Model	39
5.3.1	Determinate Lattice Tower Model	40
5.3.1.1	Mathematical Model of the Determinate Tower	41
5.3.1.2	Calculation of the Maximum Stress in the Determinate Tower Members	42
5.3.1.3	Experimental Strain Measurements in the Determinate Tower Members	45
5.3.1.4	Evaluation of the Theoretical and Experimental Stresses in the Determi- nate Tower Members	46
5.3.2	Indeterminate Lattice Tower Model	53
5.3.2.1	Mathematical Model of the Indeterminate Tower	54
5.3.2.2	Calculation of the Maximum Stress in the Indeterminate Tower Members.	54
5.3.2.3	Experimental Strain Measurements in the Indeterminate Tower Members	56
5.3.2.4	Evaluation of the Theoretical and Experimental Stresses in the Indeterminate Tower Model.	58
5.3.3	Comparison of the Determinate and Indeterminate Lattice Tower Models	64
5.4	Design of a Chair Lift Pipe Tower Model	65
5.4.1	Calculation of the Theoretical Stresses in the Pipe Tower Model	66
5.4.2	Experimental Strain Measurements in the Pipe Tower Model	66
5.4.3	Evaluation of the Theoretical and Experimental Stresses in the Pipe Tower Model	67

Chapter		Page
5.5	Design of a Chair Lift Hexagonal Tower Model	71
5.5.1	Calculation of the Theoretical Stresses in the Hexagonal Tower Model	72
5.5.2	Experimental Strain Measurements in the Hexagonal Tower Model	72
5.5.3	Evaluation of the Theoretical and Experimental Stresses in the Hexagonal Tower Model	73
6	Engineering of a Chair Lift Installation	78
6.1	Location of the Chair Lift Intermediate Towers	80
6.2	Sag and Tension Calculations for a Chair Lift Rope	81
7	Conclusion	84
Appendix A	Digital Computer Program for the Analysis of a Determinate, Pin-Jointed, Planar Truss	85
A.1	Description of the Program	86
A.2	Method of Solution	87
A.3	Program Error Messages	90
A.4	Definition of Variables and Fortran Names	91
A.5	Data Input Instructions	93
A.6	Sample Problem	95
A.7	Computer Analysis of a Determinate Lattice Chair Lift Tower Model	103
Appendix B	Digital Computer Program for the Analysis of an Indeterminate, Pin-Jointed, Planar Truss	116
B.1	Description of the Program	117
B.2	Method of Solution	121

Chapter		Page
B.3	Subroutine DTRUSS	125
B.4	Choice of Redundants	125
B.5	Definition of Variables and Fortran Names	126
B.6	Data Input Instructions	129
B.7	Sample Problem	132
B.8	Computer Analysis of an Indeterminate Lattice Chair Lift Tower Model	145
Appendix C	Calculation of the Theoretical Stresses in the Pipe Tower Model	158
C.1	External Loads on the Pipe Tower	159
C.2	Calculation of the Stress at Point A	160
C.2.1	Compressive Bending Stress at Point A	160
C.2.2	Compressive Direct Stress at Point A	160
C.2.3	Total Stress at Point A	161
C.3	Calculation of the Stress at Point B	161
C.3.1	Tensile Bending Stress at Point B	161
C.3.2	Compressive Direct Stress at Point B	162
C.3.3	Total Stress at Point B	162
C.4	Calculation of the Stress at Point C	162
C.4.1	Compressive Bending Stress at Point C	162
C.4.2	Compressive Direct Stress at Point C	163
C.4.3	Bending Shear Stress at Point C	163
C.4.4	The Principal Stresses at Point C	164
Appendix D	Calculation of the Theoretical Stresses in the Hexagonal Tower Model	166
D.1	External Loads on the Hexagonal Tower Model	167
D.2	Calculation of the Stress at Point A	168
D.2.1	Compressive Bending Stress at Point A	168
D.2.2	Compressive Direct Stress at Point A	169
D.2.3	Total Stress at Point A	169
D.3	Calculation of the Stress at Point B	169
D.3.1	Tensile Bending Stress at Point B	170
D.3.2	Compressive Direct Stress at Point B	170
D.3.3	Total Stress at Point B	170
D.4	Calculation of the Stress at Point C	170
D.4.1	Compressive Bending Stress at Point C	171
D.4.2	Compressive Direct Stress at Point C	171

Chapter		Page
D.4.3	Bending Shear Stress at Point C	172
D.4.4	The Principal Stresses at Point C	172
Appendix E	Sag and Tension Tables for a Chair Lift Rope	174
E.1	Notation	175
E.2	Theory	177
E.3	Digital Computer Program for the Solution of the Sag and Tension Equations	183
E.3.1	Description of the Program	183
E.3.2	Definition of Variables and Fortran Names	184
E.3.3	Data Input Instructions	186
E.3.4	Sample Problem	187
	Illustrations	191
	Bibliography Outline	227
	Bibliography	228

LIST OF ILLUSTRATIONS

Figure		Page
1	Monocable Ropeway, Drive Terminal Counterweighted	191
2	Monocable Ropeway, Drive Terminal Anchored	191
3	Monocable Ropeway, Idler Terminal Anchored	191
4	Monocable Ropeway, Idler Terminal Counterweighted	191
5	Monocable Ropeway with Fixed Drive and Movable Idler Terminals	192
6	Monocable Ropeway with Movable Drive and Fixed Idler Terminals	192
7	Platter Lift	193
8	T-Bar Lift	193
9	T-Bar Lift Showing Intermediate Tower and T-Bars	193
10	Ski Area Chair Lift, Open Chair	194
11	Sight-seeing Chair Lift, Enclosed Chair	194
12	Sight-seeing Chair Lift, Open Fiberglass Chair	194
13	Detachable Clip Small Cabin Monocable Ropeway, (Gondola Lift)	195
14	Reversible Bicable Passenger Ropeway, Large Cabin with Twin Track Ropes	195
15	Continuous Bicable Passenger Ropeway, Medium Cabin with Single Track Rope	195

Figure		Page
16	Bicable Ropeway for Material Transport	196
17	Bicable Ropeway Carriage and Carrier for Material Transport	196
18	Typical Aerial Ropeway Profile	196
19	Continuous Bicable Ropeway, Drive and Tensioning Layout	197
20	Single Reversible Bicable Ropeway, Drive and Tensioning Layout	198
21	Double Reversible Bicable Ropeway, Drive and Tensioning Layout	199
22	Two Parallel Tautline Cableways with Fixed Needle Type Towers	200
23	Typical Tautline Cableway Showing Area of Operation for Fixed Towers with Lateral Swing	200
24	Tautline Cableway with Fixed Towers	201
25	Tautline Cableway with Movable Towers	201
26	Tautline Cableway Fixed Tower Detail	202
27	Tautline Cableway Radial Tower Detail	202
28	Rope Reeving Diagram for a Tautline Cableway	203
29	Slackline Cableway Excavator	203
30	Chair Lift, Pipe Tower	204
31	Material Handling Ropeway, Tapered Square Tower	204
32	Chair Lift, Hexagonal Tower	205
33	Material Handling Ropeway, Light Reinforced Concrete Tower	205

Figure		Page
34	Material Handling Ropeway, Heavy Reinforced Concrete Tower	205
35	Chair Lift, Lattice Tower	206
36	Gondola Lift, Lattice Tower	206
37	Material Handling Bicable Ropeway, Lattice Tower	206
38	Construction Details, Lattice Tower	207
39	Large Passenger Bicable Ropeway, Lattice Tower	207
40	A Series of Chair Lift Hold-up Pipe Towers	208
41	Intermediate Tower Idler Assembly	208
42	A Chair Lift Hold-down Lattice Tower	208
43	Lattice Tower Showing Chordload and Windloads	209
44	Four Sheave Idler Assembly Showing Maximum Breakover Angle	209
45	Determinate Lattice Tower Model Showing Chordload (R) and Windloads (W) Applied	210
46	Square Lattice Type Tower with Straight Legs	211
47	Determinate Lattice Tower Model, Chordload Planes ABEF and CDGH Prepared for Computer Analysis	212
48	Determinate Lattice Tower Model, Windload Planes ACEG and BDFH Prepared for Computer Analysis	213
49	Determinate Lattice Tower Model Showing Test Apparatus	214
50	Indeterminate Lattice Tower Model, Showing Chordload (R) and Windloads (W) Applied	215

Figure		Page
51	Indeterminate Lattice Tower Model, Chordload Planes ABEF and CDGH Prepared for Computer Analysis	216
52	Indeterminate Lattice Tower Model, Windload Planes ACEG and BDFH Prepared for Computer Analysis	217
53	Indeterminate Lattice Tower Model Showing Test Apparatus	218
54	Pipe Tower Model Showing Chordload (R) and Windloads (W) Applied	219
55	Pipe Tower Model Showing Test Apparatus	220
56	Hexagonal Tower Model Showing Chordload (R) and Windloads (W) Applied	221
57	Hexagonal Tower Model Showing Test Apparatus	222
58	Sample Problem, Determinate Truss Analysis	223
59	Sample Problem, Indeterminate Truss Analysis	224
60	Chair Lift Profile Showing the Inter- mediate Tower Locations	225
61	Hanging Rope Carrying a Horizontally Distributed Load	226

LIST OF TABLES

Table	Content	Page
1	Determinate Chair Lift Lattice Tower Model, Member Forces	50
2	Determinate Chair Lift Lattice Tower Model, Corner Angle Forces	51
3	Experimental Strain Measurements, Determinate Lattice Tower Model	52
4	Comparison of Theoretical and Experimental Member Stresses for the Design Condition (Maximum Chordloads and Windloads), Determinate Lattice Tower Model	52
5	Indeterminate Chair Lift Lattice Tower Model, Member Forces	60
6	Indeterminate Chair Lift Lattice Tower Model, Corner Angle Forces	62
7	Experimental Strain Measurements, Indeterminate Lattice Tower Model	63
8	Comparison of Theoretical and Experimental Member Stresses for the Design Condition (Maximum Chordload and Windloads), Indeterminate Lattice Tower Model	63
9	Theoretical Stresses in the Pipe Tower Model	69
10	Experimental Strain Measurements in the Pipe Tower Model	69
11	Comparison of Theoretical and Experimental Stresses in the Pipe Tower Model for the Design Loading	70

Table	Content	Page
12	Theoretical Stresses in the Hexagonal Tower Model	76
13	Experimental Strain Measurements in the Hexagonal Tower Model	76
14	Comparison of Theoretical and Experimental Stresses in the Hexagonal Tower Model for the Design Loading	77
15	Computer Output, Sag and Tension Chart	190

1. INTRODUCTION

Aerial ropeways are perhaps one of the more obscure forms of land transportation in this country. They have always been the popular mode of passenger movement in the ski areas, and in our affluent society their use is increasing as a sight-seeing device.

The terminology used in describing systems of transportation by means of wire rope is loose and indefinite. It is advisable at this stage to set down some basic definitions to be used as guideposts. Although this mode of transportation has a long history, even the general classification of wire rope aerial transportation is confusing to the uninitiated.

Three terms are interchangeably used to describe these systems: Aerial Tramways, Aerial Ropeways and Cableways. The United States authors use the first and last terms and only sometimes discriminate between the two. However, the European and English practice is to use the term "Aerial Ropeway" since the word "Tramway" connotes streetcar or railway surface-haulage installations. The term "Cableway" is reserved for that particular type of wire rope installation where a load car or carriage may be traversed back and forth over a single suspension span.

and so arranged that the load may be raised or lowered at any point in the traverse. This is alternately known as a "Cable Crane"

The words "Aerial Ropeway" and "Cableway" will be used as defined by the European practice throughout this work, as these words seem more consistent with the description of systems that use wire rope as their basic ingredient.

Another point of confusion is the alternate use of the words "wire rope" and "cable". Even in the Wire Rope Manufacturing Industry little attempt is made to differentiate or be consistent. Hereafter, the term "wire rope" will be used to describe the ropes used in Ropeways. The word "rope" in this text implies wire rope. "Cable" is more appropriately used in describing stranded electrical conductors, but the word has been used as part of the name of some ropeway systems.

A brief description of the types of ropeways at this point will be helpful in understanding the historical development of this industry. Classification in greater detail is covered in section 3.

An aerial ropeway is a machine used to transport people or materials in carriers suspended from wire rope, and is composed of one or more spans extending from a loading point to a discharge point usually some distance

away. There are two distinct aerial ropeway systems:

- (1) Monocable System
- (2) Bicable System
 - (a) Continuous
 - (b) Reversible

Monocable ropeways use a single moving flexible wire rope, spliced endless, which both supports and hauls the carriers.

The bicable ropeway uses a stationary high-tensioned track rope to support the carriers which are hauled by a separate moving traction rope. The continuous system is constructed such that the carriers move in a continuous circuit from the loading terminal to the discharge terminal, the empty carrier returning to the loading point on the light side of the line.

The reversible system (sometimes called a "to and fro" or "jig back" system) has only two carriers, one on each side of the system. When one carrier is at the loading point, the other is at the discharge station.

The aerial ropeway is best utilized where material or people are to be transported for long distances over rough country. Some inherent advantages of ropeways are:

1. The shortest route can be taken between terminals. Ropeways are in general independent of the ground contour. They cross over highways, railways, rivers,

mountains and valleys. Their construction does not require bridges or tunnels.

2. The cost of operation is usually low compared with other systems of transportation moving between the same end points.

3. Wide varieties of materials can be handled, such as ores, sand, gravel, logs, sawed lumber, bananas, explosives and glassware. Passenger transport over rugged terrain is another important use of ropeways.

4. Materials can be transported between given points without rehandling. Loading and unloading can be completely automated.

5. Ropeways are quite flexible. The positive hauling system for the movement of the carriers enables gradients to be safely and dependably overcome which would not be practical with other means of transportation.

6. They are not as subject to interruptions in service due to extremes of weather as other transport systems.

7. Loads can be automatically discharged at any desired point in the line.

8. It is usually simpler to acquire rights-of-way for ropeways than for other systems. The wire ropes can be placed at heights necessary to clear highways, railways, buildings and cultivated land.

There are two distinct types of cableway systems:

- (1) Tautline System
- (2) Slackline System

The tautline cableway uses a single, or occasionally multiple, stationary high-tensioned track rope to support the lifting carriage. The track rope tension remains constant.

The track rope tension in a slackline cableway is never constant. The track rope is slackened to lower the lifting carriage to the working area, then tensioned and thus lifting the load clear to be hauled away by a separate rope.

The tautline cableway system is usually applied to handle material used in the construction of concrete dams. On such projects the work is generally confined to a relatively small area that can be spanned in whole or in part by a cableway. If the construction is in a deep gorge where it is difficult, if not impractical, to employ other equipment, the cableway is particularly applicable. In general it is found that, if the initial cost of the supply and installation of a tautline cableway does not greatly exceed equivalent costs of other material-handling equipment, the former will be the more economical and least hazardous. It should be considered that cableways are practically immune to the hazards of high water, flash floods or ice

runoffs. Although the preponderance of application is connected with dam construction, tautline cableways are used advantageously for other work as well, where they have not received as much publicity. Other applications include bridge building, and material handling in congested areas.^{H1}

The slackline cableway is used extensively in the construction and logging industry. The construction slackline cableway is most successful as an excavator where the material to be removed has a good depth and will cave or flow into the excavation.

A number of slackline systems are used in the logging industry to haul cut and trimmed bolt length logs from the stump to a central gathering area.

2. HISTORICAL

2.1 Aerial Ropeway History^{A4,A5,A6,A10,A11,A12,E35}

The first authenticated ropeway was constructed by a Dutchman, Adam Wybe, in 1644, for the city of Dantzic. This ropeway connected the city ramparts with a hill outside town. A single endless hemp rope passed over pulleys suspended on high posts, and carried a number of small buckets which were filled with earth on the hill and discharged at a certain point on the ramparts to strengthen the fortifications.

It was not until 1843, with the introduction of wire ropes that the modern ropeway became possible. It is interesting to note here, that, although wire ropes were known to the Romans centuries ago, (a fine specimen of bronze rope was found in the buried city of Pompeii and is now preserved in the Museo Borbonico, Naples), they were not used as a machine element until the latter nineteenth century. Wallis Taylor in his book "Aerial or Wire Ropeways"^{A10} states, "Over fifteen hundred years ago, wire ropes were known to the Chinese, and were employed as ropeways for crossing rivers". This statement is not confirmed by any other authorities on the subject.

The first ropeway of note was a monocable system built by Baron von Ducker in the Harz Mountains, Germany, in 1860. The same man constructed a ropeway using the bicable system between the years 1868 and 1870.

Charles Hodgson received the first English ropeway patent in 1868 for a monocable system. This is the man usually credited for founding the engineering of ropeways. In 1871, Theobald Obach, from Vienna, was granted the privilege of constructing a bicable continuous movement ropeway. This is probably the first patent granted for this type of ropeway. These dates mark the start of a tremendous development of freight ropeways all over the world.

This new method of transportation was considered too risky to be used for passenger travel until the start of the twentieth century. After some pilot installations began operating in Germany and Spain, the decisive success was achieved by "Simmeringer Maschinen and Waggonfabrik" in Vienna, who opened the first passenger ropeway designed for permanent operation in the vicinity of Bolzano, Italy. A similar ropeway went into operation in Switzerland at about the same time. The experience gained with military ropeways in Alpine Areas during the First World War greatly contributed to further development in the field of passenger and freight transport.

It was in this period that Luis Zuegg, an engineer from Merano, Italy, created a ropeway system which was to remain the leading design for decades. His "reversible" or "to-and-fro" moving system was originally used for passenger ropeways, as it proved to offer the highest measure of safety in high Alpine areas.

In the booming years after the First World War, the bicable ropeway for material transport underwent many improvements such as automatic loading and dumping, the twinning of the support cable producing the twin-cable system, and generally larger and longer systems. Prominent firms in this evolution of design were A. Bleichert Transportanlagen, J. Pohlig Aktiengesellschaft, of Germany; Ceretti and Tanfini of Italy; and John A. Roeblings' Sons Co., Riblet Tramway Co., Broderick and Bascomb, and the American Steel and Wire Company in America.

In the skiing industry, ropeway transportation evolved from the surface lifts. These are the T-Bar, J-Bar, or Platter Lifts, which pull the skier, riding on the snow surface on his skis, up the hill by means of devices attached to a continuous overhead moving rope. The Alpine T-Bar Lift was patented by M. Constam about 1930 in Germany and at approximately the same time Fred Pabst of Austria developed and patented the J-Bar. These lifts became a must for the progressive ski area in North America by the

early to mid 1950's.

The chairlift, in which the skier rides above the snow surface suspended in a chair from a continuous moving rope, was born about the same time as the surface lifts, again in central Europe. But the chairlift did not enjoy the popularity of the surface lifts due to cost and limited capacity. Originally the chairs were designed to seat one person, and it was only when the concept of the double chair arrangement, (two seater), with its resulting higher capacity was proved, that the chair lift became economically feasible for ski areas. The double chairlift, unlike the surface lift, is principally a North American development.

The ropeway manufacturer today is being pressed by the customer to extend the existing knowledge even further. The principal barrier to be broken is that of increasing the capacity of a given ropeway system. This means more tons per hour of material for freight ropeways, or people per hour for passenger ropeways. Increased travelling speeds, larger vehicles, better and faster loading and unloading facilities are some of the ways of tackling this problem. The tremendous increase of the summer tourist and winter skier has prompted development of ropeway systems in some of the most rugged mountainous areas of Europe and America. The ropeway manufacturer

has learned to deal with this type of terrain with its consequent extremely long spans between support towers, (the Zugspitze ropeway in the German Alps has one free hanging span of 8500 feet^{E15}), and with the inaccessibility of its support tower locations. In these situations much of the construction of the ropeway is aided by helicopters.

2.2 Cableway History ^{H1,H3,H4}

A booklet written in Italian by G. Ceretti of the firm Ceretti and Tanfini, about 1890, makes the first known reference to the cableway system. In this booklet, cableways are referred to quite casually as a new development introduced by J. Lidgerwood in the United States.

The Lidgerwood invention solved the problem of raising or lowering a load from a carriage that could be traversed between two terminal points of a suspended wire rope.

The first cableway was sold by the Lidgerwood Manufacturing Company in 1884 to Andrew and Locke, Wilmington, Delaware. It had 8 tons capacity and was powered by a steam winch. Both terminal towers were fixed, but data as to span length is missing in the literature. The next step in the evolution of cableways was the installation of four 8-ton Lidgerwood-type travelling

cableways sold in 1894. The travelling cableway incorporated the innovation of lateral moving terminal towers, allowing a greater area of work coverage. In 1897, 4-ton cableways equipped with electric hoists were produced, and in 1902 the first 10-ton unit was installed. In 1908 the Isthmian Canal Commission of the U. S. Government purchased thirteen 6-ton travelling cableways, electrically powered with steel towers operating on common parallel trackways for use on the construction of the Panama Canal.

So began the trend for heavy-duty cableways, particularly for use on the construction of large concrete dams. A major construction project on which modern electric Lidgerwood-type cableways were employed was Shasta Dam on which seven radial cableways of span lengths ranging from 710 to 2,670 feet, with capacities of 8 cubic yards of concrete, were connected to and radiated about a common radial head tower 450 feet high.

In the early 1900's, the slackline cableway was developed and soon found application in the logging industry to skid bolt length logs from the bush to a gathering area, and in the construction industry as an excavator.

The evolution of tautline cableways to date is completed with two of the largest and most modern installations. The first is a unit purchased in 1932 by the U. S.

Bureau of Reclamation for permanent installation at Boulder Dam.^{H1} It has a hook load capacity of 150 tons, has been test loaded to 160 tons, has a span length of 1,250 feet and the carriage is supported by multiple track ropes. It is used for handling heavy unit loads such as penstock sections, machinery and loaded railway cars. The second installation of note is the catenary cableway erected over the Volga River in 1956 during the construction of the Stalingrad Hydro-electric station.^{I9} This system uses four stationary heavy catenary cables to support a series of suspended frames which in turn carry four parallel cableway ropes with a capacity of 225 tons an hour each. This is much the same construction as a suspension bridge with the traffic deck replaced by the cableway ropes. The span length is 2970 feet and the fixed catenary support towers are 433 feet high. This is undoubtedly the largest tautline cableway to date using capacity in tons per hour as a reference.

3. CLASSIFICATION OF AERIAL ROPEWAYS

3.1 Monocable Systems

The monocable system consists essentially of a single, endless, continuously moving rope which is carried by sheaves on intermediate towers or trestles. At each terminal the rope passes around large diameter sheaves. One of these sheaves is anchored and powered (Figure 2), the other being free to move horizontally and is attached to a suspended weight (Figure 4), usually a large block of concrete, which maintains a constant maximum tension in the hauling-support rope. This arrangement may be reversed with the driving terminal being tensioned with the counterweight, (Figure 1), and the idler terminal anchored to a concrete base, (Figure 3). The two tensioning methods used in the monocable system are shown schematically in Figures 5 and 6.

Monocable ropeways have two main subdivisions. The fixed clip system and the detachable clip system.

3.1.1 Fixed Clip Monocable System

In this type, the carriers are attached permanently to the hauling-support rope, usually by a bolted clamp. This clamp often incorporates a swivel to allow the carrier

to hang vertically no matter what angle the rope assumes.

The main advantage of a fixed clip monocable is its ability to negotiate almost any grade. It is also the cheapest form of plant within its design limitations. It operates at slow speeds (2 to 5.1 mph), low hourly capacities (10 to 100 tons per hour), and with light loads that can be loaded onto a moving carrier.^{D1} It is also limited to the length of one section. That is, the carriers can go no further than the distance between the terminals since they cannot be detached. Thus it is impossible to have an intermediate rope tension station as is used with very long detachable clip systems.

These limitations restrict the use of the fixed clip monocable to rather special applications. The most common use today is probably in ski areas. In the ski industry, these monocable ropeways are universally known as ski lifts. Hourly production in this application sets the upper limits on the speed and capacity given above. This is due to the ability of the human cargo to deliver itself to the ropeway and load and unload itself. The normal values for material handling systems is at the low end of these figures.

Some examples of the application of the fixed clip monocable systems follow: Figure 7 shows a Platter Lift which has an expandable carrier bar fixed to the hauling-

support rope at one end, with a small plastic disc or platter about 8 inches in diameter, at the other end. The skier straddles the disc, the bar extends a spring until an equilibrium of forces occurs, and the skier is then hauled over the snow surface.

The T-Bar Lift, (Figures 8 and 9), doubles the capacity of the Platter Lift by replacing the platter with the wooden seat of a T-Bar. The advantage to the skier is the great increase in comfort of the tow to the top of the hill.

The J-Bar lift is similar to the T-Bar. The difference is that one side of the T-Bar seat is missing. Consequently the capacity matches that of the Platter Lift, but again the comfort to the skier is much improved.

It is important to note here that all the above surface lifts require the skier track, under the up-side rope, to be graded smoothly and maintained a constant distance from the hauling-support rope (usually about 13 feet). This can be a major installation cost, especially where rocky broken terrain is to be traversed.

The Chair Lift moves passengers around the circuit in chairs suspended from the hauling-support rope. In the ski areas, (Figure 10), this system is used to traverse more rugged terrain than is possible with the ground contact lifts since it is relatively independent of ground contour.

It is also used where the lift line is very steep or too lengthy (over 2000 feet) for the T-Bar Lift. The trip to the top of the hill is made with much less skier effort than is necessary with the surface lifts. However, the chairs usually travel at a height above the top of the trees so the passengers are much more exposed to the cold winter wind.

This type of lift has become quite popular as a sight-seeing novelty ride at scenic spots, (Figure 11), or at Fair Grounds, (Figure 12). Here the chairs move horizontally in a continuous circuit about 35 feet above the ground. The important feature of the chair type carrier is that it gives maximum visibility to the tourist.

On the ski slopes the disadvantage of the open chair is overcome by replacing it by a small completely enclosed cabin, (Figure 13). The small cabin system is sometimes known as a Gondola Lift. The ski lift shown in Figure 13 is actually the detachable clip monocable system. The fixed clip system is similar but with a less elaborate fixed rope clamp.

The fixed clip system is seldom used on these more elaborate Gondola lifts as the skiers must load their skis in a special attachment and enter the cabin on the run. Note that the enclosed cabin also means that the passengers cannot travel with skis attached to their feet. The

importance of this drawback, however, diminishes with lift length.

3.1.2 Detachable Clip Monocable System

In a detachable clip monocable system, the carriages are attached to the hauling-support rope by mechanically or gravity-actuated grips. At terminal stations the carriages transfer automatically from the rope to a running rail. Side mounted wheels mount an inclined rail, and release the grip, either by taking the weight off the grip or mechanically. The carriages move around the rail to the return line or to a new section by their own momentum, or are assisted manually, by gravity, or by an auxiliary chain haul.

The detachable clip monocable is generally applicable where production requirements are up to 150 tons per hour, and individual loads up to 1 ton.^{D1}

Detachable clip monocables are widely used throughout the world for the long distance (up to 47 miles^{D1}) transport of a great variety of industrial products. For the very long distances a series of tandem ropeways is constructed, and the carriers switched from one to another. The detachable clip systems are common in the mining industry.

As mentioned above, Figure 13 shows a detachable clip small cabin monocable system serving a ski area.

3.2 Bicable Systems

The bicable ropeway uses either one or two stationary highly tensioned track ropes, (when two ropes are used the system is sometimes called twincable), to support the carrier, which is hauled along by a lighter traction rope. This system is almost always operated using detachable clip carriers. The bicable ropeway has two distinct subdivisions, the continuous and the reversible systems.

3.2.1 Continuous Bicable System

The bicable continuous system, (Figures 15, 16), consists of two fixed track (support) ropes -- a heavy rope on the loaded side, and usually a somewhat lighter rope on the return (empty) side in material transport applications. The carriers are suspended from a 2- or 4-wheeled carriage which moves along the track rope, (Figure 17).

The carriage is also clipped to a continuous light traction (haulage) rope. Carriages are over-type if the haulage rope is above the track rope, and under-type if the haulage rope is below. The latter is more common

because of somewhat greater flexibility regarding grades.

The traction rope passes around a large diameter powered sheave at one terminal and a similar idler sheave at the other. The track ropes are carried on saddles located on intermediate towers, (Figure 16). The traction rope is held up by the carriages and usually supported at the towers.

At the terminals the carriers are usually released automatically from the traction rope. The traction rope grips are of the detachable type and actuated mechanically or by the weight of the load acting through the grip on the traction rope. With most systems, auxiliary wheels attached to the carriage run onto inclined rails at main stations to release the grip.

The carriers are thus transferred from the track rope to a running rail, from which they pass either to the return rope or to a second section of the ropeway.

Loading and unloading of the carriers usually takes place at the terminals, but loads can be dumped at any point along the length of the system. In any substantial commercial installation, loading, unloading, and transfer are automatic. Uniform spacing of the carriers for the designed capacity of the ropeway is obtained by an automatic timing device at the loading station.

Track support ropes are ordinarily anchored at one

end and tension maintained by freely suspended weights at the other, (Figure 19). The large diameter (10 to 15 feet) idler sheave at the return terminal of the traction (hauling) rope is mounted on a trolley and tension maintained in this rope again by a suspended counterweight. Traction ropes on short ropeway sections (up to 1/4 mile) are sometimes tensioned by springs.^{A14}

Long bicable ropeways are divided into sections which rarely exceed 5 miles^{A1}, and each section has its own endless traction rope and drive. Carriers are disengaged from the hauling rope and are either pushed or transferred automatically from one section to the next. Changes in direction may be introduced at these points.^{A1} The longest bicable ropeway is probably that which connects the mines at Boliden with those at Kristineberg in Swedish Lapland, a distance of 60 miles.^{A12} It carries gold-bearing arsenic copper-ore and sulphur pyrites. The profile of a typical bicable ropeway for passenger transport is shown in Figure 18.

Continuous, fully automated bicable or twin-cable systems are the most expensive ropeway installation. For this reason they will generally be used only where the production requirement, or individual loads, are beyond the capabilities of the monocable or bicable reversible system. The limits for the bicable ropeway are 600 tons

per hour with an individual maximum load of 5 tons.^{D1}

In addition to production and load capabilities, the continuous bicable has other advantages. It is more adaptable to full automation and more flexible as to grades. These latter features can be incorporated into monocable systems if the requirement justifies the expense.

3.2.2 Reversible (Jigback or To and Fro) Bicable System

The chief difference of this system from the conventional continuous bicable is that the carrier leaves and returns to the loading station on the same track rope. There may be only one carrier and one track rope, (Figure 20), or two carriers and two track ropes (Figure 21), the latter usually known as the double reversible system. Thus with the double reversible bicable, when one carrier is at the loading terminal, the other is at the discharge point, and the carriers -- usually one loaded, the other empty -- pass each other in transit.

This is a short length system for very special applications, and normally is of low capacity. It is used to form rubbish dumps, to dispose of industrial wastes, in collieries, and for passenger transportation. The single reversible system would have a capacity of about 20 tons per hour and a maximum length of 800 yards. The double reversible system would have twice the above capacity, but

since they are a "to and fro" operation, the capacity varies inversely to the distance travelled.^{A12}

In the field of passenger transport, (Figure 14), the double reversible bicable has achieved its widest acclaim. Here it normally assumes the character of a bus service in places where steep or rugged ground, or climatic features, would make the cost of other means of land transport prohibitive. The reversible type is given preference over the continuous system because large and medium sized cabins afford a greater comfort and better protection in bad weather than the four-seat continuous vehicles. Also, the more extensive space available in the former, permits transport of bulky packages.

Two of the modern installations are worthy of note here because of their size and capacity. The first was installed (1964) by Von Roll Limited, of Berne, Switzerland in Chamonix, France.^{E24} It has a length of 9,515 feet, rising 2,035 feet, a cabin capacity of 80 passengers and an amazing speed of 1,970 feet per minute. The second noteworthy reversible passenger ropeway was built (1963) for the Hakone National Park in Japan by Anzen Sakudo Company Limited of Osaka, Japan.^{E10} This one holds the undisputed world's record for cabin capacity -- namely, 101 persons including conductor. The ropeway length is

5,850 feet, it rises 1,940 feet, and has an operating speed of 1,580 feet per minute.

4. Classification of Cableways

The cableway is a hoisting and conveying device which operates over one clear span between terminal towers. It differs from the aerial ropeway in that the load can be raised or lowered at any point in the traverse. The bicable system is used to support and haul the hoisting carriage. That is, the hoisting carriage is suspended from a multi-wheeled carriage which moves along a heavy track (support) rope, and is traversed across the span by a lighter traction or conveying rope. There are two distinct cableway systems, the Tautline Cableway and the Slackline Cableway.

4.1 Tautline Cableways

The tautline cableway, (Figures 22, 23), uses a stationary track rope in which a constant high tension is maintained by a series of take-up pulleys which in turn are attached to the terminal or tail tower, or to a fixed ground anchorage, (Figures 24, 25). A separate rope and pulley system hoists the load. Figure 28 shows a typical rope reeving diagram for a tautline cableway. Tautline cableways may be further subdivided according to whether the terminal towers are fixed, radial, or movable.

4.1.1 Fixed Tautline Cableway

When a cableway has two stationary or fixed towers, it is classified as a fixed cableway. These towers may be needle-type masts, mounted on a hinge-pin or ball and socket arrangement, and held in position by guys and the track rope, (Figures 22, 23); guyed four legged towers; or stable towers, (Figures 24, 26). As they cannot be moved laterally, the area that can be serviced is necessarily confined to a straight line, or if luffing devices are used, (rope rigging used to swing the top of the needle mast in a lateral direction, Figure 23), a narrow parallelogram may be served.

The fixed tower cableway is usually applied to operations such as bridge construction. On the wider bridges, two fixed parallel cableways are used to obtain adequate lateral coverage, (Figure 22). However, for bridges of ordinary width of roadway, the load may be drifted laterally enough to give sufficient coverage.

4.1.2 Radial Tautline Cableways

Where a movable tower, (Figure 27), radiates about a stationary tower, the cableway is classified as radial. The segment of a circle represented by the radius (span length) subtended by the angle of travel of the movable tower is the area that can be serviced. The angle of

travel is usually less than 40° .^{H1} Sheaves and fittings at the fixed end are allowed to swivel in order to eliminate twisting or distortion when the travelling tower moves round the pivot end of the cableway.

The movable tower is usually counterweighted for stability to help offset the effect of the track rope tension, the fixed tower being guyed. The movable tower is supported at the four corners by spherical bearings mounted on multi-wheeled trucks designed to equalize wheel loads. These trucks move over steel rails.

4.1.3 Movable Tautline Cableway

This term applies to cableways where both terminal towers are movable (Figure 25). Usually the towers move on parallel trackways. There are installations where the trackways are segments of concentric circular arcs, but this type of installation is rare.^{H1}

The operational end, where the hoisting machinery is located, is called the "head tower". The opposite "tail tower", having no machinery as a counterbalance, usually requires a counterweight.

4.2 Slackline Cableways

This system is alternately known as a "dragline cableway excavator" or "slack-rope cableway excavator".

In the construction industry this machine is used for excavating material from rivers, pits, or other inaccessible spots. It is especially useful in removing sand or gravel in deep deposits under water.

In the past the slackline system was used extensively by the logging industry to haul the trimmed logs from the stump to a gathering area for transportation to the saw mill. Recently, however, they are being replaced by the more adaptable 4-wheeled logging vehicles with special winches attached.

The typical excavator installation (Figure 29) comprises a dragline bucket attached to a trolley or carriage, which runs on a track rope which is anchored at ground level at one end, the other end attached to a head tower by a block and tackle arrangement. The head tower height is normally 50 to 100 feet.^{H4} This difference in height is such that the loaded bucket can be dumped into an elevated hopper over washing screens or onto a large dump pile.

The block and tackle arrangement mentioned above consists of two pulley blocks, one which is attached to the head of the mast and the other to the track cable. The rope reeving of these pulleys is known as the "slack line". The track rope is thus tightened or slackened as the slack line is wound onto or off the hoist winch. A

pulling rope known as a "load line" or "dragline" leads from the front of the bucket, over a single block attached to the head tower, to a hauling winch.

A typical operating cycle is as follows: The track rope is slackened by the hoist winch through the slack line, lowering the bucket to the digging point. When the bucket rests on the material the hauling winch pulls on the dragline, and the bucket picks up its load as it is dragged forward. The slack line is hauled in tightening the track rope while at the same time the bucket of material is being rapidly pulled up the track rope by the dragline. At the desired dumping point, the rear dump gate of the bucket is opened, and the load dropped. The dragline is slackened and the bucket carriage runs down the sloping track rope by gravity to the digging point where the cycle is repeated.

5. Structural Design of a Chair Lift Intermediate Support Tower

The major purpose of this work is to examine in detail the structural design of the different types of chair lift towers currently being used.

The chair lift is a rather specialized form of the monocable fixed-clip ropeway used in the ski industry as discussed in section 3.1.1. It consists essentially of a single, endless, continuously moving rope which both supports and hauls the chairs and passengers, and is carried by sheaves on intermediate towers. At each terminal the rope passes around large diameter sheaves. One of these sheaves is anchored and powered, (usually the terminal at the bottom of the hill), the other being an idler at the top of the hill, free to move under the action of a counterweight. The centerline between these two terminals is usually straight and is called the "lift line".

The intermediate support towers are positioned on the lift line between the two terminals such that the rope is held up from the ground a distance of 30 to 40 feet. Thus they are normally situated at points of sharp change in the lift line contour.

The intermediate support towers of monocable ropeways have been constructed of steel in a number of different forms; the pipe tower (Figures 30 and 40), the tapered square tower (Figure 31), the hexagonal tower (Figure 32), and the lattice tower (Figures 35, 36, 37, 38, 39, 42). Some modern installations, where the height of the rope need not be more than 20 to 30 feet above the ground, have reinforced concrete towers (Figures 33 and 34). In general, for chair lifts, the lattice construction is used where the rope must be supported at a height over 40 feet. This type of tower offers the best combination of rigidity and economy at these heights. The pipe tower is used in the smaller lifts where the tower height would not exceed 30 feet. At greater heights, the larger diameter pipe required is not economical, and the ropeway manufacturer tends to use the fabricated tower (tapered square and hexagonal).

The hauling-support rope runs over a series of self-equalizing idler sheaves called an idler assembly, which is attached to the top cross-arm of the tower (Figure 41). The towers support the rope in two different ways. If the rope is held up from the ground, the tower is called a "hold-up" tower. Figure 40 shows a series of "hold-up" towers. The tower is called a "hold-down" tower if the rope is held towards the ground (Figure 42). The

change in angle between entering and leaving the idler assembly is known as the "breakover angle" for hold-up towers, and the "breakunder angle" for hold-down towers.

5.1 External Loads Imposed on a Chair Lift Intermediate Support Tower

In order to design any of the above types of intermediate tower, some analysis of the external loads which the tower must bear to support the rope, chairs and passengers must be made. The following loads are assumed to be acting:

- (a) The load due to the rope as it bends over the idler assemblies on each side of the tower. This is known as the "chordload" (R) and is the major external load imposed on the tower.
- (b) The loading due to wind on the tower, and on the rope, passengers and chairs in the half span to each side of the tower. This is assumed to act at right angles to the chordload.
- (c) The self weight of the tower and idler assemblies. This is considered negligible compared to loads (a) and (b).
- (d) The idler assembly reaction due to friction in the sheaves as the hauling-support rope

passes over them. This is considered negligible compared to loads (a) and (b).

- (e) The idler assembly reaction due to a chair clamp passing over each idler sheave. Since the clamp is somewhat larger in diameter than the rope, the idler sheaves experience some shock loading as the clamp passes over them. Again, this load is considered negligible compared to loads (a) and (b).

The latter three loads are important when considering the vibrational characteristics of the tower. A vibrational analysis is beyond the scope of this thesis and will not be treated here.

5.1.1 Calculation of the Maximum Chordload "R"

The magnitude of the chordload depends on the tension in the rope at the idler assembly, and the total breakover angle of the idler assembly. The maximum values of these two factors will produce the maximum design chordload.

The hauling-support rope normally used on chair lift installations is a 1-1/8 inch diameter, fiber center, improved plow steel, 6-strand wire rope. This rope has an ultimate breaking strength of 53 tons.^{F17} The diameter chosen is intended to be large enough to give the passenger

the comfortable feeling of strength. A smaller rope could be used, but since it could not be tensioned as highly, (the breaking strength being lower), the rope sag between towers may be unacceptable. However, the passengers' "peace of mind" must also be considered. To him, the smaller rope usually looks out of proportion to the size of the chair, even though the rope strength may be quite sufficient.

The hauling-support rope is tensioned by means of a hanging counterweight. The counterweight size is designed such that it imposes on the rope a load not greater than 1/5 its breaking strength, (see section 3.1.1.3, reference E27). So the maximum tension in the 1-1/8 diameter rope is:

$$T = \frac{53 \times 2000}{5} = 21.2 \times 10^3 \text{ pounds}$$

Note that this is the maximum tension that will occur anywhere in the hauling-support rope. No matter how much or how little the chairs are loaded, the tension in the rope will not exceed this value unless the counterweight is jammed against the end of its slide. This maximum tension is assumed to act at an intermediate tower.

The maximum number of idler sheaves in an idler assembly is assumed to be 4. The maximum allowable deflection of the rope over each sheave is 4° - 30', (see section 2.4.3, reference E27). For 4 sheaves, the total

breakover angle is:

$$\phi = 4 \times (4^\circ - 30') = 18^\circ$$

From Figures 43 and 44, it is evident that the maximum chordload is:

$$\begin{aligned} R &= 2T \sin (\phi/2) = 2 \times 21.2 \times 10^3 \times \sin(18^\circ/2) \\ &= 6,640 \text{ pounds.} \end{aligned}$$

This is the chordload contribution from one rope on one side of the tower only. For two ropes acting on two idler assemblies, the total maximum chordload is:

$$R = 2 \times 6,640 = 13,280 \text{ pounds}$$

The maximum allowable angle between the chordload (R) and the vertical tower centerline is to be 25°. The most efficient tower structure would be tilted on the ski hill such that its vertical centerline and the chordload were colinear. Here again the psychological feelings of the passenger must be considered, for towers that have large tilts seem to be falling downhill. Most lift manufacturers tilt the tower 5° - 10° where possible (Figure 36), however, the terrain does not always allow this.

5.1.2 Calculation of the Loading due to Wind

It is assumed that the wind acts on the tower, and on the half span of rope, chairs and passengers to each side of the tower. Reference E27, section 2.8, gives the following wind pressures to be used for design purposes:

Wind pressure on the projected area exposed to the wind is:

$$q = 6.15 \text{ lb/ft}^2 \text{ (30 kg/m}^2\text{)}.$$

This reference also suggests a resistance factor $C_r = 1.1$ be applied in calculating the wind loading on the ropes only.

The usual assumption for the half span on each side of the tower is 160 feet.^{G1} So for a single 1-1/8 inch diameter rope of total span 320 feet, the projected area is:

$$A_r = \frac{1.125}{12} \times 320 = 30.0 \text{ ft}^2,$$

and the windload on the rope alone is:

$$W_r = 30.0 \times 1.1 \times 6.15 = 203 \text{ pounds.}$$

The projected area of a passenger and chair is assumed to be 5 square feet.^{G1} The chair spacing is normally 80 feet, so in 320 feet there are $320/80 = 4$ chairs. Thus the projected area of passengers and chairs in 320 feet = $4 \times 5 = 20$ square feet. The windload on the chairs and passengers is:

$$W_p = 6.15 \times 20 = 123 \text{ pounds.}$$

So the total windload imposed on one idler assembly by the rope, passengers and chairs is:

$$W_R = W_r + W_p = 203 + 123 = 326 \text{ pounds}$$

The windload acting on the tower from two idler assemblies is thus:

$$W_R = 2 \times 326 = 652 \text{ pounds.}$$

Each idler assembly is assumed to have an exposed area of 12 square feet, so the windload acting on two idler assemblies is:

$$W_I = 2 \times 12 \times 6.15 = 150 \text{ pounds}$$

The windload acting on the tower structure itself cannot be calculated until an initial tower size is estimated. Then the projected area and windload can be determined. This will be done later for each tower design.

5.2 Design of the Chair Lift Intermediate Support Tower Models

Three types of chair lift towers will be examined in the following pages: (1) the lattice tower, (2) the pipe tower, and (3) the hexagonal section tower. A mathematical model for each of these structures will be proposed and the maximum stress calculated using known theories of stress analysis. It is desirable however, to see how the predicted stress at the critical section of each tower type agrees with a measured stress. This gives one some indication of the correctness of his method of analysis and simplifying assumptions.

In order that each type of tower have some common base for analysis, it will be assumed that all are 40 feet high, (the chordload is applied 40 feet from the base).

The magnitude of the maximum allowable chordload and its direction will also be common to the three types of towers.

It is evident that full scale load tests cannot be made in the laboratory due to the size of these structures, consequently it is necessary to carry out a theoretical and experimental analysis of true structural models.

The approach used to design the models is outlined in the following steps:

(a) The full size tower (prototype), was designed to withstand the chordload and windloads. Each structure was made large enough such that the maximum stress in the critical portion of the tower did not exceed a recommended maximum stress given in section 5.2.1, reference E27, (the maximum working stress under the most unfavorable conditions is not to be more than $1/3$ the breaking strength of the material).

(b) A length scale factor was chosen to give the towers an overall length of approximately 6 feet. This seemed a convenient size to work with. The model chordload and windloads for each tower were also calculated using the appropriate scale factor. The method of exact model design is thoroughly covered in reference G7 and will not be detailed here.

(c) Some deviation from exact models of the prototype towers was found to be necessary, since it was impossible to purchase from stock the exact thickness of steel sheet or steel pipe required for the models. This was not a serious problem however, as the basic idea of this study is to predict the theoretical stress behavior of a loaded structure and to check this experimentally, and thus it is not essential that the model be exactly to scale.

The initial design of the prototype and the subsequent scaling to a model was only useful in that it gave a rough indication of the model structure size. A completely new stress analysis is carried out on each of the models without any further reference to the prototype towers.

5.3 Design of the Chair Lift Lattice Tower Model

Two types of the lattice tower will be examined. The determinate structure and the indeterminate structure, (Figures 45, 50). The length scale factor is chosen to be $K_L = 0.153$. The model chordload is given by $R_m = (K_L)^2 R_p$, where the subscript "m" indicates model and "p" indicates prototype, therefore:

$$R_m = (0.153)^2 \times 13.280 = 311 \text{ pounds.}$$

The windload due to the ropes, passengers, chairs and idler assemblies is:

$$W_m = (K_L)^2 W_p = (0.153)^2 \times (652 + 150) \\ = 19.0 \text{ pounds}$$

The above loads apply to both the determinate and indeterminate structures. The subscript "m" will be dropped from this point onward as only the model structures will be dealt with.

5.3.1 Determinate Lattice Tower Model

The determinate lattice tower model is constructed as shown in Figure 45. It is square in cross-section and constructed of steel angle members bolted together. The overall dimensions of the tower are: a 12.25 inch square base, a 3.156 inch square top, and a height of 72.813 inches. These model dimensions were scaled from prototype dimensions of: a 7 foot square base, a 2 foot square top, and a height of 40 feet. The latter dimensions are typical of existing chair lift lattice towers.

The angle members of the model were formed from mild steel sheet to the following dimensions:

Corner and Top Angles

$$\text{Size} = 17/32 \times 17/32 \times 0.0478 \text{ inches}$$

$$\text{Cross-section area} = 0.0485 \text{ inches}^2$$

All Diagonal and Cross Angles

Size = $3/8 \times 3/8 \times 0.0299$ inches

Cross-section area = 0.0216 inches²

5.3.1.1 Mathematical Model of the Determinate Tower

The tower is considered to be made up of four planar trusses with common edges. Thus any general load "P", (Figure 46), can be resolved into three components: C_1 , parallel to the tower leg; C_2 , horizontal and lying in the plane of one adjacent face of the tower; and C_3 , horizontal and lying in the plane of the other adjacent face of the tower. G3,G4,G5,G6,G11

It is easy to show, G3,G4,G11 that load C_1 causes bar forces in the bars of leg GC only, C_2 causes forces in the bars of tower side CDGH only, and C_3 causes forces in the bars of tower side ACEG only.

Thus the bar forces due to each of the components, C_1 , C_2 , and C_3 , can be obtained by carrying out a separate planar analysis, and the total force in any bar, due to load "P" can be obtained by superposition of the effects of its three components.

Each of the tower planes is assumed to act as a true pin-jointed truss in which the members take little or no bending -- they transmit axial forces only.

5.3.1.2 Calculation of the Maximum Stress in the Determinate Tower Members

Figure 45 shows the tower with the chordload and windloads applied. These loads must be applied at the joints of the structure. From the previous discussion it is evident that tower sides ABEF and CDGH are stressed only by the chordload, and this is shared equally by each side. Similarly the wind loads are carried only by the tower sides ACEG and BDFH, again, these loads are equally shared. Note that the vertical component of the chordload does not lie exactly in the plane of the tower side due to the longitudinal taper of the tower. Since this taper is small (approximately 3°) the effect of this component on the wind load planes is neglected. If the taper was greater, however, this approximation should not be made.

In section 5.3, the maximum model chordload was found to be 311 pounds acting downward at 25 degrees to the vertical centerline. Each plane ABEF and CDGH carries one-half of this, or 155.5 pounds. Also, in each side, this load is assumed to act as two concentrated loads applied at the two top joints. So the point load at each of these joints in planes ABEF and CDGH will be 77.75 pounds. The axial load in each member of these chordload planes is calculated using the digital computer program for the analysis of a determinate, pin-jointed planar truss as detailed in Appendix A. The results of this

calculation are summarized below in Table 1.

The windload on the model tower is based on a projected area pressure of 6.15 pounds per square foot, see section 5.1.2. Note that this is the same wind pressure that acts on the prototype. No scaling is necessary. Reference G5 states: "In calculating the surface, (of a lattice-type tower), exposed to the wind, no credit should be given for the shielding of the leeward portions of the tower by the windward frames". The exposed area of the model is calculated by adding the areas of one leg of each angle in each frame of the windload planes. This area is multiplied by the design wind pressure and the resulting load applied at each successive joint on the windward side. The angle sizes used in the windload calculations are given in section 5.3.1. For example, referring to Figure 45, the windload W_1 is calculated as follows:

$$\begin{aligned}
 W_1 &= \frac{6.15}{12} \times 2 \left[2 \left(\frac{17}{32} \times 12.46 \right) + \left(\frac{3}{8} \times 16.50 \right) \right. \\
 &\quad \left. + \left(\frac{3}{8} \times 10.10 \right) \right] \\
 &= 3.78 \text{ pounds.}
 \end{aligned}$$

In this calculation, the exposed area for the bottom frame of one plane is found and multiplied by two. There are two corner angles 12.46 inches long, one diagonal angle 16.50 inches long; and one horizontal member 10.10 inches long. The remaining windloads are

calculated and summarized below:

Tower Model Windloads

W_1	=	3.78	pounds
W_2	=	3.48	pounds
W_3	=	3.04	pounds
W_4	=	2.62	pounds
W_5	=	2.30	pounds
W_6	=	2.02	pounds
W_7	=	1.70	pounds
W_8	=	1.54	pounds
W_9	=	1.64	pounds

Note that the total windload W_9 must also include the windload on the ropes, passengers, chairs and idler assemblies (see section 5.3). That is:

$$W_9 = 19.0 + 1.64 = 20.64 \text{ pounds.}$$

Each windload plane ACEG and BDFH carries one-half of the above loads.

The axial load in each member of the windload planes is calculated using the digital computer program for the analysis of a determinate, pin-jointed planar truss as detailed in Appendix A. The results of this calculation are summarized below in Table 1.

It can be seen from Figure 45 that the corner angles are stressed by both the windload and chordload planes, being common to both. The total load in each

member of the corner angles shown in Table 2 below is obtained by algebraically adding the contribution of the windload and chordload planes. Each member of the corner angle is defined by a small letter of the alphabet as shown in Figure 45. For example, member "AEa" is the bottom member of corner angle AE. The force in AEa is obtained by adding the force in member 1 of plane AB EF and member 3 of plane ACEG, $(-347.9 = -441.6 + 93.7)$.

5.3.1.3 Experimental Strain Measurements in the Determinate Tower Members

A determinate tower model was built to the dimensions shown in Figure 45. The angle members were formed from cold rolled mild steel sheet. The diagonal and cross angles were cut to length and assembled with a single bolt holding each end of the member to the corner angles.

Strain gages were fixed to the following members: (Refer to Figures 47 and 48 for member numbers).

- (1) Corner angle CG, member a.
- (2) Diagonal angle, member 34, plane AB EF - free leg.
- (3) Diagonal angle, member 34, plane AB EF - bolted leg.
- (4) Corner angle BF, member b.

- (5) Diagonal angle member 26, plane AB EF - free leg.
- (6) Diagonal angle member 26, plane AB EF - bolted leg.

The tower was fastened to a rigid base and loaded as shown in Figure 49. The windloads on the tower were simulated by hanging weights, (bags of sand and a block of lead). The chordload is simulated by the force of an air cylinder, mounted such that it pulled at 25 degrees to the tower centerline.

The windloads were applied and strain readings taken. Then the chordload was applied in 100 pound increments up to 400 pounds. The average strain readings for these load increments are shown in Table 3. The strains were recorded for the design chordload of 311 pounds (see section 5.3), while the wind loads were applied.

5.3.1.4 Evaluation of the Theoretical and Experimental Stresses in the Determinate Tower Members

Table 4 compares the predicted stress with the experimental stress at the design condition, (maximum chordload and windloads), in the members that were strain gaged. The theoretical stress is calculated by dividing the member force from Table 1 by the member cross-section area given in section 5.3.1. The experimental stress is

obtained by multiplying the strain readings from Table 3 by the modulus of elasticity for steel, taken as 29.9×10^6 pounds per square inch. The average experimental direct stress in diagonal members 26 and 34 of plane ABEF was calculated by separating this stress from the bending stress. Each of these diagonal angle members had two strain gages attached, one on the bolted leg, and one on the free leg. The strain reading from each gage and the position of the gages on the member allow one to calculate the average direct compressive stress.

The assumption that loads applied parallel to the windload planes produce forces only in the members of those planes, as explained in section 5.3.1.1, has been proven experimentally. Table 3 shows that member 34 (gages 2 and 3), and member 26 (gages 5 and 6), both of which are in the chordload plane ABEF, were not affected by the application of the windloads.

The other major assumption used in the theoretical analysis was that the members transmit only axial forces and experience little or no bending. This was not found to be valid. Both diagonal members examined show considerable bending stresses under load. This fact is quite obvious from the difference in strain readings of the bolted leg and the free leg of each angle. Some bending was expected to be present but not of this

magnitude. This large discrepancy with theory is rather difficult to justify; however, three possible explanations for it are:

- (a) Although only one bolt held each end of the member to the corner angles, the connection was a tight one and did not truly simulate the assumption of pinned joints used in the mathematical model. This means that some bending forces are transferred across the bolted joint to the diagonal members by friction.
- (b) The compressive force imposed on one leg of the angle by the bolts is not colinear with the neutral axis of the section. The neutral axis lies in the free leg of the angle and thus the angle is eccentrically loaded, producing a bending moment.
- (c) The angles used in the model were formed from a length of steel sheet, bent 90 degrees to simulate the rolled angle section that would be used in an actual chair lift tower. It should be noted, however, that in doing this it was not possible to duplicate the condition at

the corner of a rolled angle, where the outside corner is square, and the inside has a generous fillet. This means that the neutral axis in the model angles would be a greater distance from the bolted leg than would a true replica of a rolled angle. The bending moment induced by the bolt forces would thus be larger than expected.

It can be seen from Table 4 that, in general, the predicted stresses are higher than the experimental member stresses. Thus the mathematical model usually predicts stresses on the "safe" side of those actually encountered, which is good design procedure. Discrepancies between the predicted and experimental results would be due largely to the error in assuming the members transmit no bending moments. Some error must be assigned to the dimensional deviation of the built-up tower from the mathematical model. That is, the model was not perfectly square in section, or straight in length.

The model angle sizes supplied definitely varied from those requested. Unfortunately, time limitations dictated their use -- not their replacement. The corner angles were to be $17/32$ (0.531) x $17/32$ (0.531) x 0.0478 inches, however, typical sizes supplied varied from 0.522 to 0.605 inches for one leg width and 0.566 to 0.541

Table 1 Determinate Chair Lift Lattice Tower Model,
Member Forces

Note: Tension is Positive, Compression is Negative

<u>Member</u>	<u>Chordload Planes</u>		<u>Windload Planes</u>	
	<u>Plane ABEF</u> <u>Force-lbs.</u>	<u>Plane CDGH</u> <u>Force-lbs.</u>	<u>Plane ACEG</u> <u>Force-lbs.</u>	<u>Plane BDFH</u> <u>Force-lbs.</u>
1	-441.64	-461.37	-83.27	-93.68
2	-26.74	26.74	-14.12	14.12
3	320.28	300.57	93.68	83.27
4	19.36	-19.36	8.33	-10.22
5	-418.24	-441.67	-73.20	-83.28
6	-31.29	31.29	-13.46	13.46
7	300.59	277.16	83.28	73.20
8	22.28	-22.28	7.84	-9.58
9	-390.99	-418.27	-63.61	-73.21
10	-36.25	36.25	-12.77	12.77
11	277.18	249.92	73.21	63.61
12	25.67	-25.67	7.52	-9.04
13	-358.72	-391.02	-54.16	-63.62
14	-42.47	42.47	-12.44	12.44
15	249.94	217.65	63.62	54.16
16	29.70	-29.70	7.39	-8.70
17	-320.49	-358.75	-44.64	-54.16
18	-49.86	49.86	-12.40	12.40
19	217.67	179.42	54.16	44.64
20	34.47	-34.47	7.43	-8.58
21	-274.64	-320.48	-34.77	-44.64
22	-59.05	59.05	-12.72	12.72
23	179.43	133.55	44.65	34.76
24	40.18	-40.18	7.65	-8.66
25	-221.65	-274.63	-24.68	-34.76
26	-68.47	68.47	-13.03	13.03
27	133.59	80.55	34.77	24.67
28	46.78	-46.79	8.01	-8.90
29	-156.59	-221.63	-13.53	-24.67
30	-82.45	82.45	-14.12	14.12
31	80.55	15.52	24.67	13.53
32	54.89	-54.89	8.63	-9.40
33	-70.54	-156.59	0.00	-13.53
34	-104.92	104.92	-16.50	16.50
35	15.52	-70.54	13.53	0.00
36	28.41	-37.21	0.00	-10.32

Table 2 Determinate Chair Lift Lattice Tower Model,
Corner Angle Forces

Note: Tension is Positive, Compression is Negative

	Corner Angle AE	Corner Angle BF	Corner Angle DH	Corner Angle CG
<u>Member</u>	<u>Force - lbs.</u>	<u>Force - lbs.</u>	<u>Force - lbs.</u>	<u>Force - lbs.</u>
a	-347.9	403.6	206.9	-544.7
b	-334.9	373.8	193.9	-514.9
c	-317.8	340.8	176.7	-481.9
d	-295.1	304.1	154.1	-445.2
e	-266.3	262.3	125.2	-402.4
f	-230.0	214.2	89.0	-355.3
g	-187.0	158.3	45.8	-299.3
h	-131.9	94.1	-9.2	-235.1
i	-57.0	15.5	-84.0	-156.6

Table 3 Experimental Strain Measurements,
Determinate Lattice Tower Model

External Load lbs.	Gage					
	Strain in micro inches/inch x 10 ⁻⁶					
	1	2	3	4	5	6
Windloads	-18	0	0	+29	0	0
Plus						
Chordload						
100	-158	-5	-65	+70	-7	-49
200	-306	-3	-132	+110	-11	-94
300	-458	0	-202	+149	-14	-138
400	-610	+1	-264	+185	-18	-180
Design Condition, Maximum Chordload and Windloads						
311	-460	0	-220	+155	-15	-148

Table 4 Theoretical and Experimental Member Stresses
for the Design Condition (Maximum Chordload
and Windloads), Determinate Lattice Tower Model

Plane	Member	Gage	Experimental Stress - psi	Predicted Stress-psi	Per cent Error
Corner	CGa	1	-13700.	-11400.	-16.8
ABEF	34	2 and 3	-3600.	-4850.	34.8
Corner	BFb	4	4620.	7820.	69.4
ABEF	26	5 and 6	-2600.	-3170.	21.9

inches for the other leg width in an angle length of 80 inches. This is a maximum deviation in leg width of 14 per cent. The diagonal members were to be $3/8(0.375) \times 3/8(0.375) \times 0.0299$ inches. Those supplied varied from 0.412 to 0.450 inches for one leg width and 0.381 to 0.435 for the other leg width in an angle length of 60 inches. This is a maximum deviation in leg width of 20 per cent. These deviations in the cross-section of the angle members would most certainly affect the stress distribution in the tower.

5.3.2 Indeterminate Lattice Tower Model

The indeterminate lattice tower model was constructed as shown in Figure 50. Actually, the determinate lattice tower built previously was used as the basis of this structure and only the redundant diagonal angles were added to each plane. The tower is square in cross-section and constructed of steel angle members bolted together. The overall dimensions of the tower are: a 12.25 inch square base, a 3.156 inch square top, and a height of 71.813 inches.

The angle members of the model were formed from mild steel sheet to the following dimensions:

Corner and Top Angles

Size = $17/32 \times 17/32 \times 0.0478$ inches

Cross-section area = 0.0485 inches²

All Diagonal and Cross Angles

Size = 3/8 x 3/8 x 0.0299 inches

Cross-section area = 0.0216 inches²

5.3.2.1 Mathematical Model of the Indeterminate Tower

The indeterminate tower is considered to be made up of four planar trusses with common edges. Thus any general load can be resolved into its three components which act on different faces of the tower. Section 5.3.1.1 develops this statement in greater detail for a determinate tower. The same assumptions are applicable here and will not be repeated. It was proven that the total force in any bar, due to a general load, can be obtained by the superposition of its three components.

Each of the tower planes is assumed to act as a true pin-jointed truss in which the members take little or no bending -- they transmit axial forces only.

5.3.2.2 Calculation of the Maximum Stress in the Indeterminate Tower Members

Figure 50 shows the indeterminate tower model with the chordload and windloads applied. These loads must be applied at the joints of the structure. From the previous discussion, (section 5.3.1.1), it is evident that

tower sides AB_{EF} and CD_{GH} are stressed only by the chordload and this is shared equally by each side. Similarly the windloads are carried only by the tower sides ACEG and BDFH, again, these loads are equally shared. Note that the vertical component of the chordload does not lie exactly in the plane of the tower side due to the longitudinal taper of the tower. Since this taper is small (approximately 3°) the effect of this component on the wind load planes is neglected. If the taper was greater, however, this approximation should not be made.

In section 5.3, the maximum model chordload was found to be 311 pounds acting downward at 25 degrees to the vertical centerline. Each plane AB_{EF} and CD_{GH} carries one-half of this, or 155.5 pounds. Also, in each side, this load is assumed to act as two concentrated loads applied at the two top joints. So the point load at each of these joints in planes AB_{EF} and CD_{GH} will be 77.75 pounds. The axial load in each member of these chordload planes is calculated using the digital computer program for the analysis of an indeterminate, pin-jointed, planar truss as detailed in Appendix B. The results of this calculation are summarized in Table 5.

The windloads applied to the indeterminate tower are assumed to be the same as those calculated for the

determinate tower (section 5.3.1.2). This is not really true since another diagonal member has been added to each frame, but it was decided to keep the load constant in order to compare the performance of the two types of lattice tower similarly loaded.

The axial load in each member of the windload planes is calculated using the digital computer program for the analysis of an indeterminate, pin-jointed, planar truss as detailed in Appendix B. The results of this calculation are summarized in Table 5.

It can be seen from Figure 50 that the corner angles are stressed by both the windload and chordload planes, being common to both. The total load in each member of the corner angles shown in Table 6 is obtained by algebraically adding the contribution of the windload and chordload planes. Each member of the corner angles is defined by a small letter of the alphabet as shown in Figure 50. For example, member "AEa" is the bottom member of angle AE. The force in AEa is obtained by adding the force in member 2 of plane ABEF and member 4 of plane ACEG, ($-355.0 = -443.4 + 88.4$).

5.3.2.3 Experimental Strain Measurements in the Indeterminate Tower Members

The indeterminate tower model was built from the determinate tower model by adding the redundant members

in each frame. These angle members were formed from cold rolled mild steel sheet, cut to length, and assembled to the corner angles with a single bolt holding each end of the member.

Strain gages were fixed to the following members:

(Refer to Figures 51 and 52 for member numbers)

- (1) Corner angle CG, member a.
- (2) Diagonal angle, member 35, plane AB EF - free leg.
- (3) Diagonal angle, member 35, plane AB EF - bolted leg.
- (4) Corner angle BF, member b.
- (5) Diagonal angle, member 27, plane AB EF - free leg.
- (6) Diagonal angle, member 27, plane AB EF - bolted leg.
- (7) Redundant diagonal angle, member 44, plane AB EF - bolted leg.
- (8) Redundant diagonal angle, member 44, plane AB EF - free leg.
- (9) Corner angle BF, member d.
- (10) Corner angle BF, member e.

The tower was fastened to a rigid base and loaded as shown in Figure 53. The windloads on the tower were simulated by hanging weights, (bags of sand and a block

of lead). The chordload is simulated by the force of an air cylinder, mounted such that it pulled at 25 degrees to the tower centerline.

The windloads were applied and strain readings taken. Then the chordload was applied in 100 pound increments up to 400 pounds. The average strain readings for these load increments are shown in Table 7. The strains were recorded for the design chordload of 311 pounds (see section 5.3), while the windloads were applied.

5.3.2.4 Evaluation of the Theoretical and Experimental Stresses in the Indeterminate Tower Model

Table 8 compares the predicted stress with the experimental stress in the tower members that were strain gaged. The theoretical and experimental stresses were calculated as outlined in section 5.3.1.4.

The assumption that loads applied parallel to the windload planes produce forces only in the members of those planes, has been proven experimentally for the indeterminate tower. Table 7 shows that member 35 (gages 2 and 3), member 27 (gages 5 and 6) and member 44 (gages 7 and 8) all of which are in the chordload plane AB \bar{E} F, were not affected by the application of the windloads.

The diagonal members in the indeterminate tower experience the same high bending stresses as those in the determinate tower. Even the redundant member

(number 44, gages 7 and 8), which was in tension, experienced rather large bending stresses. From Table 7 it is seen that the free leg of angle member 44 has a much lower strain reading than the bolted leg. The probable reasons for these considerable bending stresses are detailed in section 5.3.1.4.

Table 8 indicates that in general the predicted stresses are higher than the experimental stresses. Thus the indeterminate structure analysis gives stresses on the "safe" side of those actually encountered, which is good design procedure. The discrepancies between the predicted and experimental results would be due to the same causes given in section 5.3.1.4 for the determinate tower and need not be repeated here.

One additional source of error in the indeterminate case is the theoretical calculation of the corner angle forces. It was assumed that the planes on each side of the common corner angle act independantly, and the force in the corner angle members could be obtained by superposition. This is a valid assumption for the determinate tower, but not when the tower becomes indeterminate. The basic analysis of indeterminate structures assumes compatibility of deflections. That is, all members framing into a joint deflect in common to keep the joint intact. This assumption, used with "Hooke's Law" for linear structures

Table 5 Indeterminate Chair Lift Lattice Tower Model
Member Forces

Note: Tension is Positive, Compression is Negative

<u>Member</u>	<u>Chordload Planes ABEF and CDGH Force - Lbs.</u>	<u>Windload Planes ACEG and BDFH Force - Lbs.</u>
1	-19.85	-5.51
2	-443.37	-88.42
3	-24.31	-6.99
4	318.44	88.41
5	13.98	-0.83
6	-422.58	-78.03
7	-25.44	-6.99
8	296.16	78.42
9	13.15	-0.56
10	-397.03	-68.25
11	-28.17	-6.58
12	271.06	68.54
13	13.39	-0.52
14	-366.94	-58.74
15	-31.62	-6.39
16	241.65	59.00
17	13.66	-0.44
18	-331.34	-49.27
19	-35.67	-6.36
20	206.75	49.52
21	13.40	0.50
22	-289.61	-39.74
23	-39.74	-6.30
24	164.41	39.65
25	13.42	-0.47
26	-239.60	-29.62
27	-45.25	-6.64
28	115.58	29.82
29	14.05	0.31
30	-180.04	-19.04
31	-52.73	-7.14
32	57.11	19.17
33	15.34	-0.17
34	-101.53	-6.51
35	-67.13	-8.56
36	-15.47	7.02
37	4.78	-4.96

<u>Member</u>	<u>Chordload Planes ABEF and CDGH Force - Lbs.</u>	<u>Windload Planes ACEG and BDFH Force - Lbs.</u>
38	2.40	7.05
39	5.85	6.47
40	8.07	6.19
41	10.85	6.05
42	14.18	6.04
43	19.30	6.42
44	23.22	6.39
45	29.73	6.98
46	37.78	7.94

Table 6 Indeterminate Chair Lift Lattice Tower Model,
 Corner Angle Forces

Note: Tension is Positive, Compression is Negative.

Member	Corner Angle AE	Corner Angle BF	Corner Angle DH	Corner Angle CG
	Force - lbs.	Force - lbs.	Force - lbs.	Force - lbs.
a	-355.0	406.8	230.0	-531.8
b	-344.1	374.6	218.2	-500.6
c	-328.5	339.6	202.8	-465.3
d	-307.9	290.7	183.0	-425.6
e	-281.8	256.3	157.5	-380.6
f	-250.0	204.1	124.7	-329.3
g	-209.8	145.4	86.0	-269.2
h	-160.8	76.3	38.1	-199.0
i	- 94.5	-8.5	-22.0	-108.0

Table 7 Experimental Strain Measurements,
Indeterminate Lattice Tower Model

External Load lbs.	Gage									
	Strain in Microinches/inch x 10 ⁻⁶									
	1	2	3	4	5	6	7	8	9	10
Windloads Plus Chordload	- 20	0	0	+ 30	0	0	0	0	+ 20	+ 15
100	-150	0	- 40	+ 64	0	- 25	+22	+ 3	+ 45	+ 38
200	-305	- 5	-105	+100	-10	- 52	+47	+ 5	+ 70	+ 60
300	-460	- 8	-160	+138	-16	- 79	+70	+ 8	+ 98	+ 85
400	-620	-10	-212	+175	-21	-103	+89	+10	+127	+110
Design Condition, Maximum Chordload and Windloads										
311	-475	- 8	-166	+142	-17	- 82	+72	+ 9	+102	+ 89

Table 8 Comparison of Theoretical and Experimental
Member Stresses for the Design Condition
(Maximum Chordload and Windloads),
Indeterminate Lattice Tower Model

Plane	Member	Gage	Experimental Stress-PSI	Predicted Stress PSI	% Error
Corner	CGa	1	-14200.	-11000.	-22.5
ABEF	35	2 and 3	-2800.	-3100.	10.7
Corner	BFc	4	4240.	7710.	81.8
ABEF	27	5 and 6	-1560.	-2100.	34.6
ABEF	44	7 and 8	-1200.	-1073.	-10.6
Corner	BFd	9	3050.	3770.	22.1
Corner	BFe	10	2660.	3250.	22.2

provides the solution for the member forces. It is difficult to estimate the error introduced by ignoring the fact that the corner member deflections must be compatible to both planes. However, it is probably small enough to be neglected. Comparing Table 4 for the determinate tower and Table 8 for the indeterminate tower would indicate that this error is about the same magnitude as that introduced by the other assumptions used in setting up the analytical model.

5.3.3 Comparison of the Determinate and Indeterminate Lattice Tower Models

Some general conclusions can be drawn from a comparison of the determinate and indeterminate towers under identical loading conditions. Comparing the theoretical member forces, (Tables 1 and 5), and the experimental member forces, (Tables 4 and 8) for the two structures it is evident that:

- (1) There is little difference in the magnitude of the corner angle forces or stresses.
- (2) The diagonal and horizontal members transmit less force in the indeterminate structure than the corresponding members in the determinate tower. This is understandable since an extra member has been added to each frame of the determinate tower to make it

indeterminate, thus the load is shared
by more members.

5.4 Design of a Chair Lift Pipe Tower Model

The pipe tower model is constructed as shown in Figure 54, and consists of a steel tube, gussets and a base plate. The overall dimensions of the model are: a 3-inch outside diameter tube 0.120 inches thick, and a height of 72 inches from the base to the point of application of the chordload. These dimensions were scaled from a prototype tower 40 feet high constructed of 20 inch outside diameter pipe.

The length scale factor is chosen to be $K_L = 0.15$. So the model chordload is: $R_m = (0.15)^2 \times 13,280$
= 300 pounds.

The windload due to the ropes, passengers, chairs, and idler assemblies is: $W_m = (0.15)^2 (652 + 150) = 18.0$ pounds. The windload on the tower itself is a distributed load based on a projected area pressure of 6.15 pounds per square foot, see section 5.1.2. The tower windload is:

$$w_m = \frac{3}{12} \times 6.15 = 1.54 \text{ pounds per foot.}$$

The chordload on the model was simulated by the force of an air cylinder, mounted such that it pulled at 25 degrees to the tower centerline, (Figure 55). The tower windload was simulated by one foot lengths of steel bar

resting along the top side of the model. It was not possible to find a bar whose weight per foot was exactly 1.54. A series of 3/4 inch square bars, one foot long were used to simulate the windload. The weight per foot was 1.91. This deviation from exact modelling is not serious since the object of this study is to predict the theoretical stress behavior of a loaded structure and check this experimentally.

5.4.1 Calculation of the Theoretical Stresses in the Pipe Tower Model

The critical section of the tower, where the maximum stress will occur, is at the top of the gussets at the base. This section is 64.375 inches from the point of application of the chordload, (Figure 54). The theoretical stresses are calculated for three points (A, B and C), around the circumference of the pipe at the critically stressed section. The details of this calculation are given in Appendix C and summarized in Table 9.

5.4.2 Experimental Strain Measurements in the Pipe Tower Model

The pipe tower model was constructed as shown in Figure 54. Strain gages were attached to the pipe at a section 64.375 inches from the point of application of the chordload. The gages were placed as follows:

- (1) In the x direction at point A.
- (2) In the x direction at point B.
- (3) In the x direction at point C.
- (4) In the y direction at point C.
- (5) At 45 degrees to gages (3) and (4) at point C.

The tower was fastened to a rigid base and loaded as shown in Figure 55. The windload on the tower was simulated by foot lengths of 3/4 inch square steel stock laid end to end along the length of the tower. The windload on the tower due to the rope, chairs, passengers and idler assemblies was simulated by a block of lead. The chordload was modelled by the force on an air cylinder.

The windloads were applied and strain readings taken. Then the chordload was applied in 100 pound increments up to 400 pounds. The average strain readings for these load increments are shown in Table 10.

5.4.3 Evaluation of the Theoretical and Experimental Stresses in the Pipe Tower Model

Table 11 compares the predicted stress with the experimental stress in the pipe tower model at the design condition, (maximum chordload and windloads). The theoretical stress is taken from Table 9. The experimental stress is obtained by multiplying the strain readings from Table 10 by the modulus of elasticity for steel, taken as 29.9×10^6 pounds per square inch. The principal stresses at

point C were calculated from the experimental strain readings of the rectangular gage rosette placed at point C. The theory of strain gage rosette analysis is covered in reference G17. With reference to Figure 54, the principal stresses at point C are calculated from the equation:

$$S_{1,2} = E \left[\frac{\epsilon_4 + \epsilon_3}{2(1-\mu)} \pm \sqrt{(\epsilon_4 + \epsilon_3)^2 + (2\epsilon_5 - \epsilon_4 - \epsilon_3)^2} \right]$$

where ϵ = strain in microinches/inch,

μ = Poissons' ratio,

= 0.287 for steel,

E = modulus of elasticity,

= 29.9×10^6 for steel.

It can be seen from Table 11 that the error in prediction of stresses for the pipe tower is small. This was expected since the pipe is a smooth symmetrical section. No major welding was required to fabricate the tower and thus distort the stress pattern. Some small error would be attributed to the deflection of the top of the tower under load. This introduces an additional moment on the structure due to the eccentricity of the axial component of the chordload. The top of the tower deflected 0.83 inches due to a chordload of 300 pounds.

Table 9 Theoretical Stresses
in the Pipe Tower Model

<u>Position</u>	<u>x-Direction</u>	Stress in PSI	
		<u>Principal Stresses</u>	
		<u>S₁</u>	<u>S₂</u>
A	-11100.		
B	10600.		
C		21.	-1791.

Table 10 Experimental Strain Measurements
in the Pipe Tower Model

<u>Load</u> <u>lbs.</u>	Strain in Microinches/inch x 10 ⁻⁶				
	<u>Position A</u>	<u>Position B</u>	<u>Position C</u>		
	<u>Gage 1</u> <u>x</u> <u>Direction</u>	<u>Gage 2</u> <u>y</u> <u>Direction</u>	<u>Gage 3</u> <u>x</u> <u>Direction</u>	<u>Gage 4</u> <u>y</u> <u>Direction</u>	<u>Gage 5</u> <u>45° to</u> <u>x and y</u>
Windloads	0	0	-45	+10	-25
Plus					
100	-130	+115	-48	+10	-34
200	-260	+233	-50	+10	-41
Design Load					
300	-395	+350	-52	+14	-49
400	-520	+461	-53	+20	-55

Table 11
Comparison of Theoretical and Experimental Stresses
 in the Pipe Tower Model for the Design Loading

<u>Position and Direction</u>	<u>Stress in PSI</u>		
	<u>Predicted</u>	<u>Experimental</u>	<u>% Error</u>
A, x Direction	-11100.	-11800.	- 5.9
B, x Direction	10600.	10570.	0.3
C, Prin. Stress S_1	21.	26.1	-19.0
C, Prin. Stress S_2	-1791.	-1650.	8.5

The largest error occurs in the correlation of experimental and theoretical stresses at point C. When attaching the strain gage rosette to the tower, it was quite difficult to ensure that gage 5 was oriented at 45 degrees to gages 3 and 4. These gages are small and hard to handle. Any deviation in the position of gage 5 would introduce some error in calculating the experimental principal stresses at point C.

5.5 Design of a Chair Lift Hexagonal Tower Model

The hexagonal tower model is constructed as shown in Figure 56. The structure is fabricated from cold rolled mild steel sheet 0.0598 inches thick, bent and welded to form the hexagonal section and tapered base. The overall dimensions of the model are: a 3-5/16 inch hexagonal section (across flats), and a height of 72 inches from the base plate to the point of application of the chordload. These dimensions were scaled from a prototype tower 40 feet high with a hexagonal section of 22 inches (across flats).

The external loads on the model are the same as those used on the pipe tower model (see section 5.4).

That is:

the chordload $R_m = 300$ pounds,

the windload on the ropes, chairs, passengers

and idler assemblies

$$W_m = 18.0 \text{ pounds,}$$

the tower windload

$$w_m = 1.91 \text{ pounds per foot.}$$

5.5.1 Calculation of the Theoretical Stresses in the Hexagonal Tower Model

The critical section of the tower, where the maximum stress will occur, is in the hexagonal section just above the top of the flared base. This section is 62 inches from the point of application of the chordload, (Figure 56). The theoretical stresses are calculated for three points (A, B and C) around the periphery of the hexagonal section at the critically stressed section. The details of this calculation are given in Appendix D and summarized in Table 12.

5.5.2 Experimental Strain Measurements in the Hexagonal Tower Model

The hexagonal tower was constructed as shown in Figure 56. Strain gages were attached to the tower at a section 62 inches from the point of application of the chordload. The gages were placed as follows:

- (1) In the x direction at point A.
- (2) In the x direction at point B.
- (3) In the y direction at point C.

(4) In the x direction at point C.

(5) At 45 degrees to gages (3) and (4) at point C.

The tower was fastened to a rigid base and loaded as shown in Figure 55. The windload on the tower was simulated by foot lengths of 3/4 inch square steel stock laid end to end along the length of the tower. The windload on the tower due to the rope, chairs, passengers and idler assemblies was simulated by a block of lead. The chordload was modelled by the force on an air cylinder.

The windloads were applied and strain readings taken. Then the chordload was applied in 100 pound increments up to 400 pounds. The average strain readings for these load increments are shown in Table 13.

5.5.3 Evaluation of the Theoretical and Experimental Stresses in the Hexagonal Tower Model

Table 14 compares the predicted stress with the experimental stress in the hexagonal tower model at the design condition, (maximum chordload and windloads). The theoretical stress is taken from Table 12. The experimental stress is obtained by multiplying the strain readings from Table 13 by the modulus of elasticity for steel, taken as 29.9×10^6 pounds per square inch. The principal stresses at point C were calculated from the experimental strain readings of the rectangular gage rosette placed at point C. The theory of strain gage rosette analysis is covered in

reference G17. Referring to Figure 54, the principal stresses at point C are calculated from the equation:

$$S_{1,2} = E \left[\frac{\epsilon_1 + \epsilon_3}{2(1-\mu)} \pm \sqrt{(\epsilon_1 + \epsilon_3)^2 + (2\epsilon_5 - \epsilon_1 - \epsilon_3)^2} \right]$$

where ϵ = strain in microinches/inch,

μ = Poissons' ratio,

= 0.287 for steel,

E = modulus of elasticity,

= 19.9×10^6 for steel.

Examination of Table 14 shows a somewhat greater error in predicting the stresses in a hexagonal tower than was the case with the pipe tower, (Table 11). There will be some error in the results predicted by the elastic theory used, but this should be small. The major portion of the difference between the predicted and experimental stresses must be allotted to the deviation of the tower model from a true hexagonal shape. The hexagonal portion of the tower was constructed of two parts, each bent longitudinally to form one-half of the hexagon shape. These halves were joined together with a longitudinal weld. The tapered hexagonal base was attached with a peripheral weld. Here again, as with the lattice tower, the parts supplied for the construction of the model

deviated significantly from the design drawings; and lack of time dictated their use. Typical dimensional discrepancies in the hexagonal cross-section were of the order of 13.2 per cent.

The welding of the parts to make the assembly caused even more distortion in the cross-section. It is evident from the non-linear behavior of gages 3, 4 and 5 under load (see Table 13), that some significant residual stresses had been set up in the tower by welding. These residual stresses would be relieved or redistributed as the external load was applied.

In general, however, the maximum stresses occurring at points A and B have been predicted with reasonable accuracy considering the distorted hexagonal cross-section used. This indicates to a certain extent the reliability of the theoretical analysis.

Table 12 Theoretical Stresses
in the Hexagonal Tower Model

Position	Stress in PSI		
	x-Direction	Principal Stresses	
		S ₁	S ₂
A	-15226.		
B	14414.		
C		57.	-2873.

Table 13 Experimental Strain Measurements
in the Hexagonal Tower Model

Load lbs.	Strain in Microinches/inch x 10 ⁻⁶				
	Position A	Position B	Position C		
	Gage 1 x Direction	Gage 2 y Direction	Gage 3 y Direction	Gage 4 x Direction	Gage 5 45° to x and y
Windloads	0	0	-30	-39	-30
Plus					
100	-155	200	-5	-32	-28
200	-320	402	-20	-31	-25
Design Load					
300	-475	598	60	-30	-10
400	-628	800	105	-30	+10

Table 14
 Comparison of Theoretical and Experimental Stresses
 in the Hexagonal Tower Model
 for the Design Loading

<u>Position and Direction</u>	<u>Stress in PSI</u>		
	<u>Predicted</u>	<u>Experimental</u>	<u>% Error</u>
A, x Direction	-15226.	-14200.	7.2
B, x Direction	14414.	17900.	-19.5
C, Prin. Stress S_1	57.	2650.	-75.0
C, Prin. Stress S_2	-2873.	470.	700.0

6. The Engineering of a Chair Lift Installation

The chair lift manufacturer uses the same basic structural elements (bottom terminal, intermediate towers, and top terminal), for a wide range of applications. The lift may be used as a sight-seeing attraction, carrying people horizontally above the ground over some route; or in a ski area transporting skiers to the top of the slope. The basic difference in most installations is the ground profile of the lift line -- the roughness, the length, and the vertical rise. Thus, once the structural elements have been designed for the maximum expected loading condition in all applications; the engineering of a chair lift installation consists of placing the intermediate support towers on the lift line. There are a number of factors that must be considered when choosing the location of these towers; such as: economy, the maximum allowable sag between towers, and the maximum and minimum allowable breakover or breakunder angles.

The economical factor is easily expressed as follows: the cost of a chair lift is directly proportional to the number of towers used to support the rope. Sharp sales competition in this field dictates the efficient use of these structures by the ropeway engineer. The ideal profile in a ski lift installation, would be

that closely approximating the hyperbolic shape in which the rope hangs. In this case only two support towers would be needed, one at each end of the lift line, to guide the rope as it enters the terminals. The rope sag would just be matched by the dip in the ground contour, thus keeping the clearance above ground constant. This ideal situation almost never occurs.

The maximum allowable rope sag is usually governed by the ground profile in the span. If it is convex, the towers must be close together to minimize the sag and maintain good rope clearance from the ground. In some applications, ski trails cross the lift line. Here, the towers must be placed such that the rope sag does not become excessive. It is good practice^{E27} to keep the clearance from the skiers' feet (hanging below the chair), to the highest expected snow profile, a minimum of 8.2 feet (2.5 meters).

Towers are usually located at the major breaks in the lift line profile. The towers are positioned on a scale drawing of the profile. A straight line drawn between the idler assemblies of adjacent towers will indicate whether the breakover or breakunder angle is excessive. The maximum allowable angle for a four sheave idler assembly is 18 degrees^{E27}. It is sometimes necessary to

provide a number of towers to divide the breakover angle up into acceptable increments, (Figure 40).

6.1 Location of the Chair Lift Intermediate Towers

The method of locating the intermediate towers is essentially an iterative one. The usual procedure is as follows:

(1) Figure 60 shows a typical ski area chair lift profile. Initially the towers are positioned at the major breaks or changes in the profile. Some judgement and experience is required in this step. The towers are drawn to scale on the profile and the idler assemblies of adjacent towers joined by straight lines. Measurement of the breakover or breakunder angles ϕ will indicate whether the maximum limit has been exceeded. If so, the towers must be shifted to decrease the angle, or more towers added to share it.

(2) Since the rope is counterweighted at the top terminal, the rope tension is known at this point. For a 1-1/8 inch diameter rope, this tension is about 21,000 pounds, (see section 5.1.1). The weight of rope, chairs and passengers is known and is assumed to be a uniform load distributed along the rope. For a loaded chair, the distributed weight per foot of rope is 12.03 pounds per foot. Thus, knowing the tension at the tower B, (see

Figure 60), the weight per foot of the rope, and the rise and run between towers A and B, the rope tension at tower A can be calculated. The maximum rope sag from the chordline, (a straight line between idler assemblies), can also be found. This procedure is repeated for the next span downhill where the tension in the upper tower A has been found by the previous calculation. When all spans have been examined, the maximum sag is drawn to scale on the profile drawing and clearances measured.

(3) If the rope sag in any span exceeds an allowable limit (section 6), the towers must be moved to reduce this excess. Once towers are moved, the whole procedure, from step (1), must be repeated.

(4) Finally, a check must be made to see that in the case of a hold-down tower (tower C, Figure 60), the maximum fully loaded sag between the towers adjacent to it (A and D) is not such that the rope sags below the idler assembly. A minimum pressure on the idler assemblies is necessary for positive control of the rope.

6.2 Sag and Tension Calculations for a Chair Lift Rope

The most time consuming part of engineering a chair lift installation is the calculation of the maximum sag of the rope between towers. The sag between towers and the rope tension at the tower locations must be checked for

two cases:

(1) the chairs fully loaded with passengers.

This condition gives the maximum sag between towers.

(2) the chairs empty. This condition gives the maximum tension of the rope at the towers.

The theory governing the behavior of a hanging rope is detailed in Appendix E. It can be seen that slide rule calculation of the sag and tension in the rope from these equations is a formidable job, made more tedious by the fact that the calculations are so repetitious. This is the type of problem that can be handled so well by digital computation.

A digital computer program has been devised to solve for the sag and tension in a hanging cable, (see Appendix E). Information fed to the computer consists of the rise and run between two adjacent towers, the weight per foot of the rope, passengers and chairs, and the tension at the uphill end of the span. The program prints out the maximum sag (half-way between the towers), the tension at the lower tower, and the angle at which the rope enters the idler assemblies measured from the chordline between them. This information is assembled in tabular form (see Table 15).

The engineer can thus start at the top of the lift, where the tension is known, and using the sag and tension

tables, quickly work down the profile. The tension at the lower tower of the previous span serves as the input tension for the span under consideration.

The author has had some experience in making these calculations by slide rule, and recently using the tables on actual lift installations. It is estimated that the tables cut three to four hours of engineering time per lift from the former method. Where a number of installations are to be examined, the savings in time and money should be significant. There are other advantages to using the tables. Once their use is understood, this type of analysis can be handled by a draftsman or technician. More important, the computer makes no calculation errors -- assuming that it has initially received the correct information to form the tables.

7. Conclusion

In the preceding pages, the structural analysis of a number of types of chair lift intermediate tower has been examined. The design of the structure to withstand the external loads is only one portion of an overall analysis. A study and comparison of the vibration characteristics of each type is another important part. Also, any recommendation of the applicability of one type or another to specific installations should include a study of fabricating costs and aesthetic appeal. For some installations, one manufacturer may prefer a welded fabrication, another a bolted lattice tower. The former probably would have a very efficient welding shop. More attention should be devoted to the eye appeal of a tower for a sight-seeing chair lift than need be the case for a ski lift.

In summation, it might be said of the methods used to design each type of tower, that the predicted stress is generally on the high or "safe side" of those stresses actually encountered in the structures. The prediction error tended to be higher with the lattice towers than with the pipe or fabricated towers. However, the results obtained give some confidence in the method of attack used.

The sag and tension tables developed in section 6 should be helpful to the ropeway engineer. With the increasing availability of the digital computer for analysis, the obvious extension to these charts is to have the computer automatically place the towers in the most efficient location. This problem is similar to the economical positioning of hydro transmission towers, which has been successfully programmed for computer solution.

APPENDIX A

Digital Computer Program
for the Analysis of a Determinate, Pin-Jointed,
Planar Truss

APPENDIX A

Digital Computer Program for the Analysis of a Determinate, Pin-Jointed, Planar Truss

This program has been adapted from an IBM Library computer program as detailed in reference G15.

A.1 Description of Program

The program solves a statically determinate, pin-connected, planar truss for the support reactions and the axial force in each member. The method of equilibrium at a joint is used to find these forces. Reactions of the truss are found by the three equations of static equilibrium.

The user must check the truss beforehand to see that it is statically determinate both internally and externally. The criterion for static determinacy is: the number of members plus 3, equals 2 times the number of joints. There are exceptions to this rule.

The maximum number of members and joints allowable is dictated by the storage capacity of the computer used. The dimension statement given in the example following may easily be expanded. The program provides for a maximum of 8 members connected at one joint.

All members and joints of the truss must be identified by numbers. A random numbering system may be used in numbering the joints and members with the exception of joints 1 and 2. These joint numbers must be assigned to the two truss supports. Joint 1 is the roller support and joint 2 the hinge support. The truss support joints 1 and 2 must not be in a vertical line. To remedy this situation, it is suggested the truss be rotated 90° , thus reversing the joint co-ordinates and loads. The X and Y co-ordinates of all joints must be known in addition to the number of members framing into each joint. The truss must be oriented so that all joints are in the first quadrant of the rectangular co-ordinate system, (all co-ordinates must be either zero or positive -- not negative). The truss may be loaded at any joint, but these loads must be defined by their vertical and horizontal components.

A.2 Method of Solution

The method used in solving for the reactions, and the member forces is outlined below:

(1) Initially the program solves for horizontal and vertical reactions at the supports. The program sums the horizontal and vertical external loads and takes moments about joint number 2. The horizontal reaction component at joint 1 is defined by the slope

of the roller support. This slope is entered into the program by means of an input variable "SLOPE", given in degrees. If the reaction at the joint is vertical, SLOPE is zero. A SLOPE of 90 degrees is not permitted.

(2) Axial forces in the truss members are found by the method of equilibrium at a joint. Joints are examined in numerical order. Each member connected to a particular joint is examined to determine if the force in that member is known. If the force is known, the horizontal and vertical components of this force are added to the summation of horizontal and vertical forces at the joint. If the force is unknown, the member number is stored as a member whose force is unknown.

(3) After all members connected to the joint have been examined, the number of members with unknown forces is determined. If there is only one member with an unknown vertical component of force, the summation of vertical forces at that joint is used as the vertical component of force for that member. The program calls the subroutine VCOMP and solves for the horizontal component and the member force.

(4) After the force in the member has been computed, or if there is more than one member with unknown vertical force components, a test is made to

determine if there is more than one member with unknown horizontal force components. If only one member has an unknown horizontal force component, the summation of horizontal forces, (including any horizontal load at the joint), is taken as the horizontal component of force in the member. The program calls the subroutine HCOMP, which solves for the vertical component and the member force.

(5) If it is found that there are only two members with unknown horizontal and vertical components of force at a joint, the program branches to a routine that solves for the vertical components of the two members simultaneously, using the principles of static equilibrium at a joint. Having solved for the vertical components, the horizontal components and member forces are then calculated.

(6) After a member force has been computed, or if there are too many unknown forces at the joint, the joint number is indexed by one and the procedure repeated for the next joint until the axial force in all members has been found. Tension forces are given a positive sign, and compression forces a negative sign.

(7) If a member is found to carry no load, it is assigned an arbitrarily small value (0.1 E-20), so the program will recognize the member has been solved and will

not print statement 111. This value is lost by truncation when involved with the calculation of other members carrying a significant force.

(8) When the program calls one of the subroutines, VCOMP or HCOMP, and solves for the vertical or horizontal components of members at a joint; then on return to the main program, the vertical or horizontal component of the external load is set equal to $1.0 \text{ E-}10$. When both $PV(J)$ and $PH(J) = 1.0 \text{ E-}10$ at a joint, their product will be $1.0 \text{ E-}20$ and statement 61 will recognize the joint as having been fully solved. Note that the program assigns these values to the external loads at each joint as it is completely solved, even if there are no real external loads applied there.

(9) Lastly, the program calls the subroutine LENGTH which calculates the length of each member from its end co-ordinates.

A.3 Program Error Messages

A number of error messages have been included in the program and are explained as follows:

(1) SOLUTION INCOMPLETE, CHECK MEMBERS WITH ZERO FORCE. This indicates the program has made $JN/2$ cycles without solving the complete truss. The program will give the member forces calculated up to that point.

Members with zero force may not have been solved and should be investigated. In general, compound and complex trusses cannot be solved by the method of joints, although some can be solved by isolating secondary trusses.

(2) REACTIONS INDETERMINATE. This occurs when the truss support joints 1 and 2 are vertically in line. This arrangement is not allowed and the truss should be rotated 90° .

A.4 Definition of Variables and Fortran Names

V(M)	Vertical component of force in member M.
H(M)	Horizontal component of force in member M.
S(M)	Total force in member M.
SV	Sum of the vertical force components at a joint.
SH	Sum of the horizontal force components at a joint.
SPV	Sum of the vertical external loads.
SPH	Sum of the horizontal external loads.
SMV	Sum of the moments about joint 1 due to the vertical loads.
SMH	Sum of the moments about joint 1 due to the horizontal loads.
V1, V2	Vertical reactions at joints 1 and 2.
H1, H2	Horizontal reactions at joints 1 and 2.
R1, R2	Resultant reactions at joints 1 and 2.
J	Joint number.

JN Total number of joints.

M Member number.

MN Total number of members.

K Index to count the number of members framing into a joint.

NJ,N(J) Total number of members framing into a joint.

LV Number of members with an unknown vertical force component at a joint.

LH Number of members with an unknown horizontal force component at a joint.

JA,JB Joints at each end of the member being investigated.

J1,J2 Joints at each end of member M.

MUV(LV) Index used to choose the member at the joint being investigated with the unknown vertical force component.

MUH(LH) Index used to choose the member at the joint being investigated with the unknown horizontal force component.

LIMIT Maximum number of cycles allowed for a complete solution. This is one-half the number of joints ($JN/2$).

SL Computed member length.

D1,D2 Slopes of two members with unknown vertical components framing into a joint.

X(J) Horizontal co-ordinate of joint J.

Y(J) Vertical co-ordinate of joint J.

SLOPE Slope in degrees of the joint 1 roller support.
PV(J) External vertical load component at joint J.
PH(J) External horizontal load component at joint J.

A.5 Data Input Instructions

In setting up the problem for computer analysis, it should be noted that the sign convention follows the rectangular co-ordinate system. Vertical loads and reactions acting upward are considered positive. Horizontal loads and reactions acting to the right are considered positive. Tension forces are positive and compression forces are negative. Any units of length and force may be used, the common practice being length in feet and load in kips.

The following defines the order of input cards:

Fortran Statement Cards

- (1) Problem Title Card -- This is a Hollerith Statement defining the title of the program. It is statement number 102 and must be entered in the main program under the heading Output Formats.

Data Cards

- (2) Header Card - Format (I4, I4, F10.3)
JN Total number of joints.

MN Total number of members.
SLOPE Slope of joint 1 roller support
 expressed in degrees from the
 horizontal.

(3) Joint Cards - Format (I4, F10.2, F10.2)

N(J) Number of members framing into
 joint J.
X(J) Horizontal co-ordinate of joint J.
Y(J) Vertical co-ordinate of joint J.

Note: The joint cards must be arranged in
 the same order as the joints were
 numbered.

(4) Member Cards - Format (I4, I4)

J1(M) Joint number at one end of member M.
J2(M) Joint number at other end of member M.

Note: The member cards must be arranged in the
 same order as the members were numbered.
 It does not matter which end of the
 member is assigned to J1 or J2.

(5) Load Cards - Format (I4), Format (F10.2, F10.2)

The method of identifying the external loads with
their appropriate joints is that the first card
is punched with the joint number and the next
card is punched with the load components PV(J)
and PH(J) at that joint. No special order is

necessary but each joint and its load must be together as detailed above. The end card must be a joint card punched with a 0, (zero). This card tells the computer it has read all the external loads.

A.6 Sample Problem

Figure 58 shows a determinate truss, which will be used as an example to show how the program is applied.

Sample Problem Input:

Fortran Statement Cards

(1) Problem Title Card

```
102 Format (1X, 43H Sample Problem, Determinate
Truss Analysis)
```

Data Cards

(2) Header Card

```
JN      MN      SLOPE
  8      13      0.000
```

(3) Joint Cards

Joint	N(J)	X	Y
1	4	40	0
2	2	80	0
3	2	0	30
4	3	20	30
5	4	20	15
6	4	40	15
7	3	60	0
8	4	60	15

(4) Member Cards

Member	J1	J2
1	2	7
2	2	8
3	7	8
4	1	7
5	1	8
6	6	8
7	1	6
8	1	5
9	5	6
10	4	6
11	4	5
12	3	5
13	3	4

(5) Load Cards

J	PV(J)	PH(J)
7	15	0
8	0	20
3	-60	-80
0		

```

C   STATICALLY DETERMINATE PIN JOINTED PLANE TRUSS ANALYSIS
    DIMENSION N(25), X(25), Y(25), PV(25), PH(25), V(40), H(40), S(40)
    1   , J1(40), J2(40), MUV(8), MUH(8)
    READ 201, JN, MN, SLOPE
C   READ IN JOINT COORDINATES
    1 DO 2 J= 1,JN
    2 READ 202, N(J), X(J), Y(J)
    DO 3 M= 1,MN
    3 READ 201, J1(M), J2(M)
C   READ IN EXTERNAL LOADS
    6 READ 203, J
    IF (J.EQ.0) GO TO 4
    READ 204, PV(J), PH(J)
    GO TO 6
    4 CONTINUE
C   CALCULATE REACTIONS
    IF (X(1) - X(2)) 13, 96, 13
    96 PRINT 113
    GO TO 99
    13 DO 9 J= 3,JN
    9 SMV= SMV - PV(J)*(X(2) - X(J))
    DO 10 J= 3,JN
    10 SMH= SMH + PH(J)*(Y(2) - Y(J))
    V1= -(SMV + SMH)/(X(1) - X(2))
    SLOPE= SLOPE/57.2957
    H1= V1*(SIN(SLOPE)/COS(SLOPE))
    DO 11 J= 1,JN
    11 SPV= SPV + PV(J)
    DO 12 J= 1,JN
    12 SPH= SPH + PH(J)
    V2= -SPV - V1
    H2= -SPH - H1
C   ADD HORIZONTAL REACTIONS TO EXTERNAL FORCES AT JOINTS 1 AND 2
    PH(1)= PH(1) + H1
    PH(2)= PH(2) + H2
C   ADD VERTICAL REACTIONS TO EXTERNAL FORCES AT JOINTS 1 AND 2
    PV(1)= PV(1) + V1
    PV(2)= PV(2) + V2
    R1= SQRT((ABS(V1))**2. + (ABS(H1))**2.)
    R2= SQRT((ABS(V2))**2. + (ABS(H2))**2.)
C   CALCULATE MEMBER FORCES
    LIMIT= JN/2
    DO 64 I= 1,LIMIT
    J= 1
    GO TO 61
    14 M= 1
C   K COUNTS THE NUMBER OF MEMBERS EXAMINED AT A JOINT
    K= 1
    SV= 0.
    SH= 0.
    LV= 0

```

```

      LH= 0
      NJ= N(J)
      DO 15 L= 1,NJ
      MUV(L)= 0
15    MUH(L)= 0
C     CHECK TO SEE IF J IS AT J1(M) OR J2(M). IF IT IS NOT, SCAN MEMBERS
C     TO FIND ONE THAT IS.
16    IF (J1(M) - J) 17, 20, 17
17    IF (J2(M) - J) 18, 19, 18
18    M= M+1
      GO TO 16
19    JA= J2(M)
      J2(M)= J1(M)
      J1(M)= JA
20    JA= J1(M)
C     FIND SUM OF KNOWN VERTICAL COMPONENTS AT A JOINT
      JB= J2(M)
      IF (V(M)) 21, 24, 21
21    IF (Y(JA) - Y(JB)) 23, 23, 22
22    SV= SV - V(M)
      GO TO 27
23    SV= SV + V(M)
      GO TO 27
24    IF (Y(JA) - Y(JB)) 26, 25, 26
25    V(M)= 0.1E-20
      GO TO 27
26    LV= LV + 1
      MUV(LV)= M
C     FIND SUM OF KNOWN HORIZONTAL COMPONENTS AT A JOINT
27    IF (H(M)) 28, 31, 28
28    IF (X(JA) - X(JB)) 30, 30, 29
29    SH= SH - H(M)
      GO TO 34
30    SH= SH + H(M)
      GO TO 34
31    IF (X(JA) - X(JB)) 33, 32, 33
32    H(M)= 0.1E-20
      GO TO 34
33    LH= LH + 1
      MUH(LH)= M
C     CHECK TO SEE IF ALL MEMBERS AT A JOINT HAVE BEEN EXAMINLD
34    IF (K - N(J)) 35, 39, 99
35    K= K + 1
      GO TO 18
39    IF (LV - 1) 49, 40, 70
40    M= MUV(1)
      JA= J1(M)
      JB= J2(M)
      V(M)= -(SV + PV(J))
      CALL VCOMP (V, H, S, X, Y, JA, JB, M)

```

```

      IF (Y(JA) - Y(JB)) 120, 99, 120
120 CONTINUE
      PV(J)= 1.0E-10
C      PV(J)= 1.0E-10 IS A TAG USED TO INDICATE THAT ALL VERTICAL
C      COMPONENTS AT JOINT J HAVE BEEN SOLVED
      49 IF (LH - 1) 60, 50, 60
      50 M= MUH(1)
          JA= J1(M)
          JB= J2(M)
          H(M)= -(SH + PH(J))
          CALL HCOMP (V, H, S, X, Y, JA, JB, M)
          IF (X(JA) - X(JB)) 123, 99, 123
123 CONTINUE
      PH(J)= 1.0E-10
C      INDEX TO NEXT JOINT
      60 J= J+1
          IF (J-JN) 61, 61, 62
C      STATEMENT 61 INDICATES IF WE HAVE SOLVED FOR ALL THE VERTICAL AND
C      HORIZONTAL COMPONENTS AT JOINT J
      61 IF (PV(J)*PH(J) - 1.0E-20) 14, 60, 14
C      ALL JOINTS ARE ANALYZED TO SEE IF ALL MEMBERS ARE SOLVED
      62 DO 63 M= 1,MN
          IF (S(M)) 63,64, 63
      63 CONTINUE
          GO TO 80
      64 CONTINUE
          I= I-1
          PRINT 111
          GO TO 80
C      SOLUTION OF TWO UNKNOWN MEMBERS AT A JOINT
      70 IF (LV-2) 99, 71, 49
      71 IF (LH-2) 49, 72, 60
      72 IF (MUV(1) - MUH(1)) 60, 73, 60
      73 IF (MUV(2) - MUH(2)) 60, 74, 60
      74 SV= SV + PV(J)
          SH= SH + PH(J)
          M1= MUV(1)
          M2= MUV(2)
          JA= J1(M1)
          JB= J2(M1)
          D1= (X(JA) - X(JB))/(Y(JA) - Y(JB))
          JA= J1(M2)
          JB= J2(M2)
          D2= (X(JA) - X(JB))/(Y(JA) - Y(JB))
          IF (D2 - D1) 76, 60, 76
      76 V(M2)= (SV*D1 - SH)/(D2 - D1)
          V(M1)= -(SV + V(M2))
          M= M1
          JA= J1(M1)
          JB= J2(M1)
          CALL VCOMP (V, H, S, X, Y, JA, JB, M)

```

```

      IF (Y(JA) - Y(JB)) 121, 99, 121
121 CONTINUE
      PV(J)= 1.0E-10
      M= M2
      JA= J1(M2)
      JB= J2(M2)
      CALL VCOMP (V, H, S, X, Y, JA, JB, M)
      IF (Y(JA) - Y(JB)) 122, 99, 122
122 CONTINUE
      PH(J)= 1.0E-10
      GO TO 60
C     PRINT OUTPUT
      80 PRINT 101
      PRINT 102
      PRINT 103
      PRINT 104, V1, V2
      PRINT 105, H1, H2
      PRINT 106, R1, R2
      PRINT 107
      DO 81 M= 1,MN
      CALL LENGTH (S, X, Y, JA, JB, M, J1, J2, SL)
      81 PRINT 108, M, SL, S(M)
      99 PRINT 112, I
C     INPUT FORMATS
      201 FORMAT (I4, I4, F10.3)
      202 FORMAT (I4, F10.2, F10.2)
      203 FORMAT (I4)
      204 FORMAT (F10.2, F10.2)
C     OUTPUT FORMATS
      101 FORMAT (/1X, 27H DETERMINATE TRUSS ANALYSIS )
      102 FORMAT (1X, 44H SAMPLE PROBLEM - DETERMINATE TRUSS ANALYSIS )
      103 FORMAT (//1X, 9HREACTIONS, 10X, 7HJOINT 1, 7X, 7HJOINT 2 )
      104 FORMAT (2X, 8HVERTICAL, F16.2, F14.2)
      105 FORMAT (2X, 10HHORIZONTAL, F14.2, F14.2)
      106 FORMAT (2X, 9HRESULTANT, F15.2, F14.2)
      107 FORMAT (/1X, 6HMEMBER, 6X, 6HLENGTH, 4X, 12HMEMBER FORCE )
      108 FORMAT (I4, F14.2, F14.2)
      111 FORMAT (1X, 48HSOLUTION INCOMPLETE, CHECK MEMBERS WITH 0 FORCE )
      112 FORMAT (1X, 15HNO. OF CYCLES =, I3 )
      113 FORMAT (1X, 23HREACTIONS INDETERMINATE )
      END
$IBFTC VCOMP
C     SUBROUTINE FOR THE SOLUTION OF MEMBER FORCE WHEN VERTICAL
C     COMPONENT IS KNOWN
      SUBROUTINE VCOMP (V, H, S, X, Y, JA, JB, M)
      DIMENSION V(40), H(40), S(40), Y(25), X(25)
      IF (V(M)) 502, 501, 502
      501 V(M)= 0.1E-20
      H(M)= 0.1E-20
      S(M)= 0.1E-20

```

```

      RETURN
502 IF (Y(JA) - Y(JB)) 504, 505, 503
503 V(M)= -V(M)
504 H(M)= V(M)*ABS((X(JA) - X(JB))/(Y(JA) - Y(JB))) + 0.1E-20
      S(M)= V(M)*SQRT((ABS(H(M)/V(M)))**2. + 1.)
505 RETURN
      END
$IBFTC HCOMP
C      SUBROUTINE FOR THE SOLUTION OF MEMBER FORCE WHEN HORIZONTAL
C      COMPONENT IS KNOWN.
      SUBROUTINE HCOMP (V, H, S, X, Y, JA, JB, M)
      DIMENSION V(40), H(40), Y(25), X(25), S(40)
      IF (H(M)) 512, 511, 512
511 H(M)= 0.1E-20
      V(M)= 0.1E-20
      S(M)= 0.1E-20
      RETURN
512 IF (X(JA) - X(JB)) 514, 515, 513
513 H(M)= -H(M)
514 V(M)= H(M)*ABS((Y(JA) - Y(JB))/(X(JA) - X(JB))) + 0.1E-20
      S(M)= H(M)*SQRT((ABS(V(M)/H(M)))**2. + 1.)
515 RETURN
      END
$IBFTC LENGTH
C      SUBROUTINE FOR THE SOLUTION OF MEMBER LENGTH
      SUBROUTINE LENGTH (S, X, Y, JA, JB, M, J1, J2, SL)
      DIMENSION S(40), X(25), Y(25), J1(40), J2(40)
      JA= J1(M)
      JB= J2(M)
      SL= SQRT((ABS(Y(JA) - Y(JB))**2.) + (ABS(X(JA) - X(JB))**2.))
      RETURN
      END

```

INPUT DATA

\$ENTRY

```

      8 13      0.000
      4      40.      0.
      2      80.      0.
      2      0.      30.
      3      20.      30.
      4      20.      15.
      4      40.      15.
      3      60.      00.
      4      60.      15.
      2      7
      2      8

```

7	8		
1	7		
1	8		
6	8		
1	6		
1	5		
5	6		
4	6		
4	5		
3	5		
3	4		
7			
	15.00	00.00	
8			
	00.00	20.00	
3			
	-60.00	-80.00	
0			

\$IBSYS

COMPUTER OUTPUT

DETERMINATE TRUSS ANALYSIS
 SAMPLE PROBLEM - DETERMINATE TRUSS ANALYSIS

REACTIONS	JØINT 1	JØINT 2
VERTICAL	165.00	-120.00
HØRIZØNTAL	0.00	60.00
RESULTANT	165.00	134.16

MEMBER	LENGTH	MEMBER FØRCE
1	20.00	-100.00
2	25.00	200.00
3	15.00	-15.00
4	20.00	-100.00
5	25.00	-175.00
6	20.00	320.00
7	15.00	120.00
8	25.00	-300.00
9	20.00	160.00
10	25.00	200.00
11	15.00	-120.00
12	25.00	-100.00
13	20.00	160.00

NØ. ØF CYCLES = 3

A.7 Computer Analysis of a Determinate Lattice Chair Lift Tower Model

The forces in the determinate tower members due to the external loads, (see section 5.3.1.2) are found using the preceding computer program. Each plane of the determinate tower is prepared for computer analysis as shown in Figures 47 and 48. Note that the chordload on each plane must be divided into its two components:

$$\begin{aligned} PV(19) = PV(20) &= -\frac{R}{4} \cos 25^\circ = -\frac{311}{4} \cos 25^\circ \\ &= -70.40 \text{ pounds,} \end{aligned}$$

$$\begin{aligned} \text{and } PH(19) = PH(20) &= \frac{R}{4} \sin 25^\circ = \frac{311}{4} \sin 25^\circ \\ &= 32.81 \text{ pounds.} \end{aligned}$$

The data input and computer output for each plane of the tower is given in the following pages. Each plane must be examined separately since the diagonal members in the two chordload or windload planes are in opposite directions.

INPUT DATA

102 FORMAT (/IX, 64H CHAIR LIFT LATTICE TOWER MODEL - PLANE AB EF ANALY
 1S1S //)

\$ENTRY

20	36	3.5736	
1		0.0000	0.0000
2		12.2500	0.0000
4		0.7767	12.4375
4		11.4733	12.4375
4		1.4773	23.6560
4		10.7727	23.6560
4		2.0920	33.5000
4		10.1580	33.5000
4		2.6385	42.2500
4		9.6115	42.2500
4		3.1204	49.9690
4		9.1296	49.9690
4		3.5478	56.8130
4		8.7022	56.8130
4		3.9118	62.6410
4		8.3382	62.6410
4		4.2386	67.8750
4		8.0114	67.8750
3		4.5470	72.8130
2		7.7030	72.8130
2	4		
2	3		
1	3		
3	4		
4	6		
4	5		
3	5		
5	6		
6	8		
6	7		
5	7		
7	8		
8	10		
8	9		
7	9		
9	10		
10	12		
10	11		
9	11		
11	12		
12	14		
12	13		

11	13		
13	14		
14	16		
14	15		
13	15		
15	16		
16	18		
16	17		
15	17		
17	18		
18	20		
18	19		
17	19		
19	20		
19			
	-70.40	32.81	
20			
	-70.40	32.81	
0			

\$IBSYS

COMPUTER OUTPUT

DETERMINATE TRUSS ANALYSIS

CHAIR LIFT LATTICE TOWER MODEL - PLANE ABEF ANALYSIS

REACTIONS	JØINT 1	JØINT 2
VERTICAL	-319.64	460.44
HØRIZØNTAL	-19.96	-45.66
RESULTANT	320.26	462.70

MEMBER	LENGTH	MEMBER FORCE
1	12.46	-441.64
2	16.92	-26.74
3	12.46	320.28
4	10.70	19.36
5	11.24	-418.24
6	15.03	-31.29
7	11.24	300.59
8	9.30	22.28
9	9.86	-390.99
10	13.12	-36.25
11	9.86	277.18
12	8.07	25.67
13	8.77	-358.72
14	11.54	-42.47
15	8.77	249.94
16	6.97	29.70
17	7.73	-320.49
18	10.09	-49.86
19	7.73	217.67
20	6.01	34.47
21	6.86	-274.64
22	8.83	-59.05
23	6.86	179.43
24	5.15	40.18
25	5.84	-221.65
26	7.54	-68.47
27	5.84	133.59
28	4.43	46.78
29	5.24	-156.59
30	6.65	-82.45
31	5.24	80.55
32	3.77	54.89
33	4.95	-70.54
34	6.03	-104.92
35	4.95	15.52
36	3.16	28.41

NØ. ØF CYCLES = 7

INPUT DATA

102 FORMAT (/1X, 64H CHAIR LIFT LATTICE TOWER MODEL - PLANE CDGH ANALY
 1SIS //)

\$ENTRY

20	36	-3.5736	
1	12.2500	0.0000	
2	0.0000	0.0000	
4	0.7767	12.4375	
4	11.4733	12.4375	
4	1.4773	23.6560	
4	10.7727	23.6560	
4	2.0920	33.5000	
4	10.1580	33.5000	
4	2.6385	42.2500	
4	9.6115	42.2500	
4	3.1204	49.9690	
4	9.1296	49.9690	
4	3.5478	56.8130	
4	8.7022	56.8130	
4	3.9118	62.6410	
4	8.3382	62.6410	
4	4.2386	67.8750	
4	8.0114	67.8750	
2	4.5470	72.8130	
3	7.7030	72.8130	
1	4		
2	4		
2	3		
3	4		
4	6		
3	6		
3	5		
5	6		
6	8		
5	8		
5	7		
7	8		
8	10		
7	10		
7	9		
9	10		
10	12		
9	12		
9	11		
11	12		
12	14		
11	14		

11	13		
13	14		
14	16		
13	16		
13	15		
15	16		
16	18		
15	18		
15	17		
17	18		
18	20		
17	20		
17	19		
19	20		
19			
	-70.40	32.81	
20			
	-70.40	32.81	
0			
\$IBSYS			

COMPUTER OUTPUT

DETERMINATE TRUSS ANALYSIS

CHAIR LIFT LATTICE TOWER MODEL - PLANE CDGH ANALYSIS

REACTIONS	JØINT 1	JØINT 2
VERTICAL	460.44	-319.64
HØRIZØNTAL	-28.76	-36.80
RESULTANT	461.34	321.76

MEMBER	LENGTH	MEMBER FORCE
1	12.46	-461.37
2	16.92	26.74
3	12.46	300.57
4	10.70	-19.36
5	11.24	-441.67
6	15.03	31.29
7	11.24	277.16
8	9.30	-22.28
9	9.86	-418.27
10	13.12	36.25
11	9.86	249.92
12	8.07	-25.67
13	8.77	-391.02
14	11.54	42.47
15	8.77	217.65
16	6.97	-29.70
17	7.73	-358.75
18	10.09	49.86
19	7.73	179.42
20	6.01	-34.47
21	6.86	-320.48
22	8.83	59.05
23	6.86	133.55
24	5.15	-40.18
25	5.84	-274.63
26	7.54	68.47
27	5.84	80.55
28	4.43	-46.79
29	5.24	-221.63
30	6.65	82.45
31	5.24	15.52
32	3.77	-54.89
33	4.95	-156.59
34	6.03	104.92
35	4.95	-70.54
36	3.16	-37.21

NØ. ØF CYCLES = 9

INPUT DATA

102 FORMAT (/1X, 64H CHAIR LIFT LATTICE TOWER MODEL - PLANE ACEG ANALY
 1SIS //)

\$ENTRY

20	36	3.5736	
1		0.0000	0.0000
2		12.2500	0.0000
4		0.7767	12.4375
4		11.4733	12.4375
4		1.4773	23.6560
4		10.7727	23.6560
4		2.0920	33.5000
4		10.1580	33.5000
4		2.6385	42.2500
4		9.6115	42.2500
4		3.1204	49.9690
4		9.1296	49.9690
4		3.5478	56.8130
4		8.7022	56.8130
4		3.9118	62.6410
4		8.3382	62.6410
4		4.2386	67.8750
4		8.0114	67.8750
3		4.5470	72.8130
2		7.7030	72.8130
2	4		
2	3		
1	3		
3	4		
4	6		
4	5		
3	5		
5	6		
6	8		
6	7		
5	7		
7	8		
8	10		
8	9		
7	9		
9	10		
10	12		
10	11		
9	11		
11	12		
12	14		
12	13		

11 13
13 14
14 16
14 15
13 15
15 16
16 18
16 17
15 17
17 18
18 20
18 19
17 19
19 20

3

0.00 1.89

5

0.00 1.74

7

0.00 1.52

9

0.00 1.31

11

0.00 1.15

13

0.00 1.01

15

0.00 0.89

17

0.00 0.77

19

0.00 10.32

0

\$IBSYS

COMPUTER OUTPUT

DETERMINATE TRUSS ANALYSIS

CHAIR LIFT LATTICE TOWER MODEL - PLANE ACEG ANALYSIS

REACTIONS	JØINT 1	JØINT 2
VERTICAL	-93.49	93.49
HØRIZENTAL	-5.84	-14.76
RESULTANT	93.67	94.65

MEMBER	LENGTH	MEMBER FORCE
1	12.46	-83.27
2	16.92	-14.12
3	12.46	93.68
4	10.70	8.33
5	11.24	-73.20
6	15.03	-13.46
7	11.24	83.28
8	9.30	7.84
9	9.86	-63.61
10	13.12	-12.77
11	9.86	73.21
12	8.07	7.52
13	8.77	-54.16
14	11.54	-12.44
15	8.77	63.62
16	6.97	7.39
17	7.73	-44.64
18	10.09	-12.40
19	7.73	54.16
20	6.01	7.43
21	6.86	-34.77
22	8.83	-12.72
23	6.86	44.65
24	5.15	7.65
25	5.84	-24.68
26	7.54	-13.03
27	5.84	34.77
28	4.43	8.01
29	5.24	-13.53
30	6.65	-14.12
31	5.24	24.67
32	3.77	8.63
33	4.95	0.00
34	6.03	-16.50
35	4.95	13.53
36	3.16	0.00

NØ. ØF CYCLES = 7

INPUT DATA

102 FORMAT (/1X, 64H CHAIR LIFT LATTICE TOWER MODEL - PLANE BDFH ANALY
 1SIS //)

\$ENTRY

20	36	-3.5736	
1		12.2500	0.0000
2		0.0000	0.0000
4		0.7767	12.4375
4		11.4733	12.4375
4		1.4773	23.6560
4		10.7727	23.6560
4		2.0920	33.5000
4		10.1580	33.5000
4		2.6385	42.2500
4		9.6115	42.2500
4		3.1204	49.9690
4		9.1296	49.9690
4		3.5478	56.8130
4		8.7022	56.8130
4		3.9118	62.6410
4		8.3382	62.6410
4		4.2386	67.8750
4		8.0114	67.8750
2		4.5470	72.8130
3		7.7030	72.8130
1	4		
2	4		
2	3		
3	4		
4	6		
3	6		
3	5		
5	6		
6	8		
5	8		
5	7		
7	8		
8	10		
7	10		
7	9		
9	10		
10	12		
9	12		
9	11		
11	12		
12	14		
11	14		

11 13
13 14
14 16
13 16
13 15
15 16
16 18
15 18
15 17
17 18
18 20
17 20
17 19
19 20

3	0.00	1.89
5	0.00	1.74
7	0.00	1.52
9	0.00	1.31
11	0.00	1.15
13	0.00	1.01
15	0.00	0.89
17	0.00	0.77
19	0.00	10.32

0
\$IBSYS

COMPUTER OUTPUT

DETERMINATE TRUSS ANALYSIS

CHAIR LIFT LATTICE TOWER MODEL - PLANE BDFH ANALYSIS

REACTIONS	JØINT 1	JØINT 2
VERTICAL	93.49	-93.49
HØRIZØNTAL	-5.84	-14.76
RESULTANT	93.67	94.65

MEMBER	LENGTH	MEMBER FORCE
1	12.46	-93.68
2	16.92	14.12
3	12.46	83.27
4	10.70	-10.22
5	11.24	-83.28
6	15.03	13.46
7	11.24	73.20
8	9.30	-9.58
9	9.86	-73.21
10	13.12	12.77
11	9.86	63.61
12	8.07	-9.04
13	8.77	-63.62
14	11.54	12.44
15	8.77	54.16
16	6.97	-8.70
17	7.73	-54.16
18	10.09	12.40
19	7.73	44.64
20	6.01	-8.58
21	6.86	-44.64
22	8.83	12.72
23	6.86	34.76
24	5.15	-8.66
25	5.84	-34.76
26	7.54	13.03
27	5.84	24.67
28	4.43	-8.90
29	5.24	-24.67
30	6.65	14.12
31	5.24	13.53
32	3.77	-9.40
33	4.95	-13.53
34	6.03	16.50
35	4.95	0.00
36	3.16	-10.32

NØ. ØF CYCLES = 9

APPENDIX B

Digital Computer Program for the Analysis
of an Indeterminate, Pin-Jointed, Planar Truss

APPENDIX B

Digital Computer Program for the Analysis of an Indeterminate, Pin-Jointed, Planar Truss

B.1 Description of the Program

The program solves a statically indeterminate, pin-connected, planar truss for the axial force in each member. The indeterminacy must be due to the presence of internal redundant members, not redundant supports. The truss must have determinate supports.

The flexibility matrix method is used to calculate the force in the redundant members and the method of superposition is used to calculate the force in the remaining members.

The flexibility and superposition methods are dealt with in detail in reference G13. Similar developments appear in references G3, G4, G6, G8 and G11, however, these do not use the matrix approach. In these latter texts this analysis is sometimes called the force method. A brief description of the flexibility matrix method is given here to help clarify the program.

The traditional force method of solving an indeterminate structure consists of transforming the

structure into a statically determinate form called the primary structure. This is done by cutting the internal member forces that make the structure indeterminate. These forces are called redundants, and are not required for truss stability. The deformations in the primary structure due to two separate loading conditions, are found. These loading conditions are: (1) the external loads, (2) the loads imposed by the redundant members.

The deformations at the cut in the redundant members due to loading conditions (1) and (2) must be compatible. These compatibility conditions are "n" in number, thereby giving "n" equations which can be solved for the "n" unknown redundant forces.

Figure 59a shows an indeterminate loaded truss. This truss is indeterminate to degree two since one member from each of the center panels can be removed without affecting the stability of the truss. The redundant members are chosen to be numbers 14 and 15.

Figure 59b shows the same truss with the redundant members cut to give the statically determinate primary structure. The redundant forces are labelled X_{14} and X_{15} , and are calculated by the following matrix equation:

$$X_n = -[\beta^T \phi \beta]^{-1} \cdot [\beta^T \phi \alpha] \cdot q \quad \text{--- (a)}$$

where:

β is the redundant force matrix obtained by applying

1 pound axial tension loads in place of each of the redundant members in turn. Each column of this matrix consists of the member forces in the primary determinate structure caused by these unit redundant forces.

β^T is the transposed Beta matrix. The transpose matrix β^T of the Beta matrix is developed by interchanging the rows and the columns of the Beta matrix.

ϕ is the force deformation matrix. This is made up of the influence coefficients ϕ_{ij} ; where ϕ_{ij} is the deformation at joint "i" caused by a unit force at joint j. For a truss,

$$\phi_{ij} = \left[\frac{L_m}{A_m E} \right] \quad \text{—————(b)}$$

where "A" is the member cross-section area, "L" is the member length, and "E" is the modulus of elasticity of the member.

α is the load force matrix. Each column of the matrix is made up of the member forces in the primary determinate structure caused by a unit load acting in the same direction and point of application as the external loads.

q is the external load matrix. This is a column matrix. The member forces (P_n) are then calculated from the

matrix equation:

$$P_n = \alpha q + \beta X_n \quad \text{————— (c)}$$

The program generates the Alpha, Beta and Phi matrices and combines them according to the above matrix equations to solve for the member forces.

The user must check the truss beforehand to see that it is externally determinate. The support reactions must be obtainable from the equations of statics alone.

The maximum number of members and joints allowable is dictated by the storage capacity of the computer used. The dimension statement given in the example following may be easily expanded. The program provides for a maximum of 8 members connected at one joint.

All members and joints of the truss must be identified by numbers. A random numbering system may be used in numbering the joints with the exception of joints 1 and 2. These joint numbers must be assigned to the two truss supports. Joint 1 is the roller support and joint 2 the hinge support. The truss support joints 1 and 2 must not be in a vertical line. To remedy this situation, it is suggested the truss be rotated 90°, thus reversing the joint co-ordinates and loads. The X and Y co-ordinates of all joints must be known in addition to the number of members framing into each joint. The truss must be oriented so that all joints are in the first quadrant of

the rectangular co-ordinate system, (all co-ordinates must be either zero or positive -- not negative).

The redundant members must be numbered last. Only after all the members of the primary structure have been assigned numbers can the redundant members be numbered. The redundant members may then be numbered at random.

The truss may be loaded at any joint, but these loads must be defined by their vertical and horizontal components.

B.2 Method of Solution

The method used in solving for the member forces is outlined below:

(1) The program first solves for the length of each member from its end co-ordinates.

(2) The Alpha matrix is calculated next. Each joint is scanned in turn to see if there is an external load applied. When a joint is found that carries an external load, the program first checks to see if the load has a vertical component. If so, this vertical component is transferred into a working array where it will be the only load. The magnitude of the vertical component is then normalized, (given a value of unity). The program calls the subroutine DTRUSS, (see Appendix A), which

solves for the member forces in the primary structure due to this unit external load. These member forces form one column of the Alpha matrix.

If the joint also has a horizontal load component, the working array is cleared and the horizontal component entered and normalized. Again, the subroutine DTRUSS is called and the member forces of the primary structure form another column of the Alpha matrix.

This procedure continues until all joints have been examined, the working array being cleared each time. Thus the Alpha matrix will have "MN" rows and "NP" columns. Where "MN" is the total number of members -- including redundant members, and "NP" is the total number of external load components. Note that the member forces in the cut redundant members will be entered as zero at the end of each column of the matrix.

(3) The Beta matrix is formed next. Data is supplied to the program which details the vertical and horizontal components of the unit redundant member load. The program chooses each redundant member in turn, picks out the joint at each end of the member, and transfers the redundant load components at these joints into a working array. Subroutine DTRUSS is then called, and the primary structure member forces due to each redundant load are

calculated.

This procedure continues until all the redundant members have been examined, the working array having been cleared each time. Thus the Beta matrix will have "MN" rows and "NX" columns, where "MN" is the total number of members including redundant members, and "NX" is the number of redundant members. Note that the member force in the cut redundant member being examined will be entered as 1.0 in the appropriate place in each column of the Beta matrix. All other redundant member forces will be zero in that column.

(4) The matrix multiplication $[\beta^T \Phi \beta]$ is performed next. Here, the sparseness of the Phi matrix is used to advantage since this matrix has only the main diagonal terms. Examining equations (a) and (b) we see that the common term "E", (the modulus of elasticity), cancels out in equation (a). Thus one can consider the Phi matrix to be:

$$\Phi_{ij} = [L_m/A_m] \quad \text{--- (d)}$$

The first term of equation (a) is obtained in the following manner:

$$[\beta^T \Phi \beta]_{ij} = \sum_{m=1}^{MN} [\beta_{mi}^T \frac{L_m}{A_m} \beta_{mj}] \quad \text{--- (e)}$$

The program generates only the diagonal and the terms to one side of the diagonal. The $[\beta^T \Phi \beta]$ matrix is of size "NX" by "NX" where "NX" is the number

of redundant members. Since the matrix is a symmetric one:

$$[\beta^T \Phi \beta]_{ij} = [\beta^T \Phi \beta]_{ji} \quad \text{for } i \neq j.$$

The first term of equation (a) is then inverted by calling the MINVSE subroutine. This is a "built in" subroutine of the McMaster Computer.

(5) Next, the program generates the product $[\beta^T \Phi \alpha]$. The $[\beta^T \Phi \alpha]$ matrix has "NX" rows and "NP" columns; where "NX" is the number of redundant members and "NP" is the number of external load components.

The second term of equation (a) is obtained as follows:

$$[\beta^T \Phi \alpha]_{ij} = \sum_{m=1}^{MN} \left[\beta_{mi} \frac{L_m}{A_m} \alpha_{mj} \right] \quad \text{--- (f)}$$

(6) The two terms of equation (a) are then multiplied together and stored in a working matrix.

(7) The external load components are numbered consecutively and the redundant forces calculated by multiplying the above working matrix by the external load component array.

(8) The member forces of the indeterminate structure are then calculated using equation (c). Tension forces are given a positive sign, and compression forces a negative sign.

(9) An error statement, "MATRIX DID NOT INVERT", is incorporated in the main program. This statement, if printed, means the BTPHIB matrix was not successfully

inverted. This indicates probable trouble with either the Beta or Phi matrix.

B.3 Subroutine DTRUSS

This subroutine solves for a statically determinate, pin-jointed, planar truss. The method of solution is covered in detail in Appendix A and will not be repeated here. Some minor differences occur in the subroutine used here and the program in Appendix A. This is primarily because the program is used as a subroutine and called a number of times, and thus must clear itself of all previous calculation.

Since the same indicies and variables are used in the main program, and in the subroutine, some false arrays are used so the main program will not be affected by changes in these quantities in the subroutine.

The subroutine has error statements as outlined in section A.3, Appendix A. The user should ensure the primary truss is statically determinate both externally and internally to avoid print out of these error statements.

B.4 The Choice of Redundants^{G13}

As stated in section B.1, the only restriction on the choice of redundants is that they must not be members necessary for stability. However, some choices are better

than others because of the effects of numerical errors due to round-off and truncation. In general, the best choice of redundants is that which results in the matrix $\beta^T \Phi \beta$ having dominant diagonal terms. It is usually possible to select the redundants so this will be achieved.

A diagonal element of any flexibility matrix represents the displacement at point "i" produced by a unit load at point "i". To obtain diagonal terms of the $\beta^T \Phi \beta$ matrix, (the redundant flexibility matrix), which are much larger than the nondiagonal terms, the redundants should be selected so they cause their largest displacements at their point of application. This gives a "well-conditioned" matrix.

B.5 Definition of Variables and Fortran Names

(1) Main Program

NX	Number of redundant members.
NP	Total number of external load components.
RV(J)	Unit redundant force vertical component.
RH(J)	Unit redundant force horizontal component.
AREA(M)	Cross-section area of the truss members.
JJ, MN	Total number of members including redundant members.
K	An index used to correctly place the columns

of the Alpha and Beta matrices.

WV(L) Working array used to choose one external vertical load component at a time.

WH(L) Working array used to choose one external horizontal load component at a time.

ALPHA(I,K) A matrix giving the member forces in the primary structure due to each external load component.

II The first redundant member number.

UV(J) Working array used to choose the unit redundant horizontal load component imposed by each redundant member in turn.

BETA(I,K) A matrix giving the member forces in the primary structure due to each unit redundant force.

BTPHIB(I,J) A matrix developed by the multiplication of the Beta transposed matrix by the Phi matrix by the Beta matrix.

IND An indicator used in the subroutine MINVSE.

NI A storage matrix for the subroutine MINVSE.

TEM A storage matrix for the subroutine MINVSE.

BTPHIA(I,J) A matrix developed by the multiplication of the Beta transposed matrix by the Phi matrix by the Alpha matrix.

TM(I,J) A matrix developed by the multiplication

of BTPHIB by BTPHIA.

- XX(I) An array of the redundant forces.
- Q(L) Working array used to number the external load components consecutively.
- P(I) Member forces of the indeterminate truss.

(2) Subroutine DTRUSS

The variables have the same definition as outlined in section A.3, Appendix A, with the following added:

- NN(J) An array used to transfer the array N(J) into the subroutine so as not to affect the main program values.
- XA(J) An array used to transfer the array X(J) into the subroutine so as not to affect the main program values.
- YA(J) An array used to transfer the array Y(J) into the subroutine so as not to affect the main program values.
- LJ1(M) An array used to transfer the array J1(M) into the subroutine so as not to affect the main program values.
- LJ2(M) An array used to transfer the array J2(M) into the subroutine so as not to affect the main program values.

B.6 Data Input Instructions

In setting up a problem for computer analysis, it should be noted that the sign convention follows the rectangular co-ordinate system. Vertical loads acting upwards are considered positive. Horizontal loads acting to the right are considered positive. Tension forces are positive and compression forces are negative. Any units of length and force may be used, the common practice being length in feet and load in kips.

The following defines the order of input cards:

Fortran Statement Cards

- (1) Problem Title Card -- This is a Hollerith Statement defining the title of the program. It is statement number 603 and must be entered in the main program under the heading "Output Formats".

Data Cards

- (2) Header Card - Format (I4, I4, F10.3)
- | | |
|-------|---|
| JN | total number of joints. |
| MN | total number of members including redundant members. |
| SLOPE | Slope of joint 1 roller support expressed in degrees from the horizontal. |
- (3) Joint Cards - Format (I4, F10.2, F10.2)
- | | |
|------|---|
| N(J) | Number of members framing into joint J, excluding the redundant members. These values |
|------|---|

are read from the primary structure.

X(J) Horizontal co-ordinate of joint J.

Y(J) Vertical co-ordinate of joint J.

Note: The joint cards must be arranged in the same order as the joints were numbered.

(4) Member Cards - Format (I4, I4)

J1(M Joint number at one end of member M.

J2(M) Joint number at other end of member M.

Note: The member cards must be arranged in the same order as the members were numbered. The member cards include the redundant members. It does not matter which end of the member is assigned to J1 or J2.

(5) Load Cards - Format (I4), Format (F10.2, F10.2)

The method of identifying the external loads with their appropriate joints is that the first card is punched with the joint number and the next card is punched with the load components PV(J) and PH(J) at that joint. No special order is necessary but each joint and its load must be together as detailed above. The end card must be a joint card punched with a 0, (zero). This card tells the computer it has read all the external loads.

(6) Indeterminate Index Card - Format (I4, I4)

NX Number of redundant members.

NP Total number of external load components.

- (7) Unit Redundant Load Components - Format (I4), Format (2F10.4)

The redundant load components are found by calculating the slope of the redundant member and taking the sine and cosine of this angle. The method of identifying these components with their appropriate joints is that the first card is punched with the joint number and the next card is punched with the load components RV(J) and RH(J) at that joint. No special order is necessary but each joint and its load must be together as detailed above. The end card must be a joint card punched with a 0 (zero). This card tells the computer it has read all the redundant loads.

- (8) Area Cards - Format (F10.4)

A(M) The member cross-section area. These cards should be arranged in the same sequence as the members have been numbered. For convenience, the units of area used are square inches. It does not matter that these units are not the same as those used to measure the joint coordinates since the units cancel in the multiplication of equation (a).

B.7 Sample Problem

Figure 59(a) shows an indeterminate truss which will be used as an example to show how the program is applied. The redundant members are chosen to be the diagonal from each of the center panels. Consequently these are given the last member numbers 14 and 15.

Figure 59(b) shows the redundant members cut and the unit redundant load components applied.

Sample Problem Input:

Fortran Statement Cards

(1) Problem Title Card

```
603 Format (/1X, 50H Sample Problem, Indeterminate
          Truss Analysis /)
```

Data Cards

(2) Header Card

JN	MN	SLOPE
8	15	0.000

(3) Joint Cards

Joint	N(J)	X	Y
1	2	64.00	0.00
2	2	0.00	0.00
3	4	16.00	20.00
4	4	32.00	0.00
5	4	32.00	20.00
6	4	48.00	0.00
7	3	48.00	20.00
8	3	16.00	0.00

(4) Member Cards

Member	J1	J2
1	2	8
2	2	3
3	8	4
4	8	3
5	3	4
6	3	5
7	4	6
8	4	5
9	5	6
10	5	7
11	6	1
12	6	7
13	1	7
14	5	8
15	4	7

(5) Load Cards

J	PV(J)	PH(J)
8		
4	-10.00	0.00
6	-10.00	0.00
0	-10.00	0.00

(6) Indeterminate Index Cards

NX	NP
2	3

(7) Unit Redundant Load Components

J	RV(J)	RH(J)
8	0.7809	0.6247
5	-0.7809	-0.6247
4	0.7809	0.6247
7	-0.7809	-0.6247
0		

(8) Area Cards

Member	Area
1	1.0000
2	1.0000
3	1.0000
4	1.0000
5	1.0000
6	1.0000
7	1.0000
8	1.0000
9	1.0000
10	1.0000
11	1.0000
12	1.0000
13	1.0000
14	1.0000
15	1.0000

```

C      STATICALLY INDETERMINATE PIN JOINTED PLANE TRUSS ANALYSIS
      DIMENSION N(25), X(25), Y(25), PV(25), PH(25), WV(25), WH(25),
1     S(60), J1(60), J2(60), ALPHA(50, 15), ELL(60), UV(25), UH(25),
2     BETA(50,15), RV(25), RH(25), BTPHIA(10,10), BTPHIB(10,10),
3     TM(10,10), XX(10), AREA(60), TEM(10), NI(40), Q(60), P(60)
      READ 201, JN, MN, SLOPE
C      READ IN JOINT COORDINATES
1     DO 2 J= 1,JN
2     READ 202, N(J), X(J), Y(J)
      DO 3 M= 1,MN
3     READ 201, J1(M), J2(M)
C      READ IN EXTERNAL LOADS
6     READ 203, J
      IF (J.EQ.0) GO TO 4
      READ 204, PV(J), PH(J)
      GO TO 6
4     CONTINUE
C      READ IN DEGREE OF INDETERMINACY AND NO. OF EXTERNAL LOADS
      READ 300, NX, NP
C      READ IN UNIT LOAD COMPONENTS IMPOSED BY INDETERMINATE MEMBERS
316    READ 203, J
      IF (J.EQ.0) GO TO 317
      READ 205, RV(J), RH(J)
      GO TO 316
317    CONTINUE
C      READ IN MEMBER AREA
      DO 40 M= 1,MN
40     READ 206, AREA(M)
C      CALCULATE MEMBER LENGTH
      DO 310 M= 1,MN
      JA= J1(M)
      JB= J2(M)
310    ELL(M)= SQRT((ABS(Y(JA) - Y(JB))**2.) + (ABS(X(JA) - X(JB))**2.))
      PRINT 307
      PRINT 603
      PRINT 311
      DO 312 M= 1,MN
312    PRINT 313, M, ELL(M)
      MN= MN - NX
C      CALCULATION OF THE ALPHA MATRIX
      K= 1
      DO 303 J= 1,JN
      DO 601 L= 1,JN
C      WH(J) AND WV(J) ARE WORKING ARRAYS USED TO CHOOSE ONE EXTERNAL
C      LOAD COMPONENT PER CYCLE
      WV(L)= 0.
601    WH(L)= 0.
      WV(J)= PV(J)
      IF (WV(J)) 302, 301, 315
302    WV(J)= -1.0

```

```

      GO TO 339
315 WV(J)= +1.0
339 DO 340 I= 1,MN
340 S(I)= 0.
      CALL DTRUSS (JN, MN, SLOPE, N, X, Y, J1, J2, WV, WH, S)
      JJ= MN + NX
      DO 304 I= 1,JJ
304 ALPHA(I,K)= S(I)
      K= K + 1
301 DO 602 L= 1,JN
      WV(L)= 0.
602 WH(L)= 0.
      WH(J)= PH(J)
      IF (WH(J)) 305, 303, 314
305 WH(J)= -1.0
      GO TO 341
314 WH(J)= +1.0
341 DO 342 I= 1,MN
342 S(I)= 0.
      CALL DTRUSS (JN, MN, SLOPE, N, X, Y, J1, J2, WV, WH, S)
      JJ= MN + NX
      DO 306 I= 1,JJ
306 ALPHA(I,K)= S(I)
      K= K + 1
303 CONTINUE
C   CALCULATION OF THE BETA MATRIX
      K= 1
      II= MN + 1
      JJ= MN + NX
      DO 318 M= II,JJ
      DO 600 L= 1,JN
C   UV(L) AND UH(L) ARE WORKING ARRAYS USED TO CHOOSE THE UNIT
C   REDUNDANT LOADS IMPOSED BY EACH REDUNDANT MEMBER IN TURN
      UV(L)= 0.
600 UH(L)= 0.
      DO 343 I= 1,JJ
343 S(I)= 0.
      J= J1(M)
      UV(J)= RV(J)
      UH(J)= RH(J)
      J= J2(M)
      UV(J)= RV(J)
      UH(J)= RH(J)
      CALL DTRUSS (JN, MN, SLOPE, N, X, Y, J1, J2, UV, UH, S)
      DO 319 I= 1,JJ
319 BETA(I,K)= S(I)
      I= M
      BETA(I,K)= 1.0
318 K= K + 1
C   CALCULATION OF THE INVERSE OF THE BTPHIE MATRIX

```

```

      MN= 1/N + NX
      DO 320 I= 1,NX
      DO 320 J= 1,NX
      BTPHIB(I,J)= 0.
      IF (I-J) 321, 321, 322
322 BTPHIB(I,J)= BTPHIB(J,I)
      GO TO 320
321 DO 320 M= 1,MN
      BTPHIB(I,J)= BTPHIB(I,J) + BETA(M,I)*BETA(M,J)*ELL(M)/AREA(M)
320 CONTINUE
      CALL MINVSE (BTPHIB, 10, NX, 1.0E-30, IND, NI, TEM)
      IF (IND.NE.0) GO TO 335
C     CALCULATION OF THE BTPHIA MATRIX
      DO 323 I= 1,NX
      DO 323 J= 1,NP
      BTPHIA(I,J)= 0.
      DO 323 M= 1,MN
323 BTPHIA(I,J)= BTPHIA(I,J) + BETA(M,I)*ALPHA(M,J)*ELL(M)/AREA(M)
C     CALCULATION OF BTPHIA MULT. BY INVERSE BTPHIB= TM(I,J)
      DO 324 I= 1,NX
      DO 324 J= 1,NP
      TM(I,J)= 0.
      DO 324 K= 1,NX
324 TM(I,J)= TM(I,J) + BTPHIB(I,K)*BTPHIA(K,J)
C     CALCULATION OF THE REDUNDANT FORCES XX(I)
      L= 1
      DO 326, J= 1,JN
      IF (PV(J)) 327, 328, 327
C     Q(L) IS A WORKING ARRAY USED TO NUMBER THE EXTERNAL LOAD
C     COMPONENTS CONSEQUITIVELY
327 Q(L)= ABS(PV(J))
      L= L + 1
328 IF (PH(J)) 329, 326, 329
329 Q(L)= ABS(PH(J))
      L= L + 1
326 CONTINUE
      DO 325 I= 1,NX
      XX(I)= 0.
      DO 325 J= 1,NP
325 XX(I)= XX(I) - TM(I,J)*Q(J)
C     CALCULATION OF THE MEMBER FORCES P(I)
      DO 330 I= 1,MN
      P(I)= 0.
      DO 330 J= 1,NP
330 P(I)= P(I) + ALPHA(I,J)*Q(J)
      DO 331 I= 1,MN
      DO 331 J= 1,NX
331 P(I)= P(I) + BETA(I,J)*XX(J)
      PRINT 332

```

```

      DO 333 I= 1,MN
333 PRINT 334, I, P(I)
C   INPUT FORMATS
201 FORMAT (I4, I4, F10.3)
202 FORMAT (I4, F10.2, F10.2)
203 FORMAT (I4)
204 FORMAT (F10.2, F10.2)
205 FORMAT (2F10.4)
206 FORMAT (F10.4)
300 FORMAT (I4, I4)
C   OUTPUT FORMATS
307 FORMAT (/1X, 30H INDETERMINATE TRUSS ANALYSIS      /)
311 FORMAT (1X, 6HMEMBER, 6X, 6HLENGTH )
313 FORMAT (1X, I4, F14.2)
332 FORMAT (/73X, 6HMEMBER, 6X, 12HMEMBER FORCE      )
334 FORMAT (1X, I5, 8X, F10.2)
603 FORMAT (/1X, 47H SAMPLE PROBLEM - INDETERMINATE TRUSS ANALYSIS /)
      STOP
335 PRINT 336
336 FORMAT (22H MATRIX DID NOT INVERT )
      END
SIBFTC DTRUSS
C   STATICALLY DETERMINATE PIN JOINTED TRUSS ANALYSIS
      SUBROUTINE DTRUSS (JN, MN, SLOPE, NN, XA, YA, LJ1, LJ2, PV, PH, S)
      DIMENSION N(25), X(25), Y(25), PV(25), PH(25), V(60), H(60),
1     S(60), J1(60), J2(60), MUV(8), MUH(8), LJ1(60), LJ2(60), XA(25),
2     YA(25), NN(25)
C   NN, XA AND YA ARE ARRAYS USED TO TRANSFER N, X AND Y INTO THE
C   SUBROUTINE BUT NOT OUT AGAIN
      DO 5 J= 1,JN
      N(J)= NN(J)
      X(J)= XA(J)
5     Y(J)= YA(J)
C   LJ1 AND LJ2 ARE ARRAYS USED TO TRANSFER J1 AND J2 INTO THE
C   SUBROUTINE BUT NOT OUT AGAIN
      DO 6 M= 1,MN
      J1(M)= LJ1(M)
6     J2(M)= LJ2(M)
      DO 7 M= 1,MN
      V(M)= 0.
7     H(M)= 0.
C   CALCULATE REACTIONS
      IF (X(1) - X(2)) 13, 96, 13
96 PRINT 113
      GO TO 99
13 SMV= 0.
      DO 9 J= 3,JN
9     SMV= SMV - PV(J)*(X(2) - X(J))
      SMH= 0.
      DO 10 J= 3,JN
10    SMH= SMH + PH(J)*(Y(2) - Y(J))

```

```

V1= -(SMV + SMH)/(X(1) - X(2))
SLOPE= SLOPE/57.2957
H1= V1*(SIN(SLOPE)/COS(SLOPE))
SPV= 0.
DO 11 J= 1,JN
11 SPV= SPV + PV(J)
SPH= 0.
DO 12 J= 1,JN
12 SPH= SPH + PH(J)
V2= -SPV - V1
H2= -SPH - H1
C ADD HORIZONTAL REACTIONS TO EXTERNAL FORCES AT JOINTS 1 AND 2
PH(1)= PH(1) + H1
PH(2)= PH(2) + H2
C ADD VERTICAL REACTIONS TO EXTERNAL FORCES AT JOINTS 1 AND 2
PV(1)= PV(1) + V1
PV(2)= PV(2) + V2
R1= SQRT((ABS(V1))**2. + (ABS(H1))**2.)
R2= SQRT((ABS(V2))**2. + (ABS(H2))**2.)
C CALCULATE MEMBER FORCES
LIMIT= JN/2
DO 64 I= 1,LIMIT
J= 1
GO TO 61
14 M= 1
C K COUNTS THE NUMBER OF MEMBERS EXAMINED AT A JOINT
K= 1
SV= 0.
SH= 0.
LV= 0
LH= 0
NJ= N(J)
DO 15 L= 1,NJ
15 MUH(L)= 0
C CHECK TO SEE IF J IS AT J1(M) OR J2(M). IF IT IS NOT, SCAN MEMBERS
C TO FIND ONE THAT IS.
16 IF (J1(M) - J) 17, 20, 17
17 IF (J2(M) - J) 18, 19, 18
18 M= M+1
GO TO 16
19 JA= J2(M)
J2(M)= J1(M)
J1(M)= JA
20 JA= J1(M)
C FIND SUM OF KNOWN VERTICAL COMPONENTS AT A JOINT
JB= J2(M)
IF (V(M)) 21, 24, 21
21 IF (Y(JA) - Y(JB)) 23, 23, 22
22 SV= SV - V(M)

```

```

      GO TO 27
23  SV= SV + V(M)
      GO TO 27
24  IF (Y(JA) - Y(JB)) 26, 25, 26
25  V(M)= 0.1E-20
      GO TO 27
26  LV= LV + 1
      MUV(LV)= M
C    FIND SUM OF KNOWN HORIZONTAL COMPONENTS AT A JOINT
27  IF (H(M)) 28, 31, 28
28  IF (X(JA) - X(JB)) 30, 30, 29
29  SH= SH - H(M)
      GO TO 34
30  SH= SH + H(M)
      GO TO 34
31  IF (X(JA) - X(JB)) 33, 32, 33
32  H(M)= 0.1E-20
      GO TO 34
33  LH= LH + 1
      MUH(LH)= M
C    CHECK TO SEE IF ALL MEMBERS AT A JOINT HAVE BEEN EXAMINED
34  IF (K - N(J)) 35, 39, 99
35  K= K + 1
      GO TO 18
39  IF (LV - 1) 49, 40, 70
40  M= MUV(1)
      JA= J1(M)
      JB= J2(M)
      V(M)= -(SV + PV(J))
      CALL VCOMP (V, H, S, X, Y, JA, JB, M)
      IF (Y(JA) - Y(JB)) 120, 99, 120
120 CONTINUE
C    PV(J)= 1.0E-10 IS A TAG USED TO INDICATE THAT ALL VERTICAL
C    COMPONENTS AT JOINT J HAVE BEEN SOLVED
      PV(J)= 1.0E-10
49  IF (LH - 1) 60, 50, 60
50  M= MUH(1)
      JA= J1(M)
      JB= J2(M)
      H(M)= -(SH + PH(J))
      CALL HCOMP (V, H, S, X, Y, JA, JB, M)
      IF (X(JA) - X(JB)) 123, 99, 123
123 CONTINUE
      PH(J)= 1.0E-10
C    INDEX TO NEXT JOINT
60  J= J+1
      IF (J-JN) 61, 61, 62
C    STATEMENT 61 INDICATES IF WE HAVE SOLVED FOR ALL THE VERTICAL AND
C    HORIZONTAL COMPONENTS AT JOINT J
61  IF (PV(J)*PH(J) - 1.0E-20) 14, 60, 14

```

```

C      ALL JOINTS ARE ANALYZED TO SEE IF ALL MEMBERS ARE SOLVED
62 DO 63 M= 1,MN
    IF (S(M)) 63,64, 63
63 CONTINUE
    GO TO 80
64 CONTINUE
    I= I-1
    PRINT 111
    GO TO 80
C      SOLUTION OF TWO UNKNOWN MEMBERS AT A JOINT
70 IF (LV-2) 99, 71, 49
71 IF (LH-2) 49, 72, 60
72 IF (MUV(1) - MUH(1)) 60, 73, 60
73 IF (MUV(2) - MUH(2)) 60, 74, 60
74 SV= SV + PV(J)
    SH= SH + PH(J)
    M1= MUV(1)
    M2= MUV(2)
    JA= J1(M1)
    JB= J2(M1)
    D1= (X(JA) - X(JB))/(Y(JA) - Y(JB))
    JA= J1(M2)
    JB= J2(M2)
    D2= (X(JA) - X(JB))/(Y(JA) - Y(JB))
    IF (D2 - D1) 76, 60, 76
76 V(M2)= (SV*D1 - SH)/(D2 - D1)
    V(M1)= -(SV + V(M2))
    M= M1
    JA= J1(M1)
    JB= J2(M1)
    CALL VCOMP (V, H, S, X, Y, JA, JB, M)
    IF (Y(JA) - Y(JB)) 121, 99, 121
121 CONTINUE
    PV(J)= 1.0E-10
    M= M2
    JA= J1(M2)
    JB= J2(M2)
    CALL VCOMP (V, H, S, X, Y, JA, JB, M)
    IF (Y(JA) - Y(JB)) 122, 99, 122
122 CONTINUE
    PH(J)= 1.0E-10
    GO TO 60
99 PRINT 112, I
C      OUTPUT FORMATS
111 FORMAT (1X, 48HSOLUTION INCOMPLETE, CHECK MEMBERS WITH 0 FORCE )
112 FORMAT (1X, 15HNC. OF CYCLES =, I3 )
113 FORMAT (1X, 23HREACTIONS INDETERMINATE )
80 RETURN
    END
$IBFTC VCOMP

```

```

C      SUBROUTINE FOR THE SOLUTION OF MEMBER FORCE WHEN VERTICAL
C      COMPONENT IS KNOWN
      SUBROUTINE VCOMP (V, H, S, X, Y, JA, JB, M)
      DIMENSION V(40), H(40), S(40), Y(25), X(25)
      IF (V(M)) 502, 501, 502
501  V(M)= 0.1E-20
      H(M)= 0.1E-20
      S(M)= 0.1E-20
      RETURN
502  IF (Y(JA) - Y(JB)) 504, 505, 503
503  V(M)= -V(M)
504  H(M)= V(M)*ABS((X(JA) - X(JB))/(Y(JA) - Y(JB))) + 0.1E-20
      S(M)= V(M)*SQRT((ABS(H(M)/V(M)))**2. + 1.) -
505  RETURN
      END
$IBFTC HCOMP
C      SUBROUTINE FOR THE SOLUTION OF MEMBER FORCE WHEN HORIZONTAL
C      COMPONENT IS KNOWN.
      SUBROUTINE HCOMP (V, H, S, X, Y, JA, JB, M)
      DIMENSION V(40), H(40), Y(25), X(25), S(40)
      IF (H(M)) 512, 511, 512
511  H(M)= 0.1E-20
      V(M)= 0.1E-20
      S(M)= 0.1E-20
      RETURN
512  IF (X(JA) - X(JB)) 514, 515, 513
513  H(M)= -H(M)
514  V(M)= H(M)*ABS((Y(JA) - Y(JB))/(X(JA) - X(JB))) + 0.1E-20
      S(M)= H(M)*SQRT((ABS(V(M)/H(M)))**2. + 1.)
515  RETURN
      END

      INPUT DATA

```

\$ENTRY

8	15	0.000	
2		64.00	0.00
2		0.00	0.00
4		16.00	20.00
4		32.00	0.00
4		32.00	20.00
4		48.00	0.00
3		48.00	20.00
3		16.00	0.00
2	8		
2	3		
8	4		
8	3		
3	4		

3	5
4	6
4	5
5	6
5	7
6	2
6	7
1	7
5	8
4	7

8		
	-10.00	0.00

4		
	-10.00	0.00

6		
	-10.00	0.00

0		
---	--	--

2	3	
---	---	--

8		
	0.7809	0.6247

5		
	-0.7809	-0.6247

4		
	0.7809	0.6247

7		
	-0.7809	-0.6247

0		
	1.0000	

	1.0000	
--	--------	--

	1.0000	
--	--------	--

	1.0000	
--	--------	--

	1.0000	
--	--------	--

	1.0000	
--	--------	--

	1.0000	
--	--------	--

	1.0000	
--	--------	--

	1.0000	
--	--------	--

	1.0000	
--	--------	--

	1.0000	
--	--------	--

	1.0000	
--	--------	--

	1.0000	
--	--------	--

	1.0000	
--	--------	--

	1.0000	
--	--------	--

\$IBSYS

COMPUTER OUTPUT

INDETERMINATE TRUSS ANALYSIS

SAMPLE PRØBLEM - INDETERMINATE TRUSS ANALYSIS

MEMBER	LENGTH
1	16.00
2	25.61
3	16.00
4	20.00
5	25.61
6	16.00
7	16.00
8	20.00
9	25.61
10	16.00
11	48.00
12	20.00
13	25.61
14	25.61
15	25.61

MEMBER	MEMBER FORCE
1	12.00
2	-19.21
3	12.18
4	10.23
5	6.11
6	-15.82
7	13.12
8	1.63
9	-1.80
10	-2.88
11	-12.00
12	-3.59
13	0.00
14	-0.29
15	4.60

B.8 Computer Analysis of an Indeterminate Lattice Chair Lift Tower Model

The forces in the indeterminate tower members due to the external loads, (see section 5.3.2.2), are found using the preceding computer program. The two chordload planes are prepared for computer analysis as shown in Figure 51. The windload planes are prepared as shown in Figure 52. Note that the chordload must be divided into its two components:

$$\begin{aligned} PV(19) = PV(20) &= -\frac{R}{4} \cos 25^\circ = -\frac{311}{4} \cos 25^\circ \\ &= -70.40 \text{ pounds,} \end{aligned}$$

$$\begin{aligned} \text{and } PH(19) = PH(20) &= \frac{R}{4} \sin 25^\circ = \frac{311}{4} \sin 25^\circ \\ &= 32.81 \text{ pounds.} \end{aligned}$$

The data input and computer output for the chordload and windload planes is given in the following pages.

A member joining the two supports (joints 1 and 2), of each plane must be included in order to get a computer solution. This is member 1 in each plane. The member is given a cross-section area of 10,000 square inches to make it appear infinitely rigid to the other members and thus simulate the fixed supports of the real tower.

The input data is entered with more precision than the sample problem shown previously. This is done to get third figure accuracy in the answers.

INPUT DATA

603 FORMAT (/1X, 64H CHAIR LIFT LATTICE TOWER MODEL, PLANES AB EF AND CD
1GH ANALYSIS /)

\$ENTRY

20	46	0.0000	
2		0.0000	0.0000
3		12.2500	0.0000
4		0.7767	12.4375
4		11.4733	12.4375
4		1.4773	23.6560
4		10.7727	23.6560
4		2.0920	33.5000
4		10.1580	33.5000
4		2.6385	42.2500
4		9.6115	42.2500
4		3.1204	49.9690
4		9.1296	49.9690
4		3.5478	56.8130
4		8.7022	56.8130
4		3.9118	62.6410
4		8.3382	62.6410
4		4.2386	67.8750
4		8.0114	67.8750
3		4.5470	72.8130
2		7.7030	72.8130
1	2		
2	4		
2	3		
1	3		
3	4		
4	6		
4	5		
3	5		
5	6		
6	8		
6	7		
5	7		
7	8		
8	10		
8	9		
7	9		
9	10		
10	12		
10	11		
9	11		
11	12		
12	14		

12 13
 11 13
 13 14
 14 16
 14 15
 13 15
 15 16
 16 18
 16 17
 15 17
 17 18
 18 20
 18 19
 17 19
 19 20
 1 4
 3 6
 5 8
 7 10
 9 12
 11 14
 13 16
 15 18
 17 20
 19

-70.40 32.81

20
-70.40 32.81

0
9 4
4
-0.72987 -0.68593

3
0.74664 0.66523

6
-0.74664 -0.66523

5
0.75002 0.66143

8
-0.75002 -0.66143

7
0.75840 0.65177

10
-0.75840 -0.65177

9
0.76535 0.64360

12
-0.76535 -0.64360

11
0.77494 0.63203

0.0485
0.0485
0.0216
0.0216
0.0216
0.0216
0.0216
0.0216
0.0216
0.0216
0.0216
0.0216

\$IBSYS

COMPUTER OUTPUT

INDETERMINATE TRUSS ANALYSIS

CHAIR LIFT LATTICE TOWER MODEL, PLANES AB EF AND CD GH ANALYSIS

MEMBER	LENGTH
1	12.25
2	12.46
3	16.92
4	12.46
5	10.70
6	11.24
7	15.03
8	11.24
9	9.30
10	9.86
11	13.12
12	9.86
13	8.07
14	8.77
15	11.54
16	8.77
17	6.97
18	7.73
19	10.09
20	7.73
21	6.01
22	6.86
23	8.83
24	6.86
25	5.15
26	5.84
27	7.54
28	5.84
29	4.43
30	5.24
31	6.65
32	5.24
33	3.77
34	4.95
35	6.03
36	4.95
37	3.16
38	16.92
39	15.03
40	13.12
41	11.54
42	10.09
43	8.83
44	7.54
45	6.65
46	6.03

MEMBER	MEMBER FORCE
1	-19.85
2	-443.37

3	-24.31
4	318.44
5	13.98
6	-422.58
7	-25.44
8	296.16
9	13.15
10	-397.03
11	-28.17
12	271.06
13	13.39
14	-366.94
15	-31.62
16	241.65
17	13.66
18	-331.34
19	-35.67
20	206.75
21	13.40
22	-289.61
23	-39.74
24	164.41
25	13.42
26	-239.60
27	-45.25
28	115.58
29	14.05
30	-180.04
31	-52.73
32	57.11
33	15.34
34	-101.53
35	-67.13
36	-15.47
37	4.78
38	2.40
39	5.85
40	8.07
41	10.85
42	14.18
43	19.30
44	23.22
45	29.73
46	37.78

INPUT DATA

603 FORMAT (/1X, 64H CHAIR LIFT LATTICE TOWER MODEL, PLANES ACEG AND BD
1FH ANALYSIS /)

\$ENTRY

20	46	0.0000	
2		0.0000	0.0000
3		12.2500	0.0000
4		0.7767	12.4375
4		11.4733	12.4375
4		1.4773	23.6560
4		10.7727	23.6560
4		2.0920	33.5000
4		10.1580	33.5000
4		2.6385	42.2500
4		9.6115	42.2500
4		3.1204	49.9690
4		9.1296	49.9690
4		3.5478	56.8130
4		8.7022	56.8130
4		3.9118	62.6410
4		8.3382	62.6410
4		4.2386	67.8750
4		8.0114	67.8750
3		4.5470	72.8130
2		7.7030	72.8130
1	2		
2	4		
2	3		
1	3		
3	4		
4	6		
4	5		
3	5		
5	6		
6	8		
6	7		
5	7		
7	8		
8	10		
8	9		
7	9		
9	10		
10	12		
10	11		
9	11		
11	12		
12	14		

12 13
 11 13
 13 14
 14 16
 14 15
 13 15
 15 16
 16 18
 16 17
 15 17
 17 18
 18 20
 18 19
 17 19
 19 20
 1 4
 3 6
 5 8
 7 10
 9 12
 11 14
 13 16
 15 18
 17 20

3	0.00	1.89
5	0.00	1.74
7	0.00	1.52
9	0.00	1.31
11	0.00	1.15
13	0.00	1.01
15	0.00	0.89
17	0.00	0.77
19	0.00	10.32
0		
9 9		
4		
-0.72987	-0.68593	
3		
0.74664	0.66523	
6		
-0.74664	-0.66523	

COMPUTER OUTPUT

INDETERMINATE TRUSS ANALYSIS

CHAIR LIFT LATTICE TOWER MODEL, PLANES ACEG AND BDFH ANALYSIS

MEMBER	LENGTH
1	12.25
2	12.46
3	16.92
4	12.46
5	10.70
6	11.24
7	15.03
8	11.24
9	9.30
10	9.86
11	13.12
12	9.86
13	8.07
14	8.77
15	11.54
16	8.77
17	6.97
18	7.73
19	10.09
20	7.73
21	6.01
22	6.86
23	8.83
24	6.86
25	5.15
26	5.84
27	7.54
28	5.84
29	4.43
30	5.24
31	6.65
32	5.24
33	3.77
34	4.95
35	6.03
36	4.95
37	3.16
38	16.92
39	15.03
40	13.12
41	11.54
42	10.09
43	8.83
44	7.54
45	6.65
46	6.03

MEMBER	MEMBER FORCE
1	-5.51
2	-88.42

3	-6.99
4	88.41
5	-0.83
6	-78.03
7	-6.99
8	78.42
9	-0.56
10	-68.25
11	-6.58
12	68.54
13	-0.52
14	-58.74
15	-6.39
16	59.00
17	-0.44
18	-49.27
19	-6.36
20	49.52
21	-0.50
22	-39.74
23	-6.30
24	39.65
25	-0.47
26	-29.62
27	-6.64
28	29.82
29	-0.31
30	-19.04
31	-7.14
32	19.17
33	-0.17
34	-6.51
35	-8.56
36	7.02
37	-4.96
38	7.05
39	6.47
40	6.19
41	6.05
42	6.04
43	6.42
44	6.39
45	6.98
46	7.94

APPENDIX C

Calculation of the Theoretical Stresses
in the Pipe Tower Model

APPENDIX C

Calculation of the Theoretical Stresses
in the Pipe Tower Model

C.1 External Loads on the Pipe Tower

Figure 54 shows the chordload (R) and windloads (W) applied to the tower. The chordload can be divided into its components:

$$R_x = -R \cos 25^\circ = -300 \cos 25^\circ = -272 \text{ pounds}$$

$$R_y = R \sin 25^\circ = 300 \sin 25^\circ = 126.8 \text{ pounds}$$

The windload on the tower itself is considered a uniformly distributed load with a magnitude of:

$$w_y = 1.91 \text{ pounds per foot.}$$

The windload due to the ropes, passengers, chairs and idler assemblies is:

$$W_y = 18.0 \text{ pounds.}$$

This is applied at the free end of the tower.

The stresses at points A, B and C on the pipe circumference, due to the above loads, will be calculated. The location of these points on the pipe is shown in Figure 54.

C.2 Calculation of the Stress at Point A

The stress at point A is the algebraic sum of two components -- the compressive stress due to bending about the z-axis, and the direct compressive stress due to the axial chordload component. The bending shear stress due to the windload and the direct shear stress are neglected.

C.2.1 Compressive Bending Stress at Point A

The bending stress is given by:

$$S_{Ab} = \frac{-M_z C}{I_z} ,$$

where M_z = bending moment about the z-axis at point A,
 $= 64.375 \times R_y = 64.375 \times 126.8$,
 $= 8.16 \times 10^3$ pound inches;

C = distance from the z-axis to the point A,
 $= 3/2 = 1.5$ inches;

I_z = second moment of area of the cross-section
 about the z-axis,
 $= 1.128$ inches⁴ (see reference G16, page 361).

The bending stress at point A due to the design loading is:

$$S_{Ab} = - \frac{8.16 \times 10^3 \times 1.5}{1.128} = -10850 \text{ psi.}$$

C.2.2 Compressive Direct Stress at Point A

The direct stress is given by:

$$S_{Ad} = \frac{R_x}{A_x} ,$$

where R_x = axial chordload component,
 = -272 pounds;

A_x = cross-section area,
 = 1.086 inches² (see reference G16, page 361).

The direct stress at point A due to the design loading is $S_{Ad} = \frac{-272}{1.086} = -250$ psi.

C.2.3 Total Stress at Point A

The total compressive stress at point A due to the design loading is:

$$S_A = S_{Ab} + S_{Ad} = -10850 - 250 = -11100 \text{ psi.}$$

C.3 Calculation of the Stress at Point B

The stress at point B is the algebraic sum of two components -- the tensile stress due to bending about the z-axis, and the direct compressive stress due to the axial chordload component. The bending shear stress due to the windload and the direct shear stress are neglected.

C.3.1. Tensile Bending Stress at Point B

Since the section is symmetrical about the z-axis, the tensile bending stress will have the same magnitude as the compressive bending stress at point A, (section C.2.1), but with opposite sign.

$$S_{Bb} = 10850 \text{ psi.}$$

C.3.2 Compressive Direct Stress at Point B

The compressive direct stress at point B will have the same magnitude and sign as that at point A, (section C.2.2).

$$S_{Bd} = -250 \text{ psi.}$$

C.3.3 Total Stress at Point B

The total stress at point B due to the design loading is:

$$S_B = S_{Bb} + S_{Bd} = 10850 - 250 = 10600 \text{ psi.}$$

C.4 Calculation of the Stress at Point C

The stress at point C is a combination of three components -- the compressive bending stress due to the windloads, the compressive direct stress due to the axial component of the chordload, and the bending shear stress due to the bending moment about the z-axis. The direct shear stresses are neglected.

C.4.1 Compressive Bending Stress at Point C

The bending stress is given by:

$$S_{Cb} = \frac{-M_y C}{I_y} ,$$

where M_y = bending moment about the y-axis due to the windloads,

$$= -64,375 \times 18.0 - \left(\frac{1.91}{12} \times \frac{64.375^3}{2} \right),$$

$$= -1.49 \times 10^3 \text{ pound inches};$$

C = distance from the y-axis to point C,

$$= -3/2 = -1.5 \text{ inches};$$

I_y = second moment of area of the cross-section about the y-axis,

$$= 1.128 \text{ inches}^4.$$

The bending compressive stress at point C due to the design loading is:

$$S_{Cb} = - \frac{1.49 \times 10^3 \times 1.5}{1.128} = -1520 \text{ psi.}$$

C.4.2 Compressive Direct Stress at Point C

The compressive direct stress at point C will have the same magnitude and sign as that at point A, (section C.2.2).

$$S_{Cd} = -250 \text{ psi.}$$

C.4.3 Bending Shear Stress at Point C

The bending shear stress is given by:

$$S_{Cs} = \frac{VQ}{2tI_z},$$

where V = shear force at point C due to the chordload component R_y ,

$$= 126.8 \text{ pounds};$$

t = thickness of the tube,

$$= 0.120 \text{ inches};$$

Q = first moment of area of one-half the cross-section,

$$= 2 \times t \times r^2, \quad r = \text{mean radius of the tube}$$

$$= 1.44 \text{ inches},$$

$$= 2 \times 0.120 \times (1.44)^2 = 0.415 \text{ inches}^3;$$

I_z = second moment of area of the cross-section about the z-axis,

$$= 1.128 \text{ inches}^4 \quad (\text{see section C.2.1}).$$

The bending shear stress at point C due to the design loading is:

$$S_{Cs} = \frac{126.8 \times 0.415}{2 \times 0.120 \times 1.128} = 194.5 \text{ psi.}$$

C.4.4 The Principal Stresses at Point C

The principal stresses at point C are given by:

$$S_{1,2} = (S_x + S_y)/2 \pm \sqrt{[(S_x - S_y)/2]^2 + (S_s)^2},$$

where S_x = stress in the x direction,

$$= -1520 - 250 = -1770 \text{ psi};$$

S_y = stress in the y direction,

$$= 0 ;$$

S_s = shear stress at point C,

$$= 194.5 \text{ psi.}$$

The principal stress at point C due to the design loading are:

$$S_{1,2} = \frac{-1770}{2} \pm \sqrt{885^2 + 194.5^2}$$
$$= -885 \pm 906 \text{ psi.}$$

So: $S_1 = -21 \text{ psi,}$

and $S_2 = -1791 \text{ psi.}$

APPENDIX D

Calculation of the Theoretical Stresses
in the Hexagonal Tower Model

APPENDIX DCalculation of the Theoretical Stresses
in the Hexagonal Tower ModelD.1 External Loads on the Hexagonal Tower

Figure 56 shows the chordload (R) and the windloads (W) applied to the tower. The chordload can be divided into its components:

$$R_x = -R \cos 25^\circ = -300 \cos 25^\circ = -272 \text{ pounds}$$

$$R_y = R \sin 25^\circ = 300 \sin 25^\circ = 126.8 \text{ pounds.}$$

The windload on the tower itself is considered a uniformly distributed load with a magnitude of:

$$w_y = 1.91 \text{ pounds per foot.}$$

The windload due to the ropes, passengers, chairs and idler assemblies is:

$$W_y = 18.0 \text{ pounds.}$$

This is applied at the free end of the tower.

The stresses at points A, B and C on the hexagonal section periphery, due to the above loads, will be calculated. The location of points A, B and C on the tower is shown in Figure 56.

D.2 Calculation of the Stress at Point A

The stress at point A is the algebraic sum of two components -- the compressive stress due to bending about the z-axis, and the direct compressive stress due to the axial chordload component. The bending shear stress due to the windload and the direct shear stress are neglected.

D.2.1 Compressive Bending Stress at Point A

The bending stress is given by:

$$S_{Ab} = \frac{-M_z C}{I_z},$$

where M_z = bending moment about the z-axis at point A,

$$= 62 \times R_y = 62 \times 126.8$$

$$= 7.85 \times 10^3 \text{ pound inches;}$$

C = distance from the z-axis to point A,

$$= 1.850 \text{ inches;}$$

I_z = second moment of area of the cross-section about the z-axis,

$$= 0.98 \text{ inches}^4 \text{ (see reference G16, page 364).}$$

The bending stress at point A due to the design loading is:

$$S_{Ab} = - \frac{7.85 \times 10^3 \times 1.850}{0.98} = -14820 \text{ psi.}$$

D.2.2 Compressive Direct Stress at Point A

The direct stress is given by:

$$S_{Ad} = \frac{R_x}{A_x},$$

where R_x = axial chordload component,

$$= -272 \text{ pounds};$$

A_x = cross-section area,

$$= 0.67 \text{ inches}^2 \text{ (see reference G16, page 364).}$$

The direct stress at point A due to the design loading is:

$$S_{Ad} = \frac{-272}{0.67} = -406 \text{ psi.}$$

D.2.3 Total Stress at Point A

The total compressive stress at point A due to the design loading is:

$$S_A = S_{Ab} + S_{Ad} = -14820 - 406 = -15226 \text{ psi.}$$

D.3 Calculation of the Stress at Point B

The stress at point B is the algebraic sum of two components -- the tensile stress due to bending about the z-axis, and the direct compressive stress due to the axial chordload component. The bending shear stress due to the windload and the direct shear stress are neglected.

D.3.1 Tensile Bending Stress at Point B

Since the section is symmetrical about the z-axis, the tensile bending stress will have the same magnitude as the compressive bending stress at point A, (section D.2.1), but with opposite sign.

$$S_{Bb} = 14820 \text{ psi.}$$

D.3.2 Compressive Direct Stress at Point B

The compressive direct stress at point B will have the same magnitude and sign as that at Point A, (section D.2.2).

$$S_{Bd} = -406 \text{ psi.}$$

D.3.3 Total Stress at Point B

The total stress at point B due to the design loading is:

$$S_B = S_{Bb} + S_{Bd} = 14820 - 406 = 14414 \text{ psi.}$$

D.4 Calculation of the Stress at Point C

The stress at point C is a combination of three components -- the compressive bending stress due to the windloads, the compressive direct stress due to the axial component of the chordload, and the bending shear stress due to the bending moment about the z-axis. The direct shear stresses are neglected.

D.4.1 Compressive Bending Stress at Point C

The bending stress is given by:

$$S_{Cb} = \frac{-M_y C}{I_y},$$

where M_y = bending moment about the y-axis due to the windloads,

$$= -62 \times 18.0 - \left(\frac{1.91}{12} \times \frac{62^2}{2} \right)$$

$$= -1.424 \times 10^3 \text{ pound inches;}$$

C = distance from the y-axis to point C,

$$= -1.6562 \text{ inches;}$$

I_y = second moment of area of the cross-section about the y-axis, ($I_y = I_z$ for a regular polygon),

$$= 0.98 \text{ inches}^4 \text{ (see section D.2.1).}$$

The bending compressive stress at point C due to the design loading is:

$$S_{Cb} = \frac{-1.424 \times 10^3 \times 1.6561}{0.98} = -2410 \text{ psi.}$$

D.4.2 Compressive Direct Stress at Point C

The compressive direct stress at point C will have the same magnitude and sign as that at point A, (section D.2.2)

$$S_{Cd} = -406 \text{ psi.}$$

D.4.3 Bending Shear Stress at Point C

The bending shear stress is given by:

$$S_{Cs} = \frac{VQ}{2tI_z},$$

where V = shear force at point C due to the chordload component R_y ,
 = 126.8 pounds;
 t = thickness of the hexagonal section,
 = 0.0598 inches;
 Q = first moment of area of the half cross-section which lies to the left of the z-axis,

$$= \int ydA = 2 \left[\int_0^{.939} y(tdy) + \int_{.939}^{1.878} y \frac{t}{\sin 30^\circ} dy \right]$$

$$= 0.368 \text{ inches}^3;$$

I_z = second moment of area of the cross-section about the z-axis,
 = 0.98 inches⁴ (see section D.2.1).

The bending shear stress at point C due to the design loading is:

$$S_{Cs} = \frac{126.8 \times 0.368}{2 \times 0.0598 \times 0.98} = 398 \text{ psi.}$$

D.4.4 The Principal Stresses at Point C

The principal stresses at point C are given by:

$$S_{1,2} = (S_x + S_y)/2 \pm \sqrt{\left[(S_x + S_y)/2\right]^2 + (S_s)^2},$$

where S_x = stress in the x direction,

$$= -2410 - 406 = -2816 \text{ psi};$$

S_y = stress in the y direction

$$= 0;$$

S_s = shear stress at point C,

$$= 398 \text{ psi}.$$

The principal stresses at point C due to the design loading are:

$$S_{1,2} = -2816 \pm \sqrt{1408^2 + 398^2},$$

$$= -1408 \pm 1465 \text{ psi},$$

So $S_1 = 57 \text{ psi}$,

and $S_2 = -2873 \text{ psi}$.

APPENDIX E

Sag and Tension Tables
for a Chair Lift Rope

APPENDIX E

Sag and Tension Tables
for a Chair Lift Rope

E.1 Notation

The following is the notation used in the development of the equations governing the behavior of a hanging rope.

<u>Symbol</u>	<u>Description</u>	<u>Dimension</u>
x	Horizontal coordinate of the rope profile.	feet
y	Vertical coordinate of the rope profile.	feet
w	Weight per foot of rope, chairs and passengers measured horizontally.	pounds/foot
Q	Weight per foot of the rope, chairs, and passengers, measured along the chord.	pounds/foot
Q_r	Weight per foot of the rope alone measured along the chord.	pounds/foot
Q_v	Weight per foot of the chairs measured along the chord.	pounds/foot
Q_p	Weight per foot of the passengers measured along the chord.	pounds/foot

L	Span length between supports.	feet
S	Horizontal distance between supports.	feet
D	Vertical distance between supports.	feet
α	Slope angle measured from a horizontal line.	degrees
T	Axial tension at any point in the rope.	pounds
H	Axial tension in the rope at the origin of coordinates -- where the tangent to the rope profile, or profile extended, becomes horizontal.	pounds
T_A	Axial tension in the rope at the lower support tower.	pounds
T_B	Axial tension in the rope at the upper support tower.	pounds
F	Rope sag, which is the vertical distance between the chord of the rope and the rope itself.	feet
$F_{max.}$	Maximum rope sag, assumed to occur at $S/2$.	feet
ϕ	The angle between the tangent to the rope profile at any point and a horizontal line.	degrees
β_A	The angle between the tangent to	

the rope profile and the chord
at point A. degrees

β_B The angle between the tangent to the
rope profile and the chord at
point B. degrees

Subscript A Lower support tower.

Subscript B Upper support tower.

Subscript C The origin of coordinates.

Subscript D Location on the rope of the maximum sag,
assumed to be at $S/2$.

Subscript E Location on the chord, joining the points
of support, which is directly above point D.

E.2 Theory

In practice, the rope of a chair lift is loaded with a series of discrete concentrated loads. These loads represent the weight of the chair, or the weight of chair plus passengers. It is usual to assume that these concentrated loads can be represented as a distributed load along the rope. It is also usual practice to assume the cable hangs in a parabolic shape -- not in a hyperbolic catenary. Since the maximum sag rarely exceeds 2 per cent of the span length, this assumption

is valid. F2, F14, F16

Figure 61 shows a hanging chair lift rope and the loads that are assumed to act on it. The location of the origin of coordinates for the parabolic rope is taken to be to the left of support tower A. This is generally the case for chair lift ropes. The origin may move between the towers in which case distance x_A would be negative.

The tension in the rope at any point is given by:

$$T = \sqrt{H^2 + w^2 x^2} \quad \text{--- (1)}$$

The equation defining the shape of the hanging rope is:

$$y = \frac{wx^2}{2H} \quad \text{--- (2)}$$

The initial step in solving for the tension at A and the maximum rope sag is to calculate H.

From Figure 61, it is seen that;

$$y_B - y_A = D, \quad \text{--- (3)}$$

$$\text{and } x_B - x_A = S; \quad \text{--- (4)}$$

$$\text{also } y_B = \frac{wx_B^2}{2H}, \quad \text{--- (5)}$$

$$\text{and } y_A = \frac{wx_A^2}{2H}. \quad \text{--- (6)}$$

Subtract equation (6) from (5),

$$y_B - y_A = \frac{w}{2H} (x_B^2 - x_A^2) \quad \text{--- (7)}$$

From equation (4), $x_A = x_B - S$,

so $x_A^2 = x_B^2 - 2x_B S + S^2$, Substitute this,

and equation (3) in equation (7):

$$\frac{2HD}{w} = x_B^2 - x_B^2 + 2x_B S - S^2,$$

$$\text{or } 2x_B S - S^2 = \frac{2HD}{w} \quad \text{--- (8)}$$

Equation (1) can be written for point B as:

$$w^2 x_B^2 = T_B^2 - H^2$$

or $x_B = \sqrt{\frac{T_B^2 - H^2}{w^2}}$. Substitute this in equation (8)

Thus, $\sqrt{\frac{T_B^2 - H^2}{w^2}} = \frac{HD}{wS} + \frac{S}{2}$. Square both sides,

$$\frac{T_B^2}{w^2} - \frac{H^2}{w^2} = \frac{H^2 D^2}{w^2 S^2} + \frac{HD}{w} + \frac{S^2}{4} \quad \text{or by rearranging terms,}$$

$$H^2 \left[\frac{D^2}{w^2 S^2} + \frac{1}{w^2} \right] + \left[\frac{D}{w} \right] H + \left[\frac{S^2}{4} - \frac{T_B^2}{w^2} \right] = 0$$

This equation has a solution:

$$H = \frac{-\frac{D}{w} \pm \sqrt{\left[\frac{D}{w}\right]^2 - 4 \left[\frac{D^2}{w^2 S^2} + \frac{1}{w^2}\right] \times \left[\frac{S^2}{4} - \frac{T_B^2}{w^2}\right]}}{2 \left[\frac{D^2}{w^2 S^2} + \frac{1}{w^2}\right]} \quad \text{--- (9)}$$

Note that the negative sign before the radical can be neglected as this gives a negative value for H which has no physical significance.

All the quantities on the right hand side of equation (9) are known, so a solution for H can be obtained.

The distance from the origin of coordinates to support A is found as follows:

From equation (4), $x_B = S + x_A$, square both sides, $x_B^2 = x_A^2 + 2Sx_A + S^2$. Substitute this in equation (7):

$$x_A^2 + 2Sx_A + S^2 - x_A^2 = \frac{2HD}{w}$$

$$\text{or } x_A = \frac{HD}{wS} - \frac{S}{2} \quad \text{--- (10)}$$

The rope tension at the lower support is:

$$\text{From equation (1), } T_A = \sqrt{H^2 + w^2 x_A^2} \quad \text{--- (11)}$$

The maximum sag is assumed to occur at the mid span ($S/2$). It is found by subtracting the vertical distance to point D on the rope from the vertical distance to point E on the chord.

$$\text{Now } y_D = \frac{wx_D^2}{2H}, \quad \text{but } x_D = x_A + S/2,$$

$$\text{so } y_D = \frac{w}{2H} \left[x_A^2 + x_A S + \frac{S^2}{4} \right] \quad \text{--- (12)}$$

The vertical distance to point E on the chord is:

$$y_E = y_A + \frac{D}{2}, \quad \text{but } y_A = \frac{wx_A^2}{2H};$$

$$\text{so } y_E = \frac{wx_A^2}{2H} + \frac{D}{2} \quad \text{--- (13)}$$

The maximum sag is obtained by subtracting equation (12) from (13).

$$F_{\max.} = y_E - y_D = \frac{wx_A^2}{2H} + \frac{D}{2} - \left[\frac{wx_A^2}{2H} + \frac{wx_A S}{2H} + \frac{wS^2}{8H} \right],$$

$$\text{or } F_{\max.} = \frac{D}{2} - \frac{wSx_A}{2H} - \frac{wS^2}{8H}. \quad \text{--- (14)}$$

The above equations are not yet in the best form for computer analysis. The weight per foot "w" of the rope, chairs and contents measured horizontally, varies with the slope angle. It would be advantageous to define "w" in terms of "Q", the weight per foot of rope, chairs and contents measured along the chord. This term is constant.

"Q" is the sum of three terms:

$$Q = Q_r + Q_v + Q_p.$$

From Figure 61, it can be shown that:

$$w = Q \sec \alpha, \quad \text{but } \sec \alpha = \frac{\sqrt{D^2 + S^2}}{S},$$

$$\text{so } w = Q \frac{\sqrt{D^2 + S^2}}{S} \quad \text{--- (14)}$$

This is substituted in equations (9), (10), (11) and (14) to give:

$$H = \frac{-\left[\frac{D \times S}{Q \sqrt{D^2 + S^2}}\right] + \left\{ \left(\frac{D \times S}{Q \sqrt{D^2 + S^2}}\right)^2 - 4 \times \left[\left(\frac{D}{Q \sqrt{D^2 + S^2}}\right)^2 + \left(\frac{S}{Q \sqrt{D^2 + S^2}}\right)^2 \right] \right.}{\left. \times \left[\left(\frac{S}{2}\right)^2 - \left(\frac{T_B \times S}{Q \sqrt{D^2 + S^2}}\right)^2 \right]^{1/2}} \quad (15)$$

$$2 \times \left[\left(\frac{D}{Q \sqrt{D^2 + S^2}}\right)^2 + \left(\frac{S}{Q \sqrt{D^2 + S^2}}\right)^2 \right]$$

$$x_A = \frac{HD}{Q \sqrt{D^2 + S^2}} - \frac{S}{2} \quad \text{-----} \quad (16)$$

$$T_A = \sqrt{H^2 + \left(Q \frac{\sqrt{D^2 + S^2}}{S} x_A \right)^2} \quad \text{-----} \quad (17)$$

$$F_{\max.} = \frac{D}{2} - \frac{Q \sqrt{D^2 + S^2}}{2H} \left[x_A + \frac{S}{4} \right] \quad \text{-----} \quad (18)$$

The angle of departure (β) of the rope from the idler assemblies at each end of a span is required since it contributes to the total breakover or breakunder angle at a tower. This angle, for each support, is calculated as follows:

The equation defining the rope profile is:

$$y = \frac{wx^2}{2H} \quad \text{-----} \quad (2)$$

The slope at any point on the rope is given by the derivative of equation (2)

$$\text{That is: } \tan \phi = \frac{2wx}{2H} = \frac{wx}{H}$$

So from Figure 61,

$$\tan \phi_B = \frac{wx_B}{H} \quad , \quad \text{--- (19)}$$

$$\text{and } \tan \phi_A = \frac{wx_A}{H} \quad \text{--- (20)}$$

$$\text{Now } \beta_B = \phi_B - \alpha \quad \text{and } \beta_A = \phi_A - \alpha \quad ;$$

$$\text{but } \alpha = \tan^{-1} \left[\frac{D}{S} \right] \quad . \quad \text{Also, } x_B = S + x_A, \quad [\text{equation (4)}],$$

and $w = \frac{Q \sqrt{D^2 + S^2}}{S}$, [equation (14)]. Substitute these into equations (19) and (20) and rearrange.

$$\beta_B = \tan^{-1} \left[\frac{Q \sqrt{D^2 + S^2}}{S} \times \frac{(S + x_A)}{H} \right] - \tan^{-1} \left[\frac{D}{S} \right] \quad \text{--- (21)}$$

$$\beta_A = \tan^{-1} \left[\frac{Q \sqrt{D^2 + S^2}}{S} \times \frac{x_A}{H} \right] - \tan^{-1} \left[\frac{D}{S} \right] \quad \text{--- (22)}$$

E.3 Digital Computer Program for the Solution of the Sag and Tension Equations

E.3.1 Description of the Program

The program solves equations (15), (16), (17), (18), (21) and (22) from section E.2 for various values of rise (D), run (S) and rope weight (Q). The computer calculates and prints out the maximum sag in a span, the tension at the lower support, the axial tension in the rope

- XA Distance from the origin of coordinates to point A.
- FMAX Maximum vertical distance from the chord to the rope, (sag).
- BETAA Angle between the tangent to the rope profile and the chord at point A.
- BETAB Angle between the tangent to the rope profile and the chord at point B.
- Q Weight per foot of rope, chairs and passengers measured along the chord.
- W Weight per foot of rope, chairs and passengers measured horizontally.
- X False variable used to calculate part of the equation for PHI.
- PHI Angle between the tangent to the rope profile at point B, and a horizontal line, (ϕ_B).
- Y False variable used to calculate part of the equation for DELT.
- DELT Angle between the tangent to the rope profile at point A, and a horizontal line (ϕ_A).
- I Index used to space the printed output on the page.
- ALPHA Slope angle measured from a horizontal line.

E.3.3 Data Input Instructions

The following defines the order of input cards.

Fortran Statement Cards

- (1) Problem Title Card - This is a Hollerith Statement defining the title of the problem. It is statement number 15 and must be entered in the main program under the heading Output Formats.

Data Cards

- (2) Header Card - Format (3I4)
ND Total number of D values in input.
NS Total number of S values in input.
NTB Total number of TB values in input.
- (3) Weight Card - Format (F10.2)
Q Weight per foot of rope, chairs and passengers measured along the chord.
- (4) Rise Cards - Format (6F10.1)
D Vertical rise in feet from support A to B.
- (5) Run Cards - Format (6F10.1)
S Horizontal run in feet between supports A and B.
- (6) Tension Cards - Format (6F10.1)
TB Axial Tension at the high support B.

E.3.4 Sample Problem

It is desired to calculate the sag and tension for a series of rise, run and tensions as shown below.

Sample Problem Input:

Fortran Statement Cards

(1) Problem Title Card

```
15 FORMAT (1X, 80H SAG AND TENSION CHARTS --
1200 PEOPLE PER HOUR, CHAIRS LOADED, 1-1/8
ROPE //)
```

Data Cards

(2) Header Card

```
ND   NS   NTB
6    6    6
```

(3) Weight Card

```
Q   12.03
```

(4) Rise Cards

```
D   120.0  110.0  100.0  90.0  80.0  70.0
```

(5) Run Cards

```
S   220.0  200.0  180.0  160.0  140.0  130.0
```

(6) Tension Cards

```
TB  20000.0  19750.0  19500.0  19250.0
      19000.0  18750.0
```

The computer program and solution (Table 15) are shown on the following pages.

```

C     SAG AND TENSION CALCULATIONS FOR A CHAIR LIFT
      DIMENSION D(40), S(40), TB(40)
      READ 40, ND, NS, NTB
      READ 10, Q
      READ 14, (D(J), J= 1,ND)
      READ 14, (S(K), K= 1,NS)
      READ 14, (TB(L), L= 1,NTB)
      PRINT 8
      PRINT 15
      PRINT 20
      I= 5
      DO 21 L= 1,NTB
      PRINT 6
      DO 21 J= 1,ND
      DO 21 K= 1,NS
      IF (0.500 - (D(J)/S(K))) 21, 21, 22
22  CONTINUE
      V1= SQRT(D(J)*D(J) + S(K)*S(K))
      V2= (D(J)*S(K))/(Q*V1)
      V3= V2**2.
      V4= (V2/S(K))**2.
      V5= (V2/D(J))**2.
      V6= (S(K)/2. )**2.
      V7= ((TB(L)*S(K))/(Q*V1))**2.
C     CALCULATE THE HORIZONTAL TENSION H
      H= (-V2 + SQRT(V3 - 4.*(V4 + V5)*(V6 - V7)))/(2.*(V4 + V5))
C     CALCULATE POSITION OF VERTEX FROM LOWER SUPPORT- XA
      XA= (H*SQRT(V4)) - (S(K)/2.)
C     CALCULATE TENSION TA AT LOWER SUPPORT
      TA= SQRT((H**2.) + ((1./V5)*XA*XA))
C     CALCULATE MAXIMUM CABLE SAG FROM CHORD LINE
      FMAX= (D(J)/2.) - (((Q*V1)/(2.0*H))*(XA + S(K)/4.0))
C     CALC. OF THE LEAD IN AND LEAD OUT ROPE-TO-CHORD ANGLES BETAB AND
C     BETAA
C     CALCULATION OF THE SLOPE ANGLE ALPHA
      ALPHA= ATAN2(D(J),S(K))
      W= Q/COS(ALPHA)
      X= ABS(W*(S(K) + XA))
      PHI= ATAN2(X,H)
      BETAB= PHI - ALPHA
      BETAB= BETAB*57.29578
      Y= ABS(W*XA)
      DELT= ATAN2(Y,H)
      BETAA= DELT - ALPHA
      BETAA= BETAA*57.29578
      I= I + 1
      IF (I.NE.50) GO TO 11
30  PRINT 7
      PRINT 15
      PRINT 20

```

```

      I= 3
11 PRINT 12, TB(L), D(J), S(K), Q, H, XA, TA, FMAX, BETAB, BETAA
21 CONTINUE
C   INPUT FORMATS
10 FORMAT (1F10.2)
14 FORMAT (6F10.1)
40 FORMAT (3I4)
C   OUTPUT FORMATS
 6 FORMAT (1H )
 7 FORMAT (1H1/ 1H-/ 1H )
 8 FORMAT (1H-/ 1HU)
12 FORMAT (1X, F10.1, 1X, F8.1, 1X, F9.1, 1X, F8.2, 4X, F9.1, 3X,
1  F10.2, 3X, F10.2, 3X, F8.2, 1X, F8.2, 1X, F7.2)
15 FORMAT (1X, 80H SAG AND TENSION CHARTS - 1200 PEOPLE PER HOUR, CHA
11RS LOADED, 1-1/8 ROPE                //)
20 FORMAT (1X,105H TENSION TB   RISE D   RUN L   WT/FT Q   TENSION H
1  DISTANCE XA   TENSION TA   SAG FMAX   BETAB   BETAA           /)
      END

```

INPUT DATA

\$ENTRY

6	6	6				
12.03						
120.0	110.0	100.0	90.0	80.0	70.0	
220.0	200.0	180.0	160.0	140.0	130.0	
20000.0	19750.0	19500.0	19250.0	19000.0	18750.0	

\$IBSYS

Table 15 Computer Output, Sag and Tension Chart

SAG AND TENSION CHARTS - 1200 PEOPLE PER HOUR, CHAIRS LOADED, 1-1/8 ROPE

TENSION TB	RISE D	RUN L	WT/FT Q	TENSION H	DISTANCE XA	TENSION TA	SAG FMAX	BETAB	BETA A
20000.0	100.0	220.0	12.03	17619.8	496.08	18799.80	4.54	3.79	-4.04
20000.0	90.0	220.0	12.03	17969.3	455.57	18919.81	4.38	3.79	-4.01
20000.0	90.0	200.0	12.03	17711.7	504.18	18919.37	3.72	3.45	-3.65
20000.0	80.0	220.0	12.03	18302.5	409.93	19039.81	4.23	3.79	-3.99
20000.0	80.0	200.0	12.03	18089.1	458.45	19039.43	3.58	3.45	-3.62
20000.0	80.0	180.0	12.03	17809.7	511.26	19039.08	2.99	3.10	-3.26
20000.0	70.0	220.0	12.03	18615.5	359.18	19159.83	4.10	3.79	-3.95
20000.0	70.0	200.0	12.03	18445.6	406.53	19159.49	3.45	3.45	-3.60
20000.0	70.0	180.0	12.03	18220.3	458.95	19159.19	2.87	3.10	-3.24
20000.0	70.0	160.0	12.03	17916.2	516.94	19158.92	2.35	2.76	-2.88
19750.0	100.0	220.0	12.03	17391.7	488.23	18549.88	4.60	3.84	-4.09
19750.0	90.0	220.0	12.03	17737.4	448.27	18669.87	4.43	3.84	-4.06
19750.0	90.0	200.0	12.03	17483.3	496.39	18669.43	3.77	3.49	-3.59
19750.0	80.0	220.0	12.03	18067.0	403.24	18789.87	4.29	3.84	-4.04
19750.0	80.0	200.0	12.03	17856.6	451.27	18789.48	3.63	3.49	-3.67
19750.0	80.0	180.0	12.03	17580.9	503.54	18789.12	3.03	3.14	-3.30
19750.0	70.0	220.0	12.03	18376.8	353.17	18909.88	4.16	3.84	-4.01
19750.0	70.0	200.0	12.03	18209.2	400.03	18909.53	3.50	3.49	-3.65
19750.0	70.0	180.0	12.03	17987.0	451.92	18909.22	2.91	3.14	-3.28
19750.0	70.0	160.0	12.03	17686.9	509.30	18908.95	2.38	2.79	-2.92
19500.0	100.0	220.0	12.03	17163.6	480.39	18299.96	4.66	3.89	-4.15
19500.0	90.0	220.0	12.03	17505.5	440.97	18419.94	4.49	3.89	-4.12
19500.0	90.0	200.0	12.03	17254.9	488.60	18419.48	3.82	3.54	-3.74
19500.0	80.0	220.0	12.03	17831.5	396.55	18539.93	4.34	3.89	-4.09
19500.0	80.0	200.0	12.03	17624.0	444.09	18539.53	3.66	3.54	-3.72
19500.0	80.0	180.0	12.03	17352.1	495.82	18539.16	3.07	3.18	-3.35
19500.0	70.0	220.0	12.03	18138.0	347.15	18659.93	4.21	3.89	-4.07
19500.0	70.0	200.0	12.03	17972.8	393.54	18659.58	3.55	3.54	-3.70
19500.0	70.0	180.0	12.03	17753.6	444.89	18659.26	2.94	3.18	-3.33
19500.0	70.0	160.0	12.03	17457.5	501.66	18658.97	2.41	2.83	-2.96
19250.0	100.0	220.0	12.03	16935.5	472.54	18050.04	4.72	3.94	-4.20
19250.0	90.0	220.0	12.03	17273.6	433.67	18170.01	4.55	3.94	-4.18
19250.0	90.0	200.0	12.03	17026.5	480.80	18169.54	3.87	3.58	-3.80
19250.0	80.0	220.0	12.03	17596.0	389.86	18290.00	4.40	3.94	-4.15
19250.0	80.0	200.0	12.03	17391.5	436.91	18289.58	3.73	3.58	-3.77
19250.0	80.0	180.0	12.03	17123.3	488.09	18289.20	3.11	3.22	-3.39
19250.0	70.0	220.0	12.03	17899.2	341.13	18409.98	4.27	3.94	-4.12
19250.0	70.0	200.0	12.03	17736.3	387.05	18409.62	3.59	3.58	-3.75
19250.0	70.0	180.0	12.03	17520.3	437.86	18409.29	2.98	3.22	-3.37
19250.0	70.0	160.0	12.03	17228.2	494.01	18409.00	2.44	2.87	-3.00
19000.0	100.0	220.0	12.03	16707.4	464.69	17800.12	4.79	3.99	-4.26
19000.0	90.0	220.0	12.03	17041.6	426.37	17920.09	4.61	3.99	-4.23
19000.0	90.0	200.0	12.03	16798.1	473.01	17919.60	3.93	3.63	-3.85
19000.0	80.0	220.0	12.03	17360.5	383.17	18040.06	4.46	3.99	-4.21



Figure 1
Monocable
Ropeway, Drive
Terminal
Counterweighted

Figure 2
Monocable Ropeway,
Drive Terminal Anchored



Figure 3
Monocable Ropeway,
Idler Terminal Anchored



Figure 4
Monocable Ropeway,
Idler Terminal Counterweighted



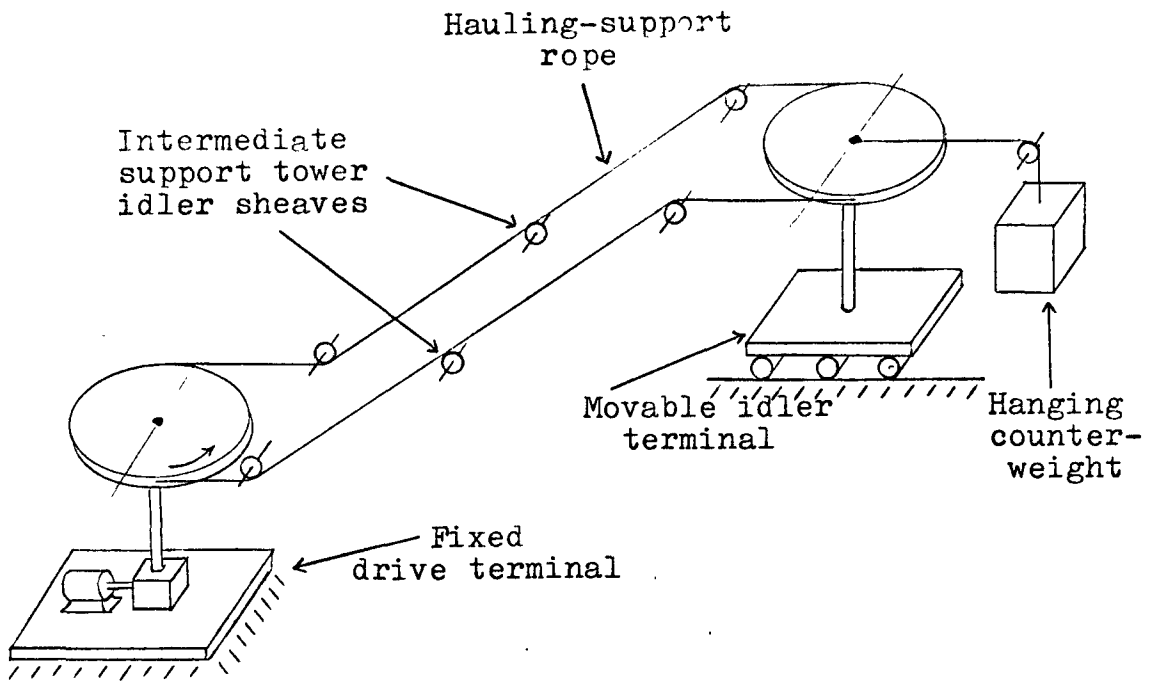


Figure 5. Monocable Ropeway with Fixed Drive and Movable Idler Terminals

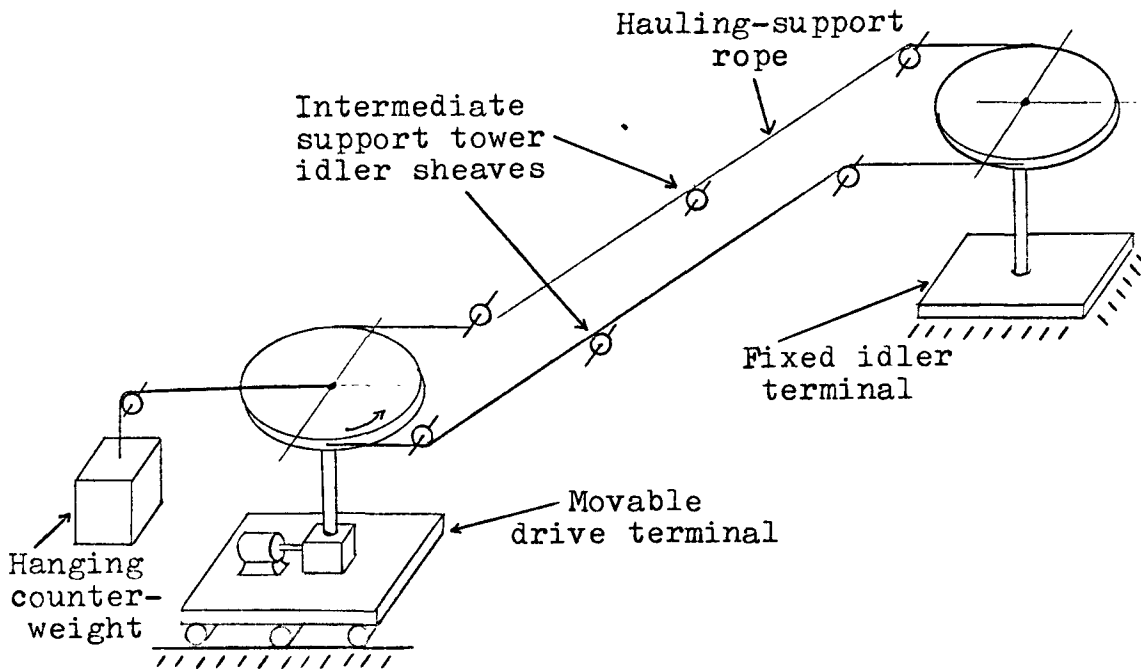


Figure 6. Monocable Ropeway with Movable Drive and Fixed Idler Terminals



Figure 8 T-Bar Lift



Figure 7 Platter Lift

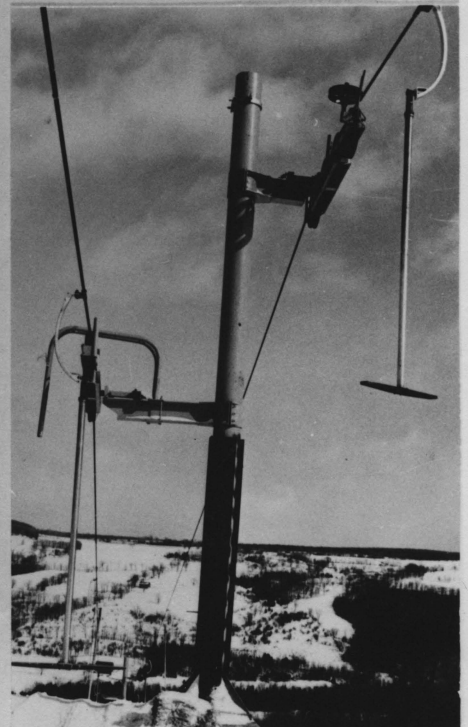


Figure 9 T-Bar Lift Showing Intermediate Tower and T-Bars



Figure 10
Ski Area Chair Lift,
Open Chair



Figure 11
Sight-seeing Chair Lift,
Open Fiberglass Chair

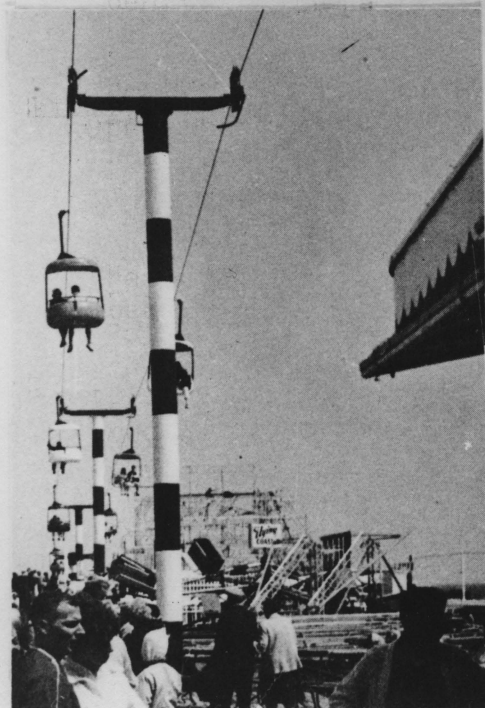


Figure 12
Sight-seeing Chair Lift,
Open Fiberglass Chair



Figure 13
Detachable Clip
Small Cabin Monocable Ropeway
(Gondola Lift)

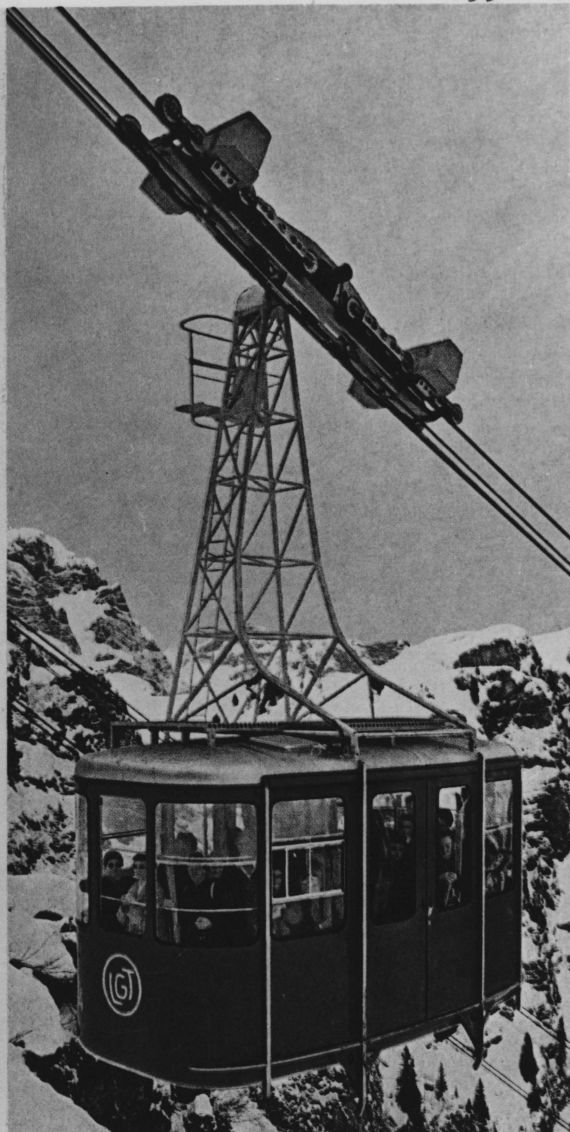


Figure 14
Reversible
Bicable Passenger Ropeway,
Large Cabin
with Twin Track Ropes



Figure 15
Continuous Bicable Passenger Ropeway,
Medium Cabin with Single Track Rope

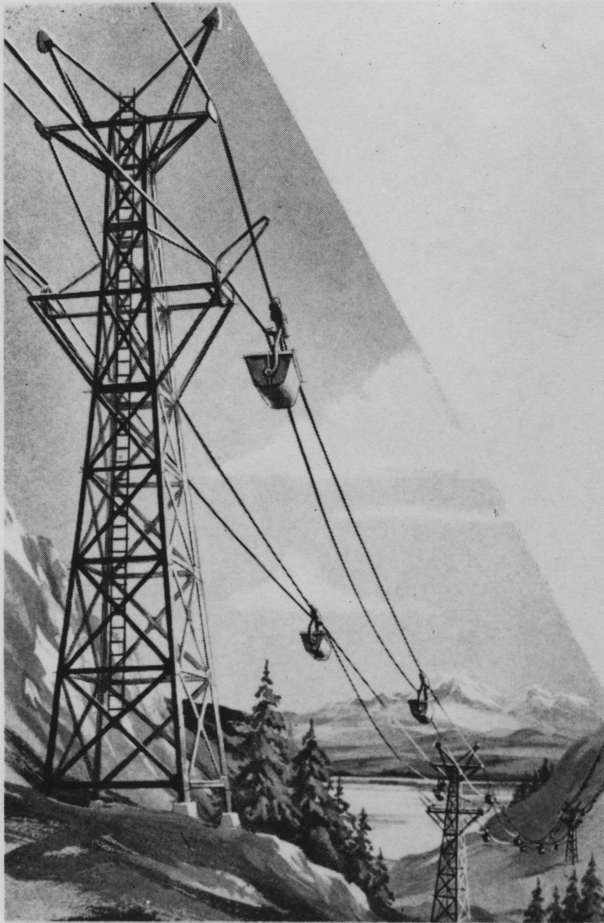


Figure 16 Bicable Ropeway for Material Transport

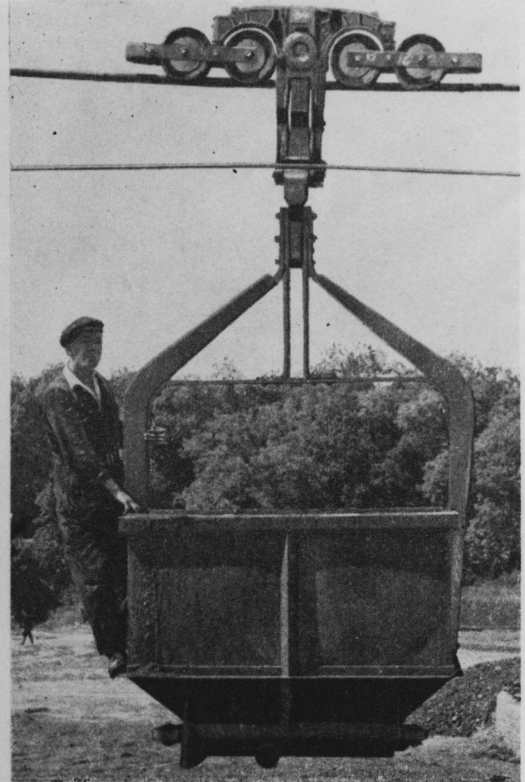


Figure 17 Bicable Ropeway Carriage and Carrier for Material Transport

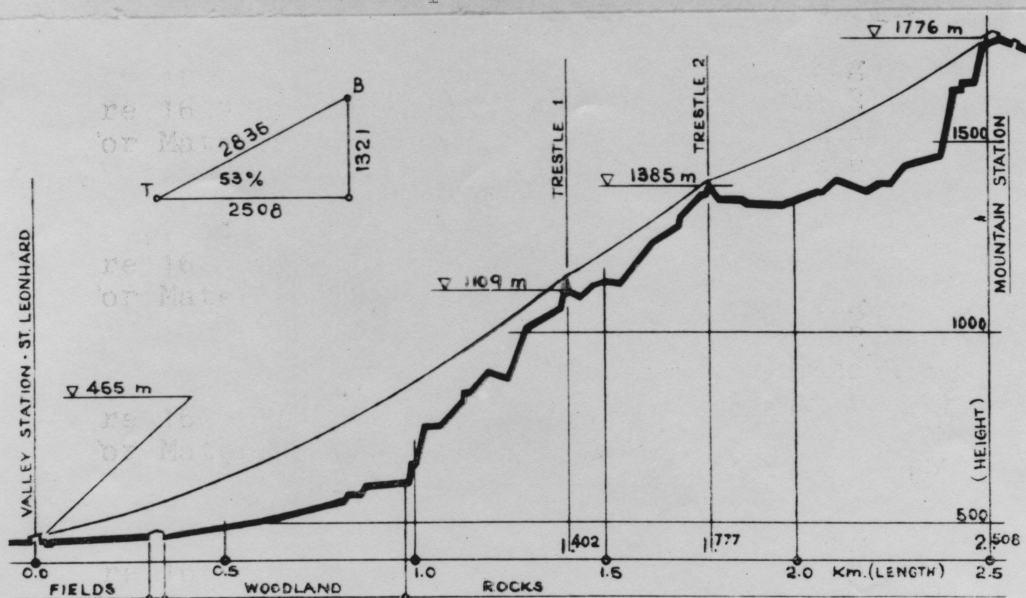


Figure 18 Typical Aerial Ropeway Profile

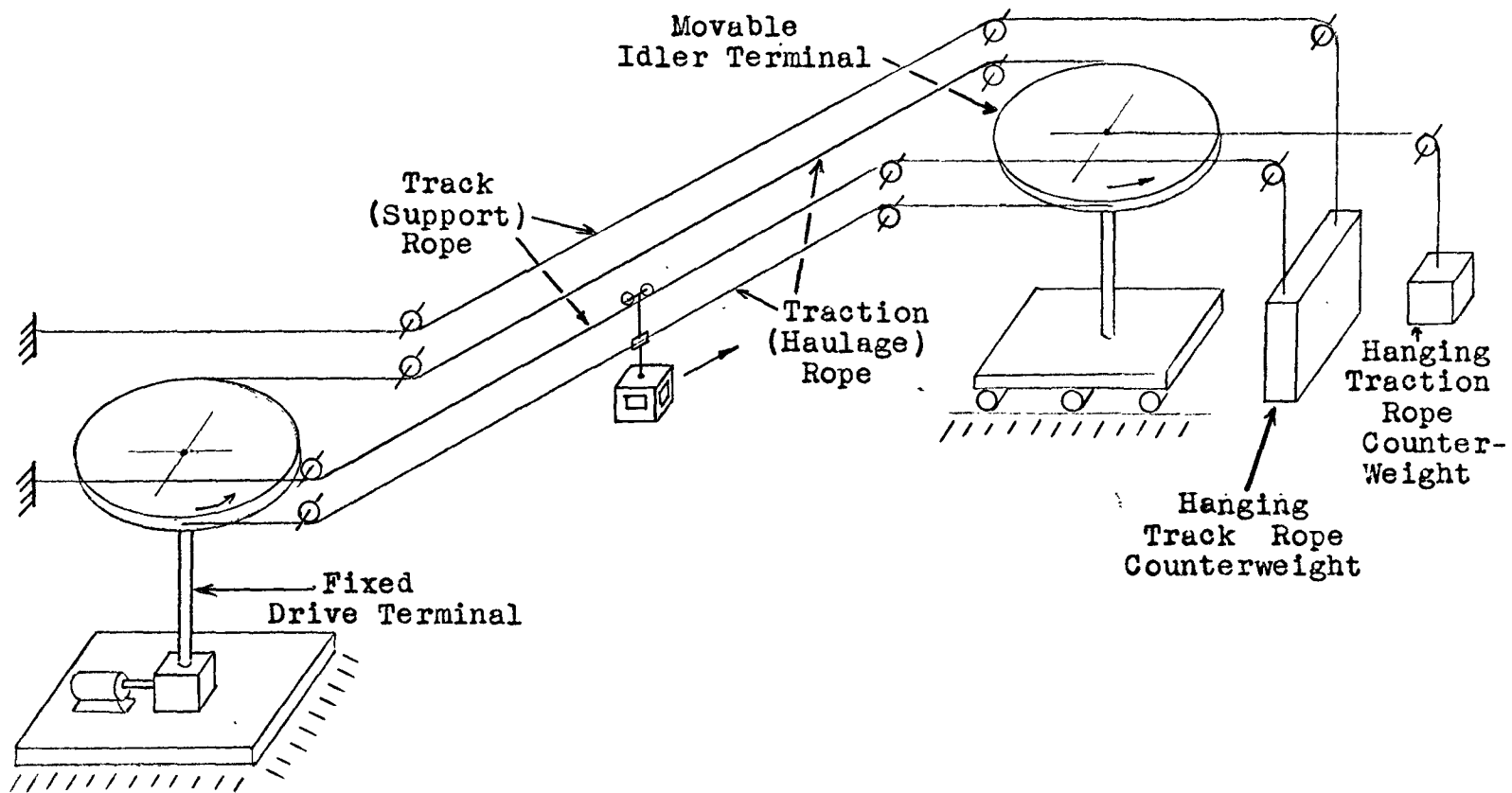


Figure 19 Continuous Bicable Ropeway
Drive and Tensioning Layout

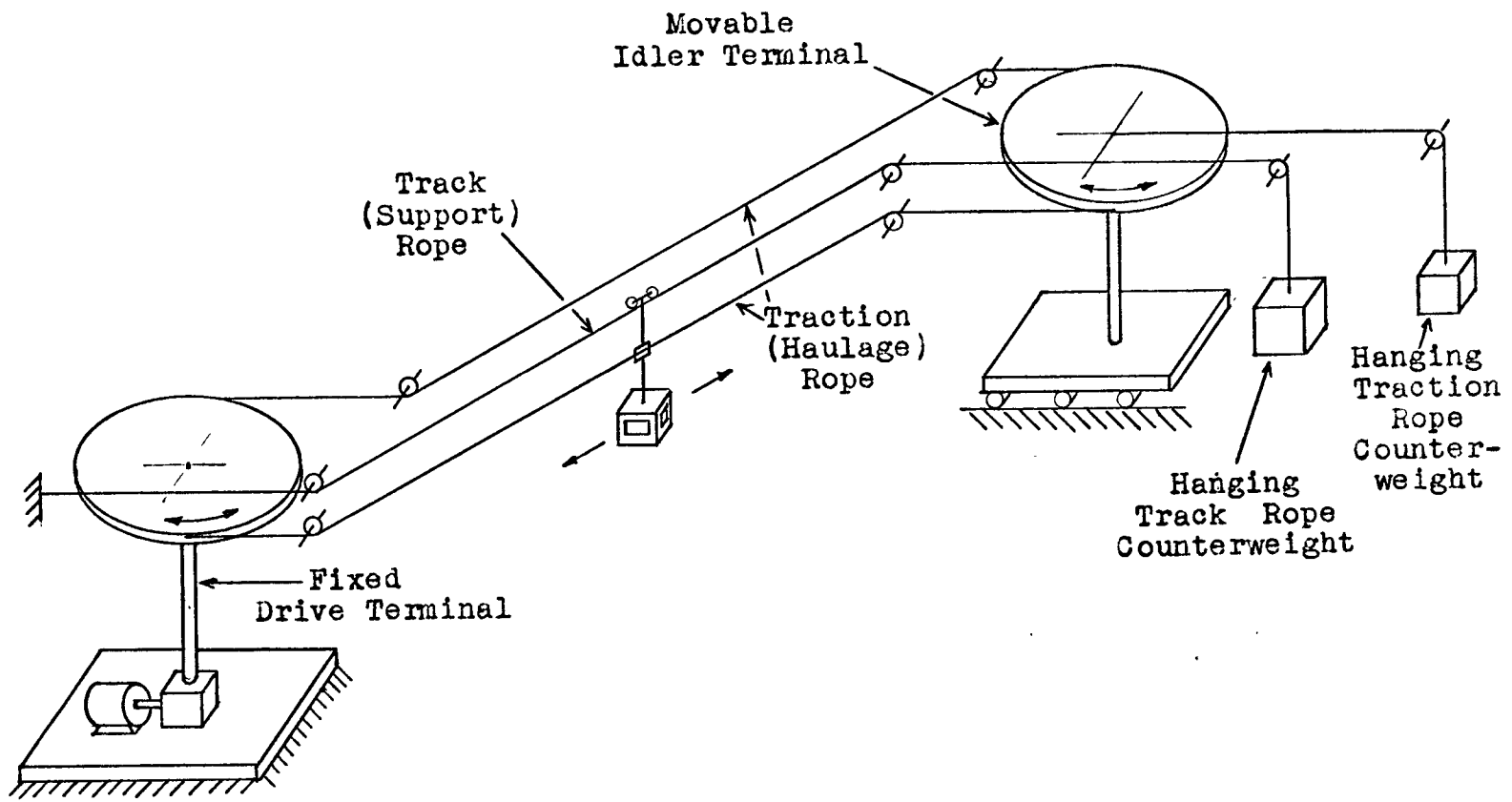


Figure 20 Single Reversible Bicable Ropeway Drive and Tensioning Layout

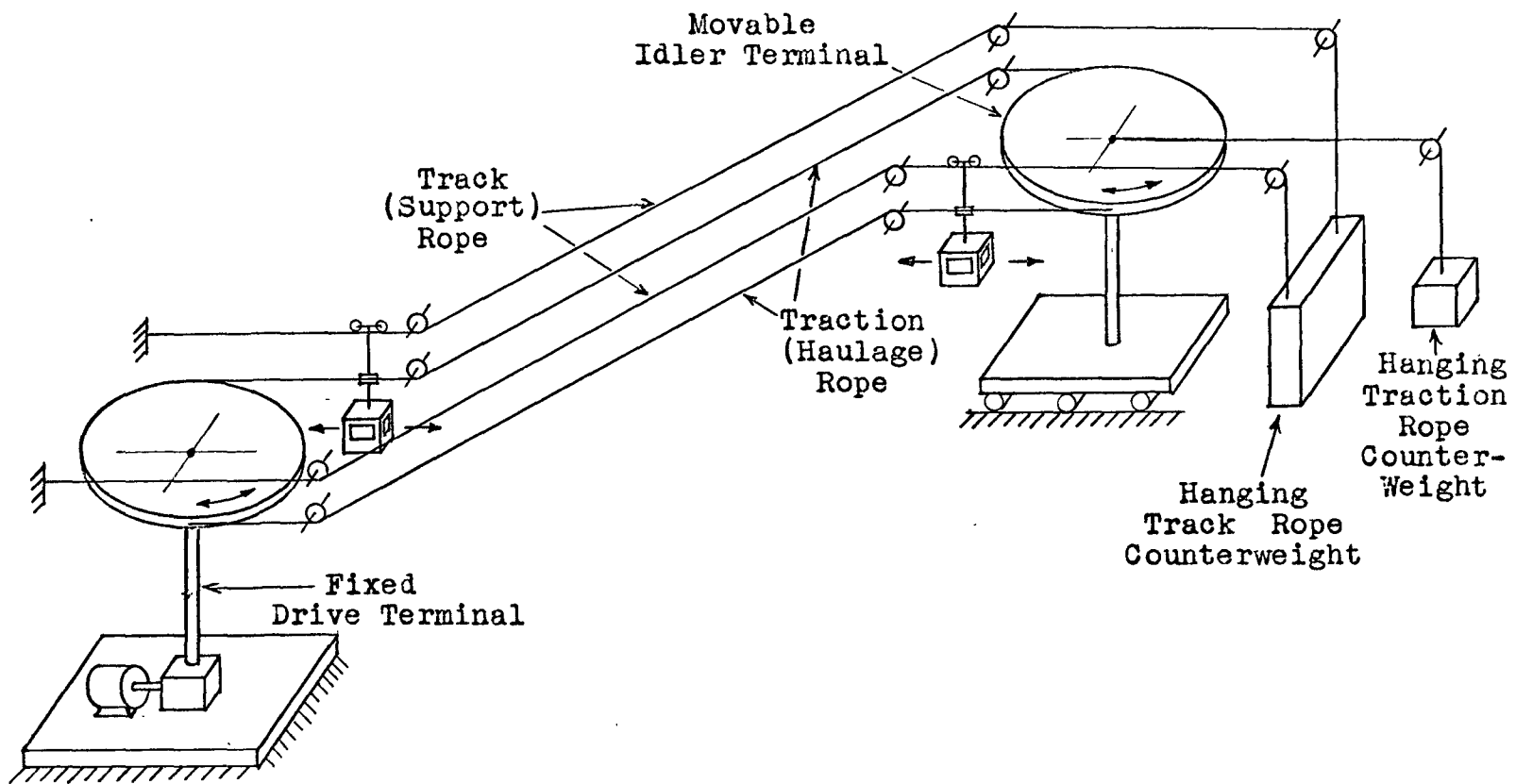


Figure 21 Double Reversible Bicable Ropeway Drive and Tensioning Layout

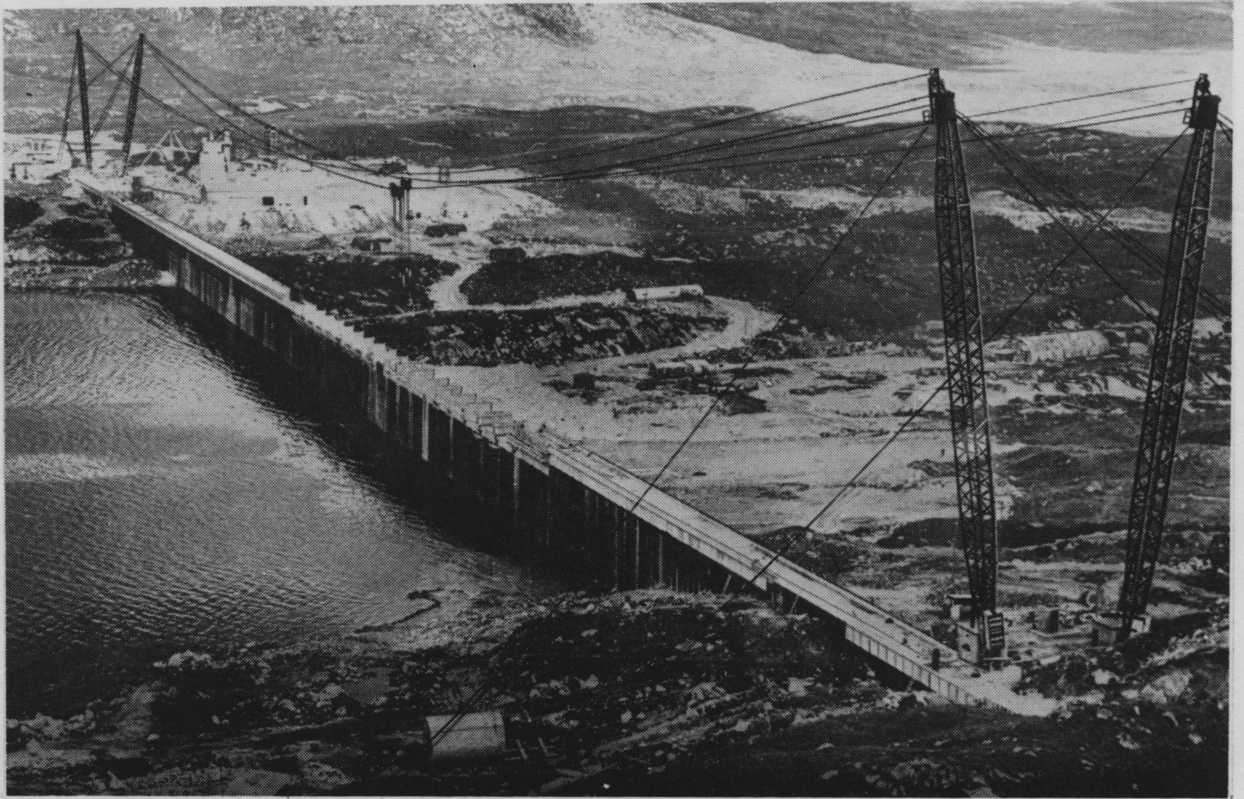


Figure 22
Two Parallel Tautline Cableways
with Fixed Needle Type Towers

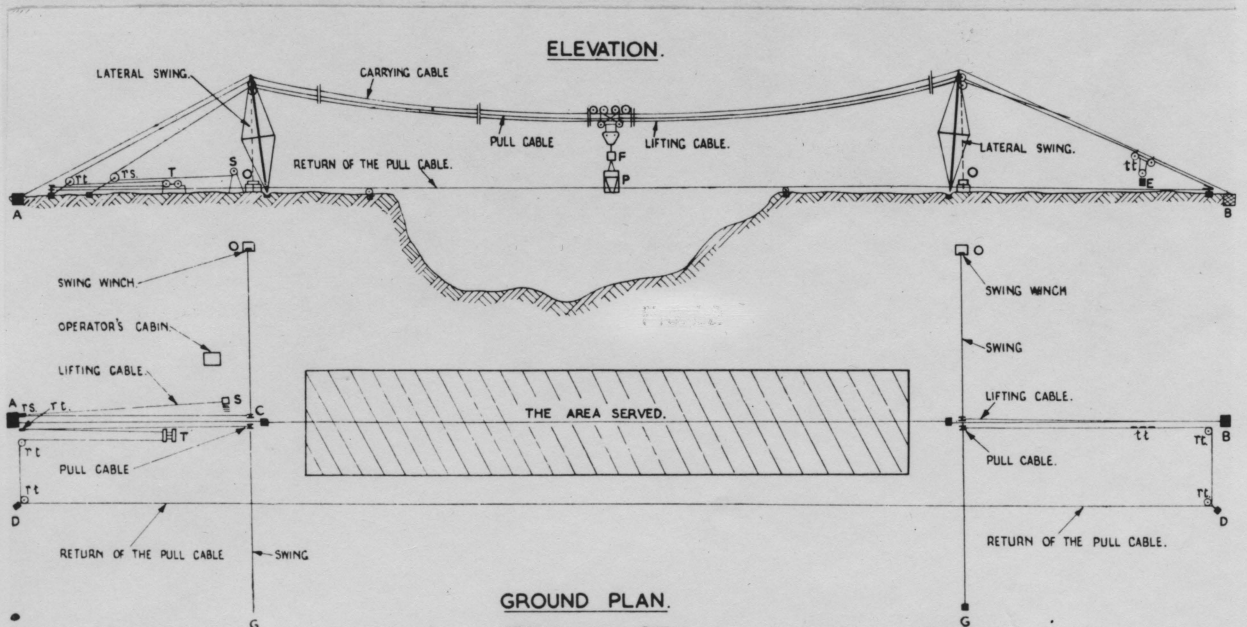


Figure 23
Typical Tautline Cableway Showing Area of Operation
for Fixed Towers with Lateral Swing

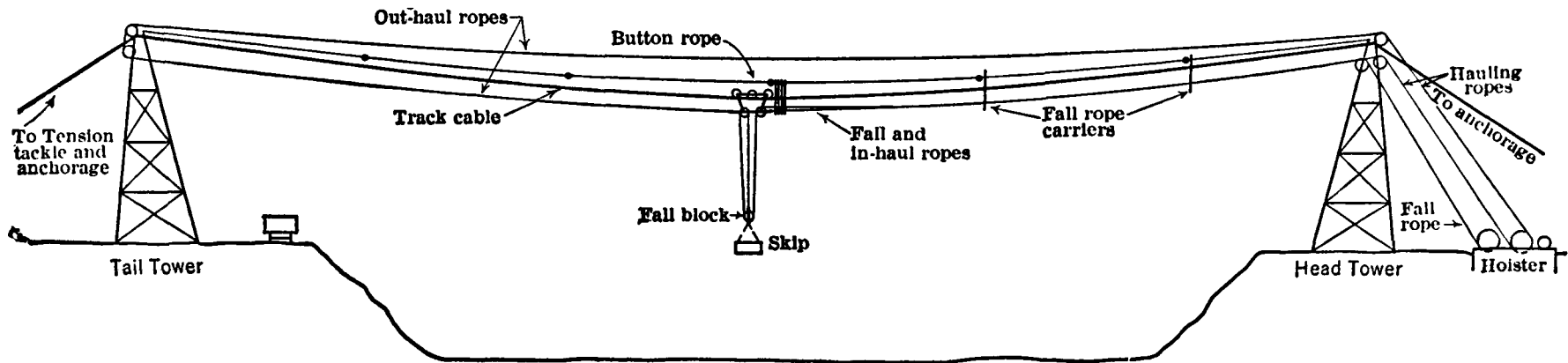


Figure 24 - Tautline Cableway with Fixed Towers

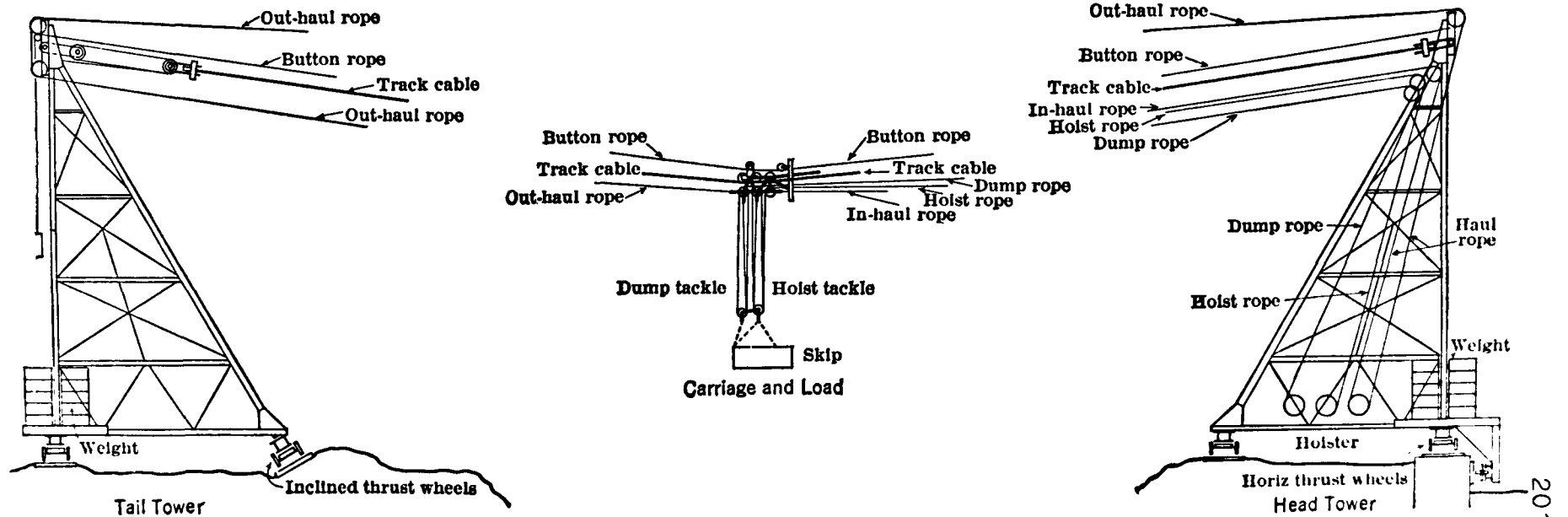


Figure 25 Tautline Cableway with Movable Towers

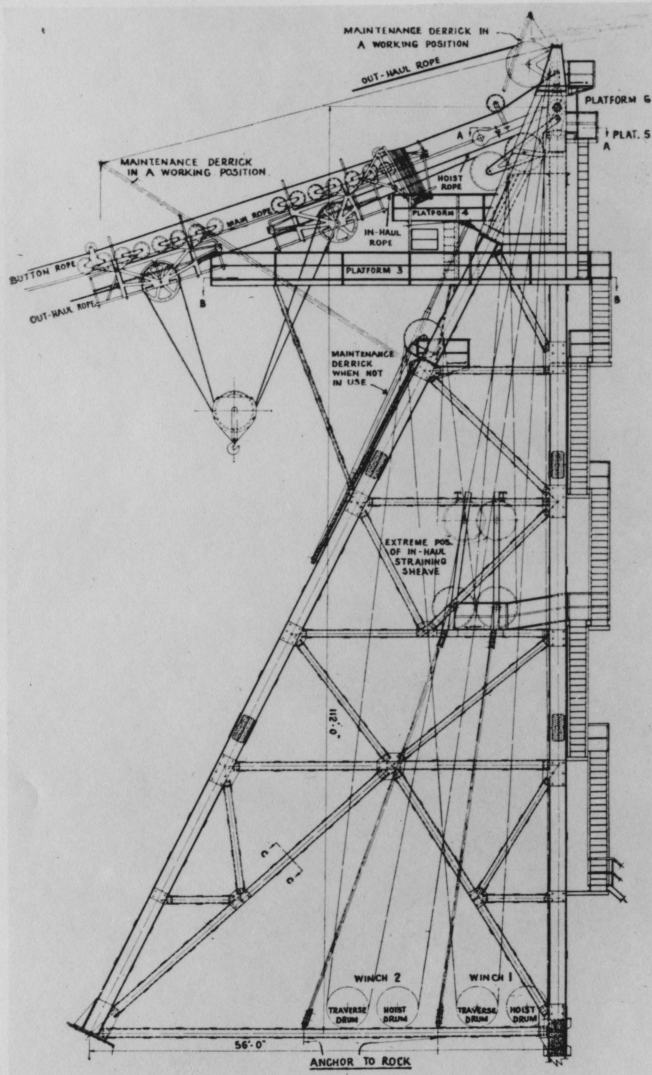


Figure 26 Tautline Cableway
Fixed Tower Detail

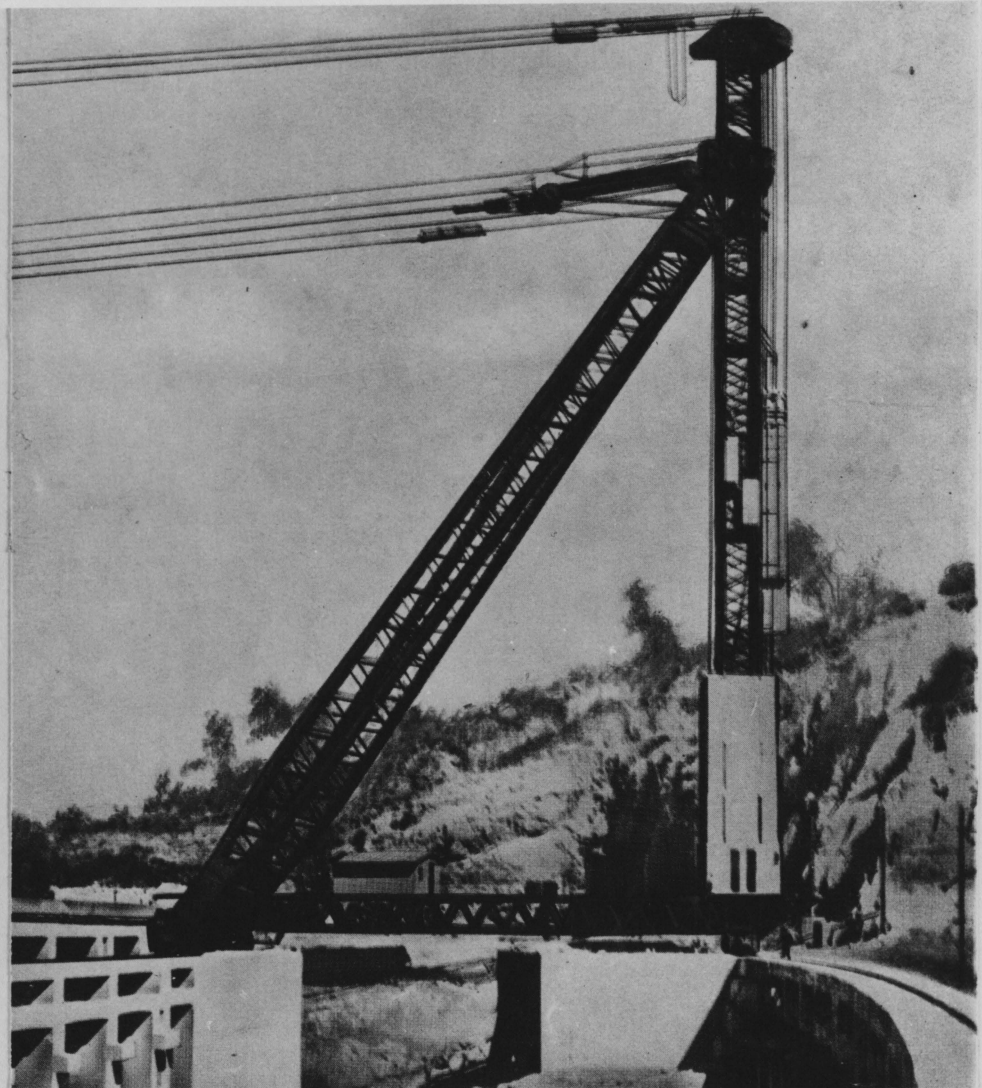


Figure 27 Tautline Cableway Radial Tower Detail

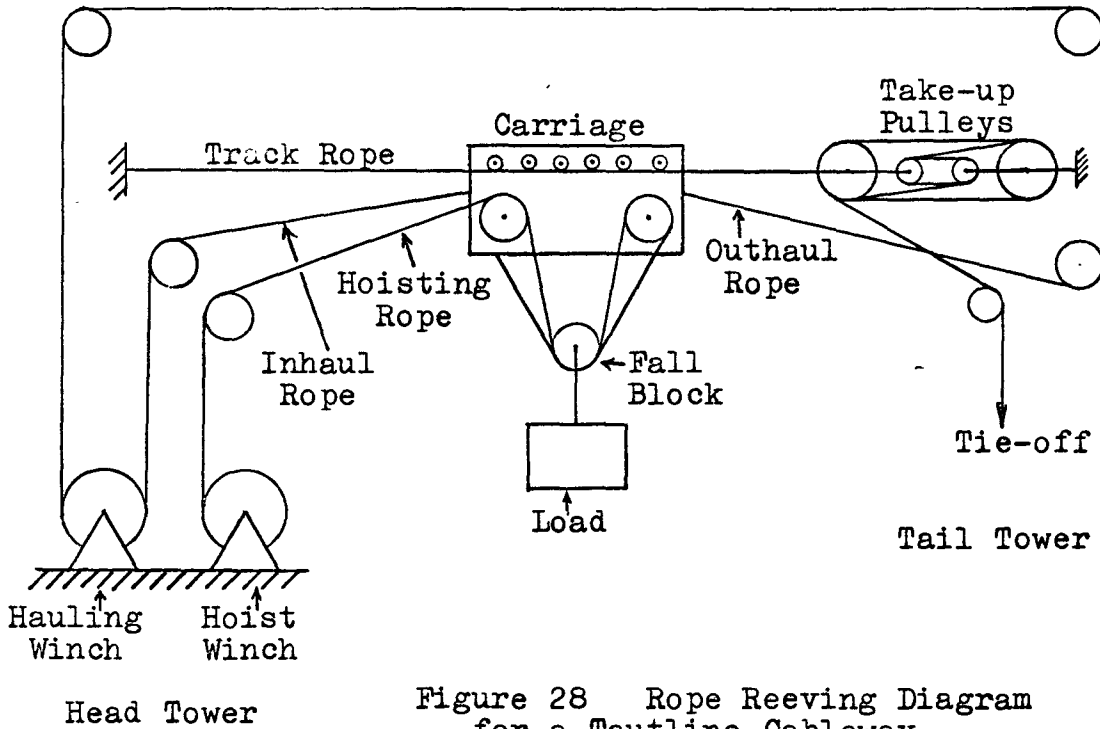


Figure 28 Rope Reeving Diagram for a Tautline Cableway

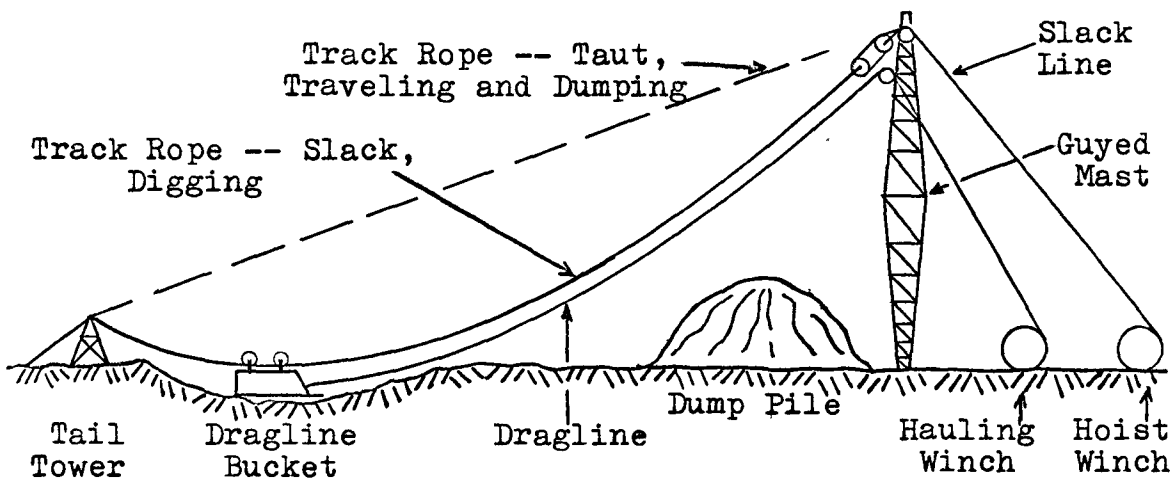


Figure 29 Slackline Cableway Excavator

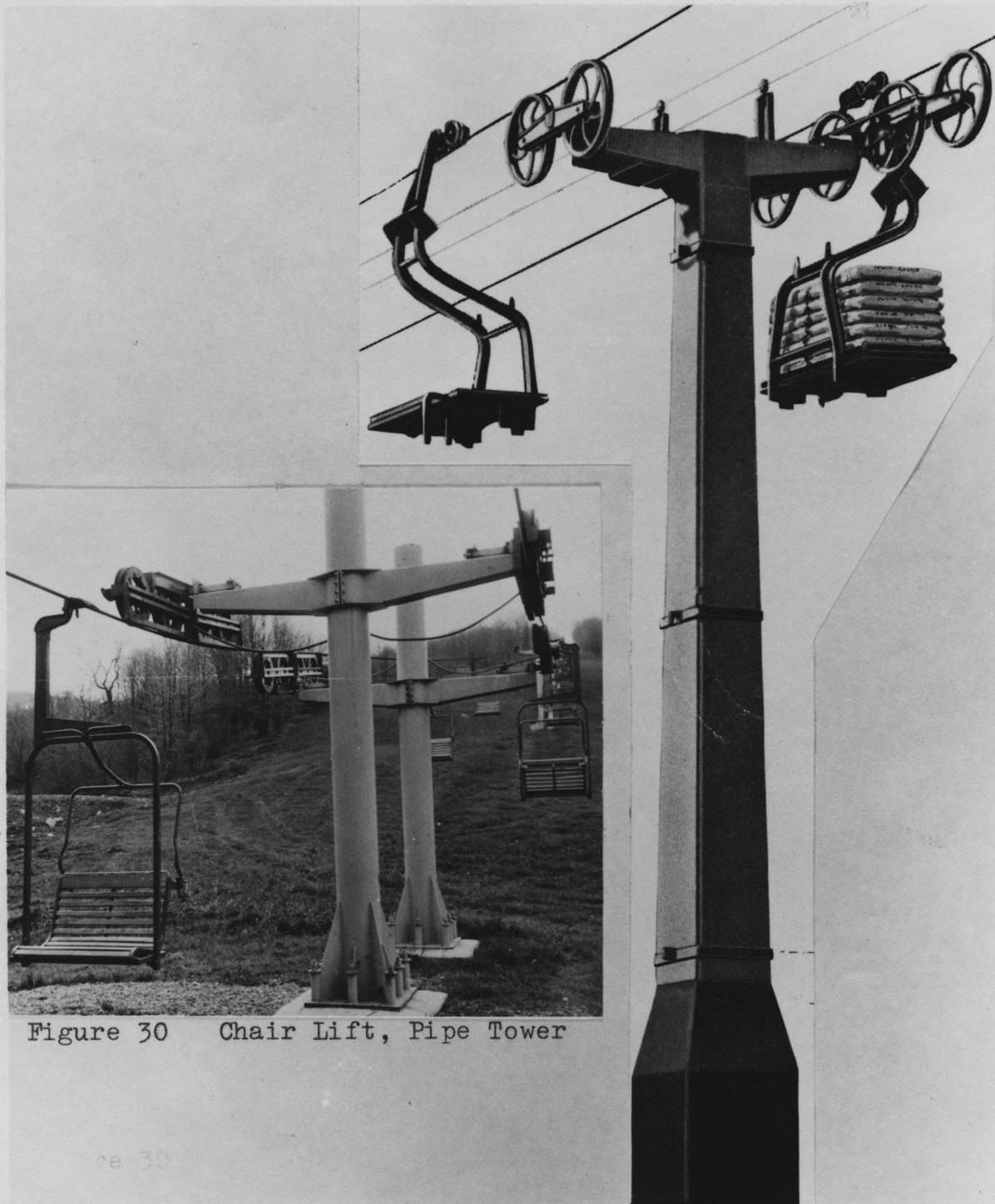


Figure 30 Chair Lift, Pipe Tower

Figure 31
Material Handling Ropeway,
Tapered Square Tower



Figure 32
Chair Lift, Hexagonal Tower

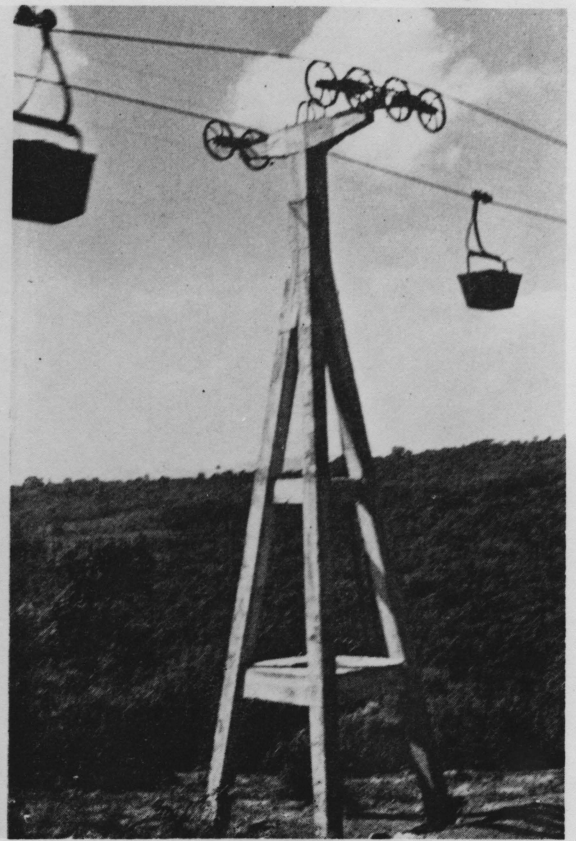


Figure 33
Material Handling Ropeway,
Light Reinforced
Concrete Tower

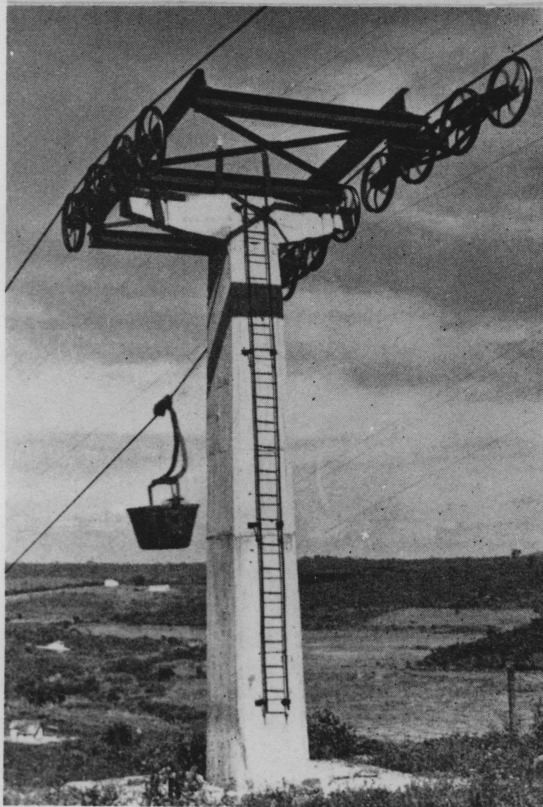


Figure 34
Material Handling Ropeway,
Heavy Reinforced Concrete Tower



Figure 35
Chair Lift,
Lattice Tower

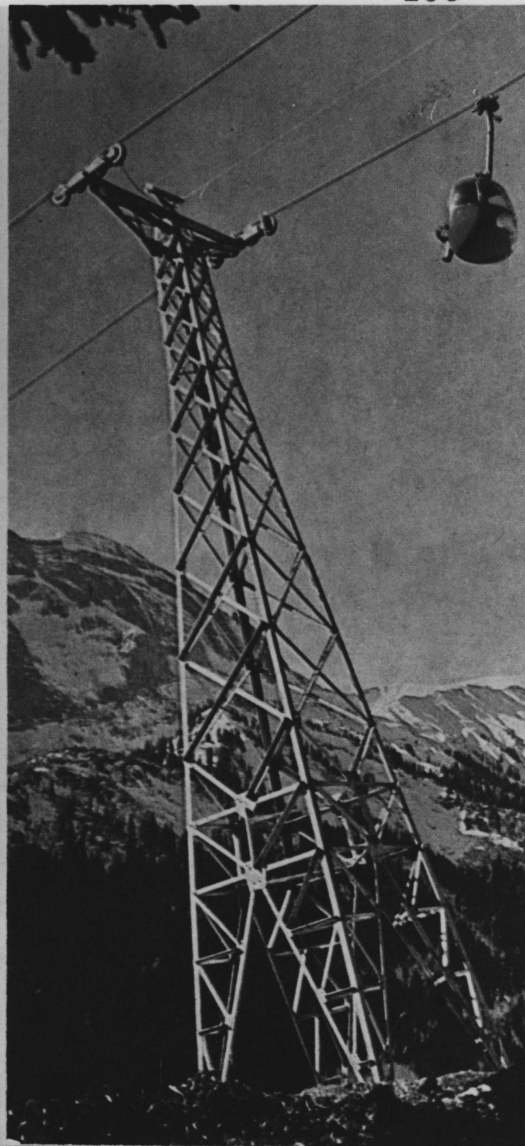


Figure 36
Gondola Lift, Lattice Tower



Figure 37
Material Handling Bicable
Ropeway, Lattice Tower

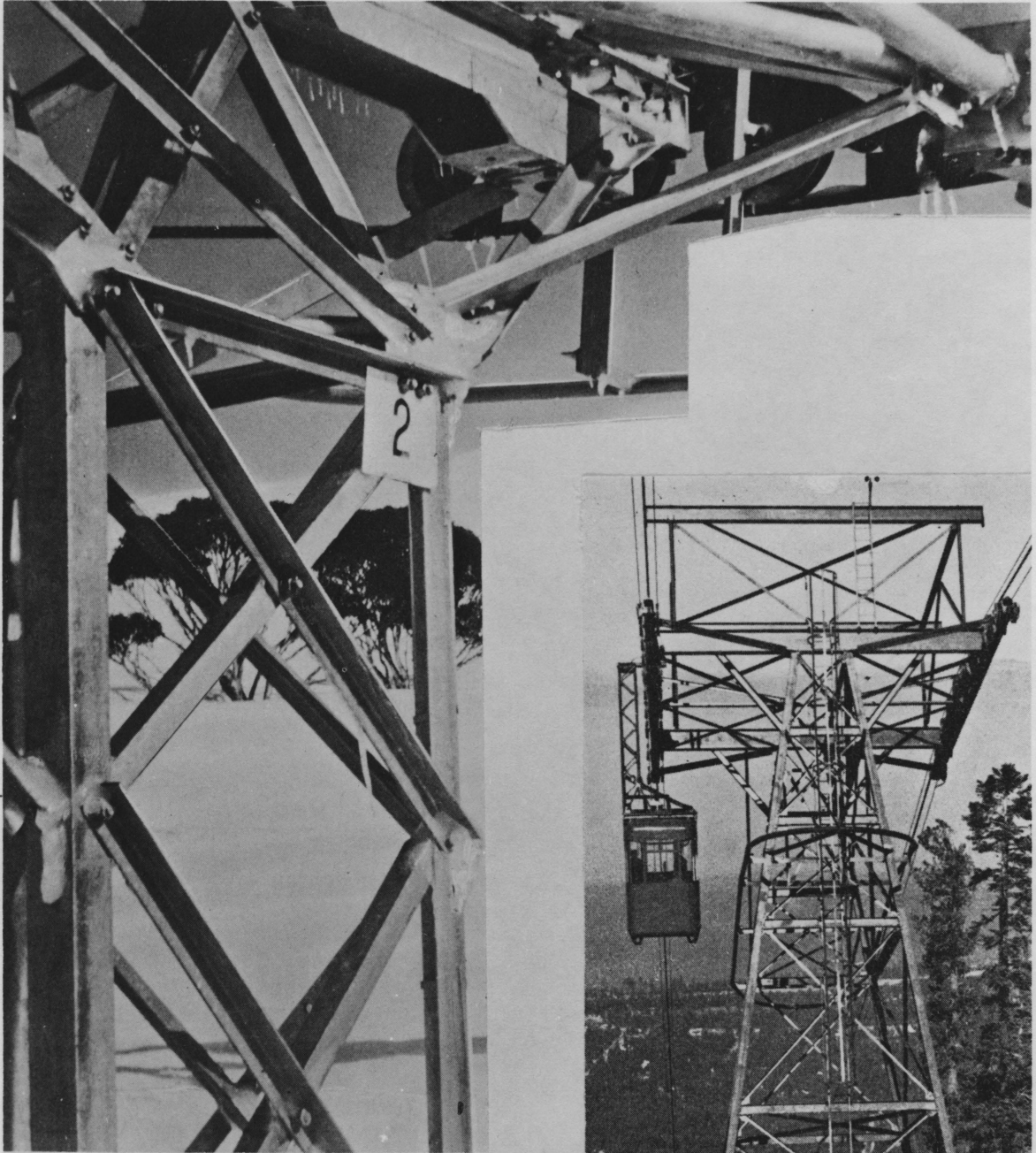


Figure 38
Construction Details,
Lattice Tower

Figure 39
Large Passenger
Bicable Ropeway,
Lattice Tower

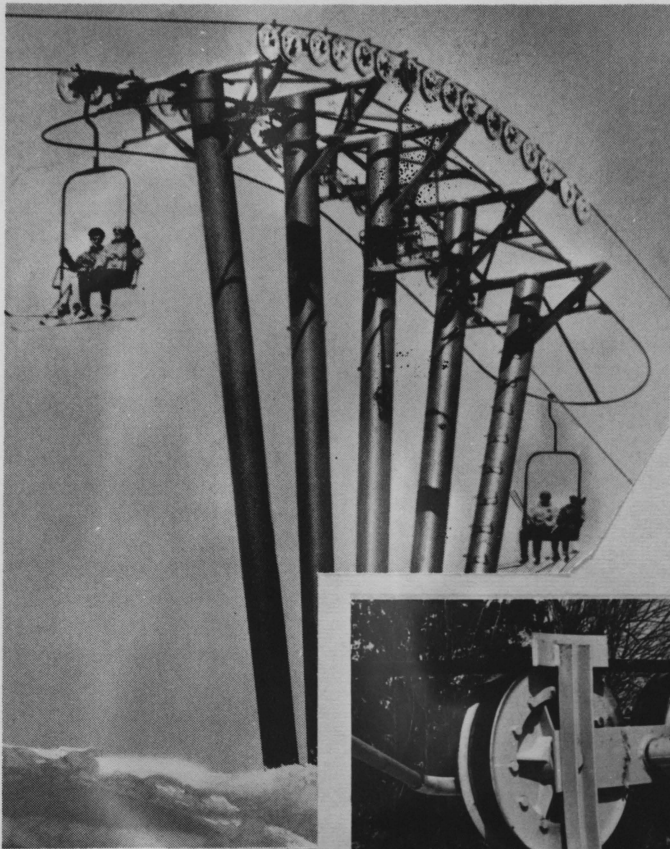


Figure 40
A Series of Chair Lift
Hold-up Pipe Towers

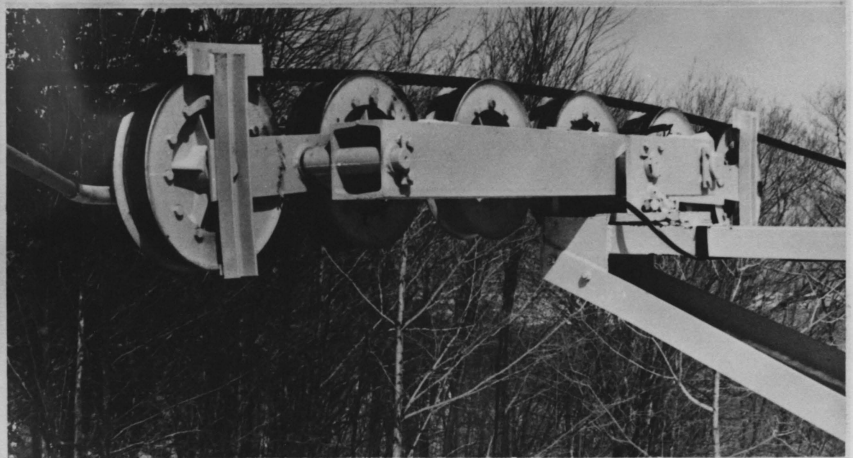


Figure 41 Intermediate Tower Idler Assembly



Figure 42
A Chair Lift Hold-down
Lattice Tower

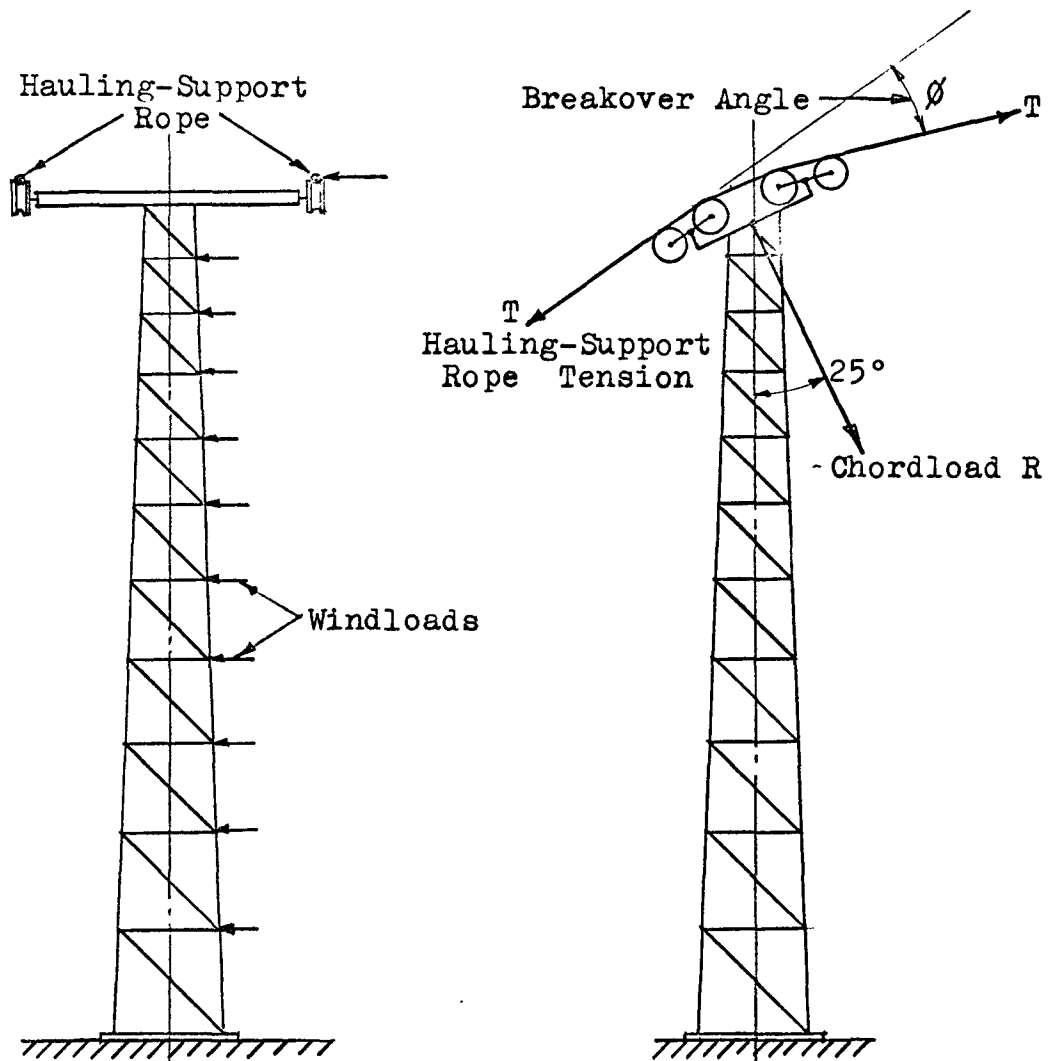


Figure 43 Lattice Tower Showing Chordload and Windloads

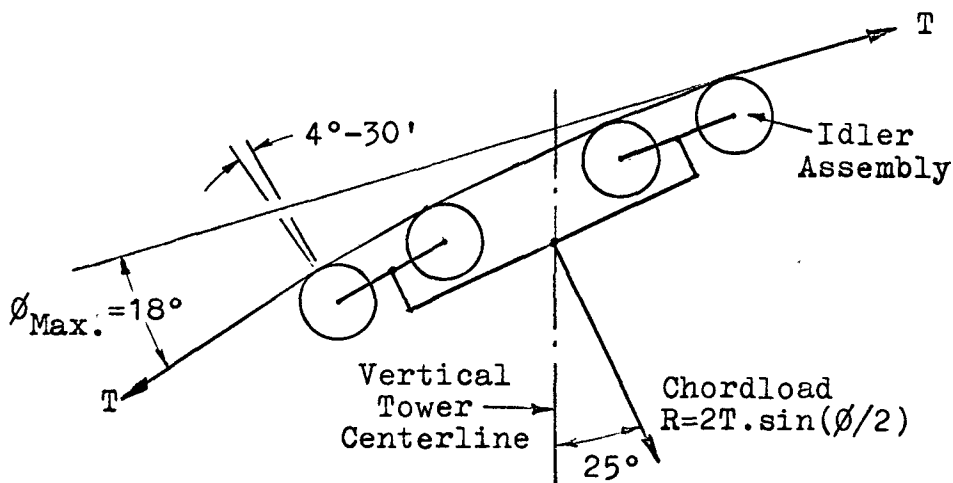


Figure 44 Four Sheave Idler Assembly Showing Maximum Breakover Angle

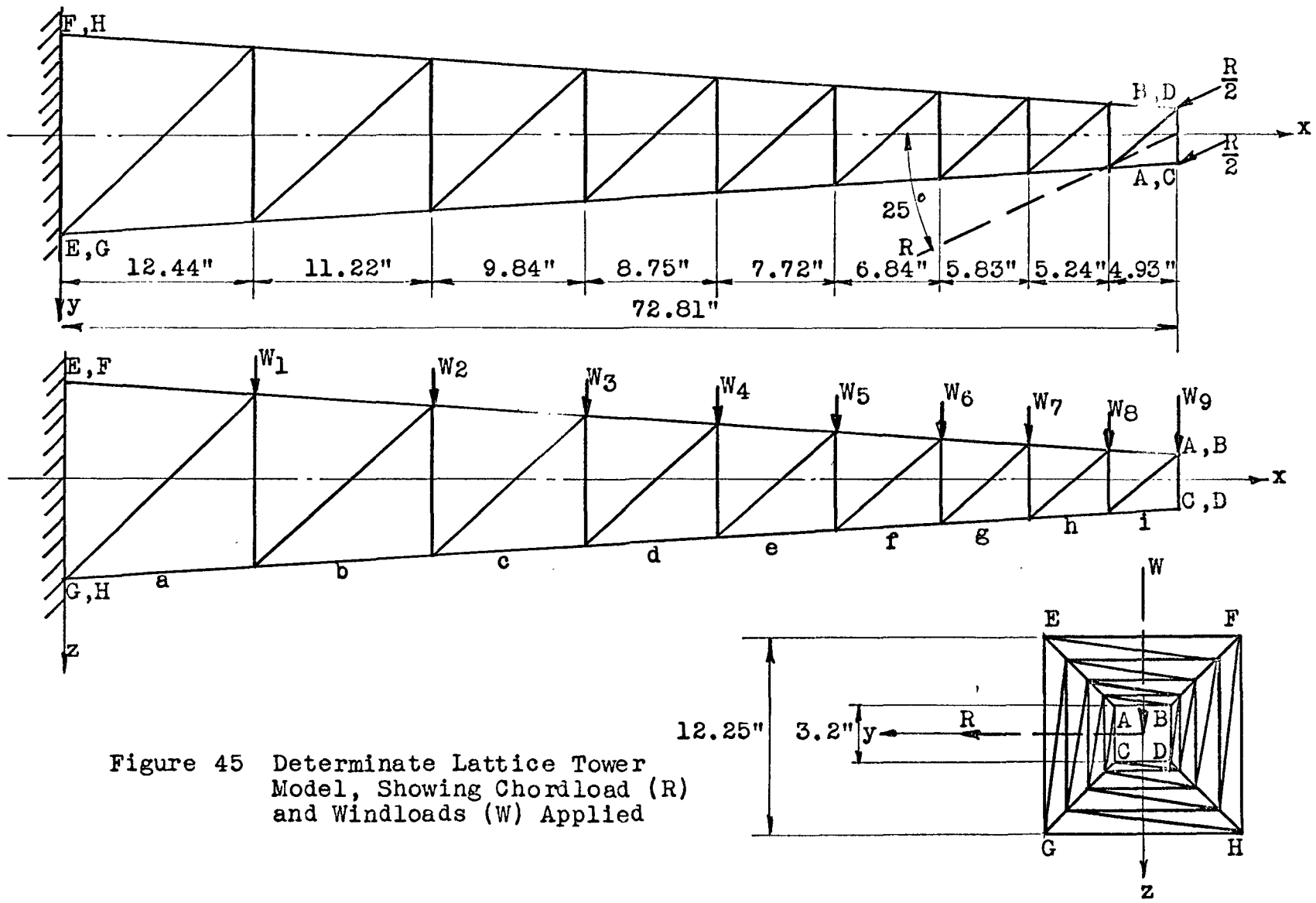


Figure 45 Determinate Lattice Tower Model, Showing Chordload (R) and Windloads (W) Applied

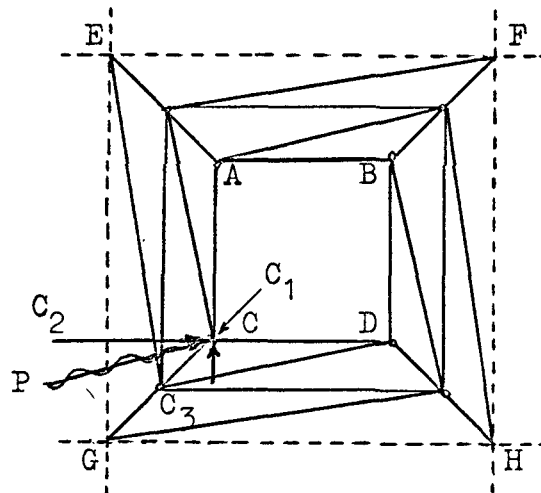
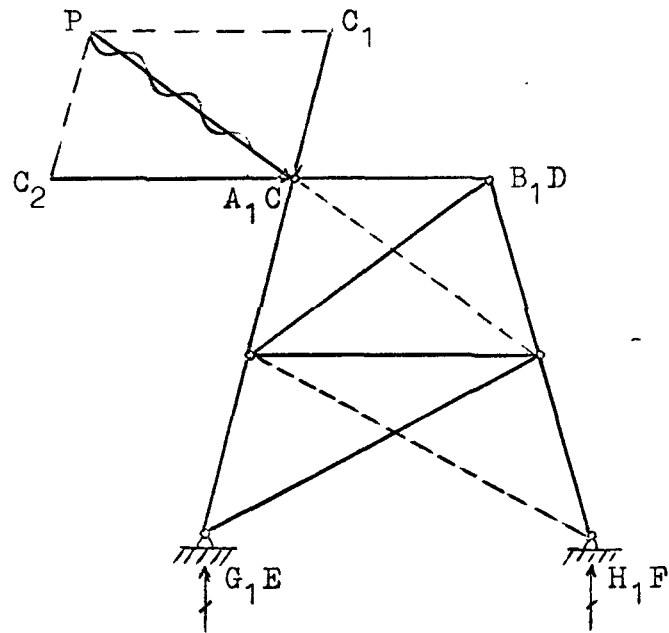
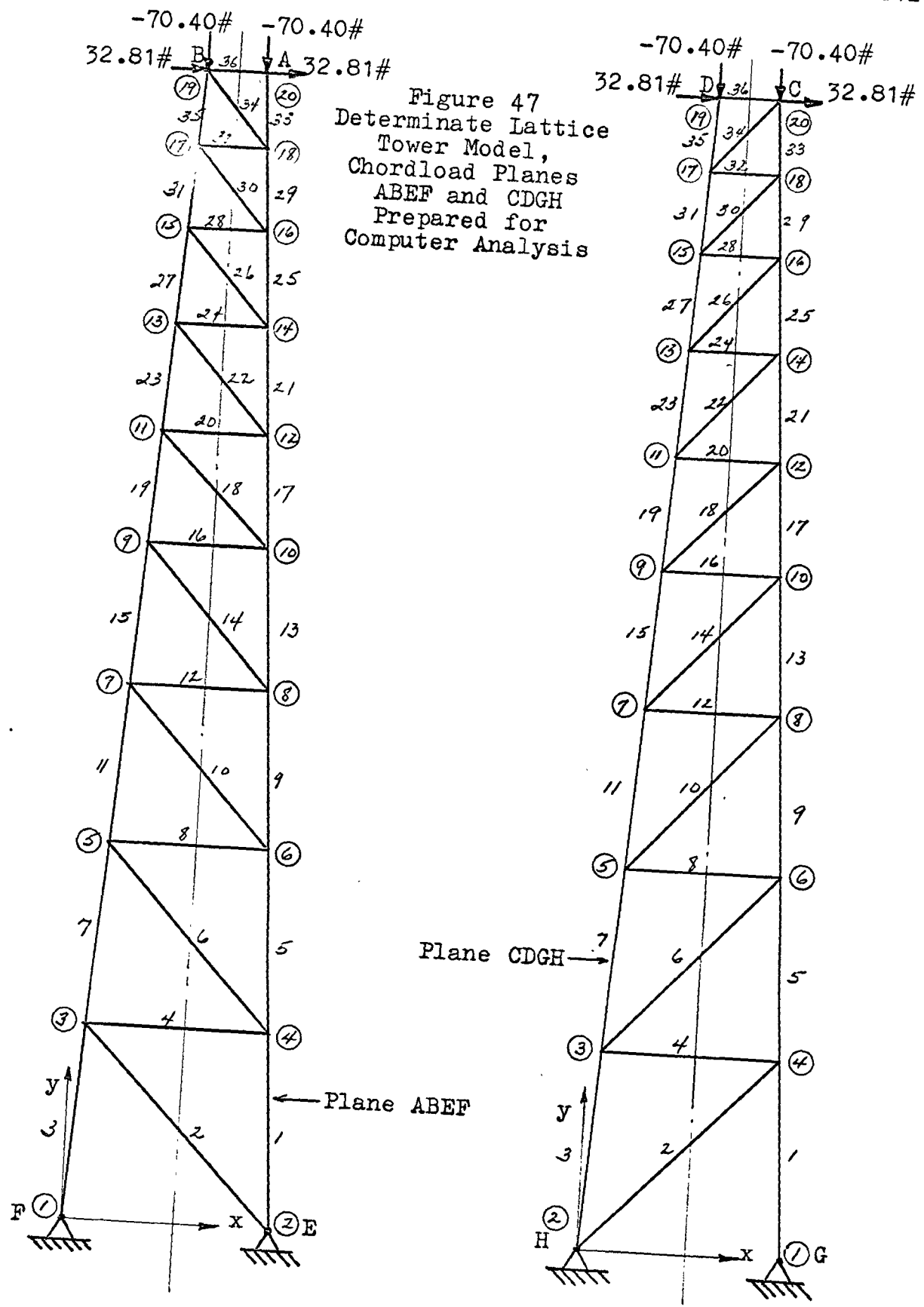


Figure 46 Square Lattice-Type Tower
With Straight Legs



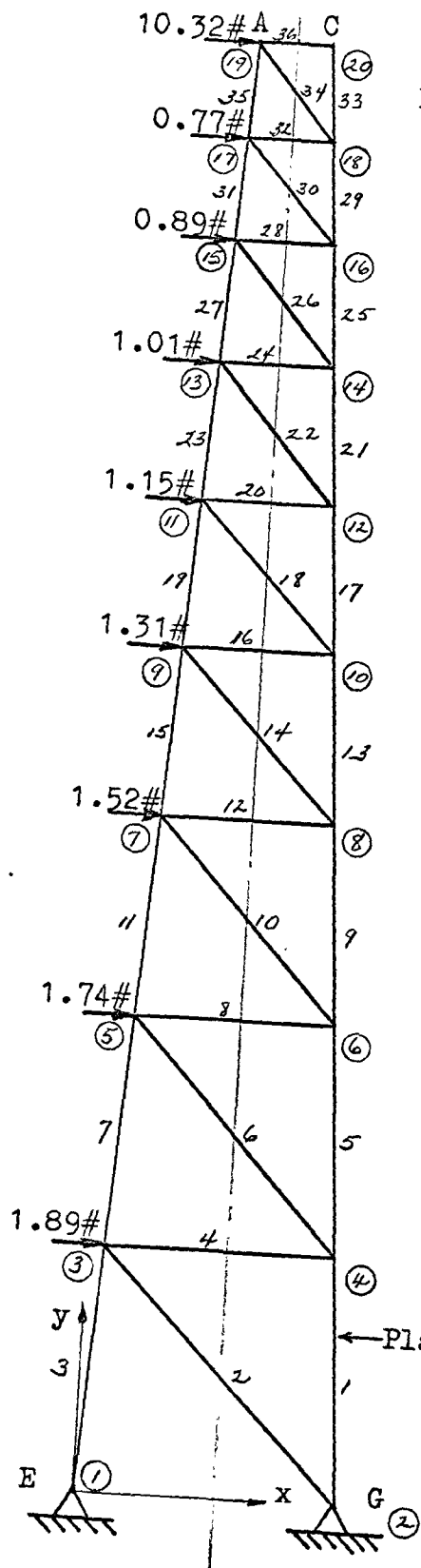
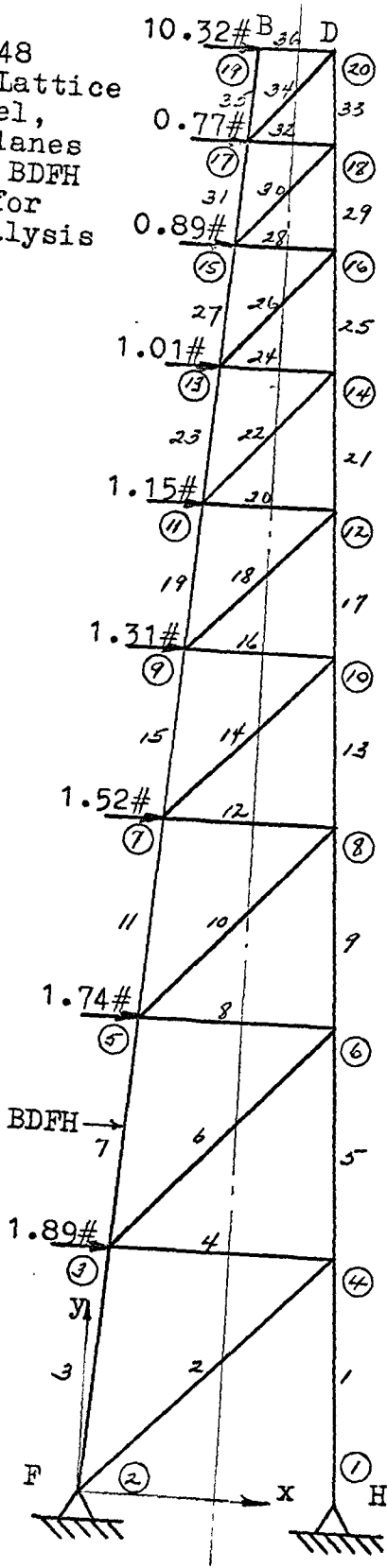


Figure 48
 Determinate Lattice
 Tower Model,
 Windload Planes
 ACEG and BDFH
 Prepared for
 Computer Analysis



Plane BDFH →

← Plane ACEG

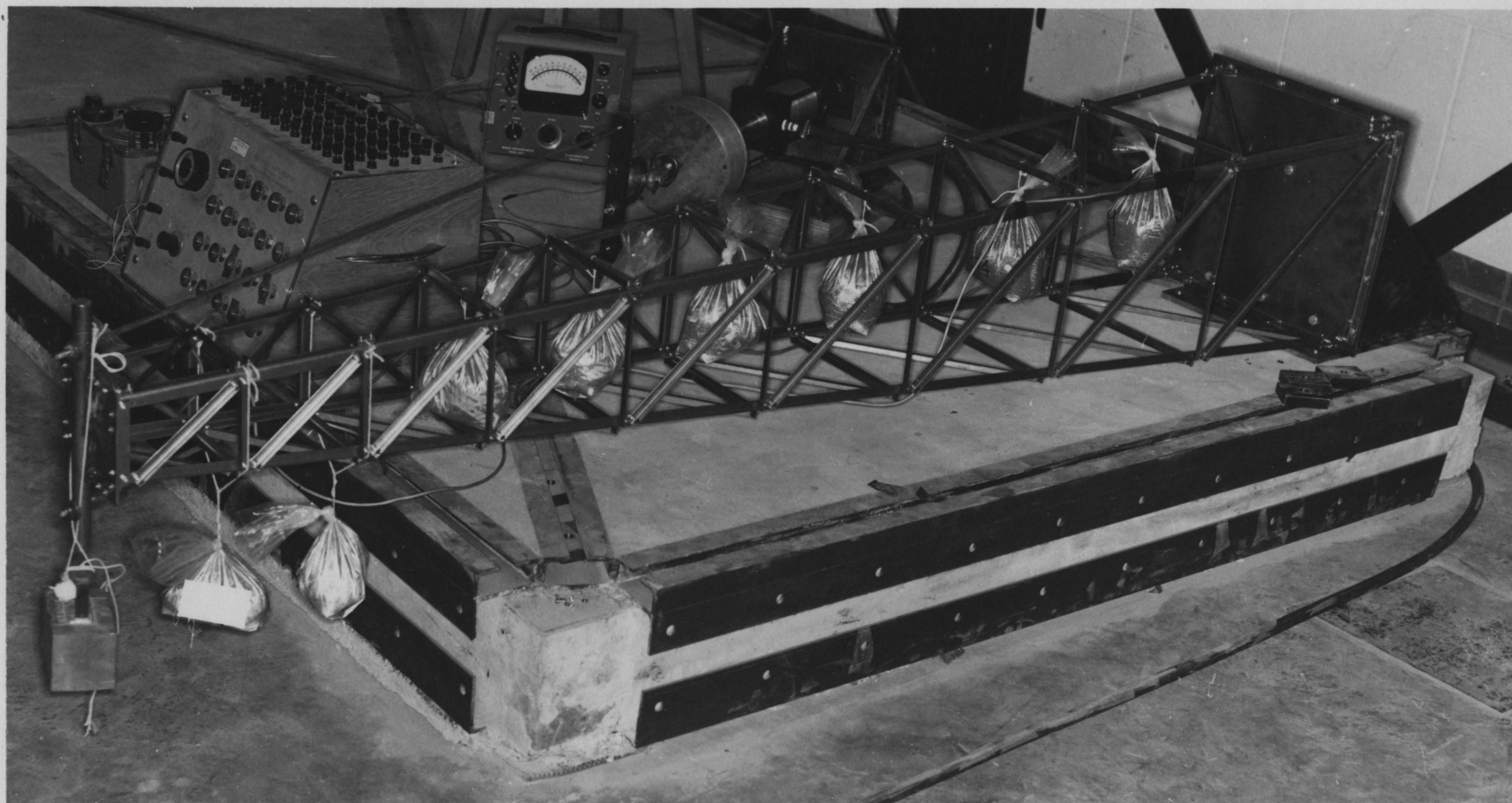


Figure 49 Determinate Lattice Tower Model
Showing Test Apparatus

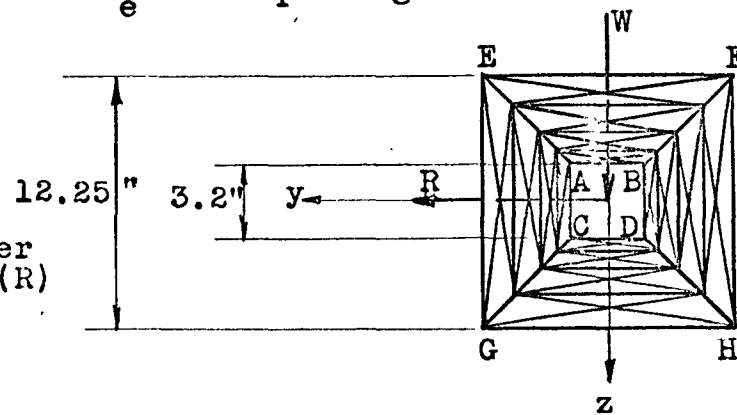
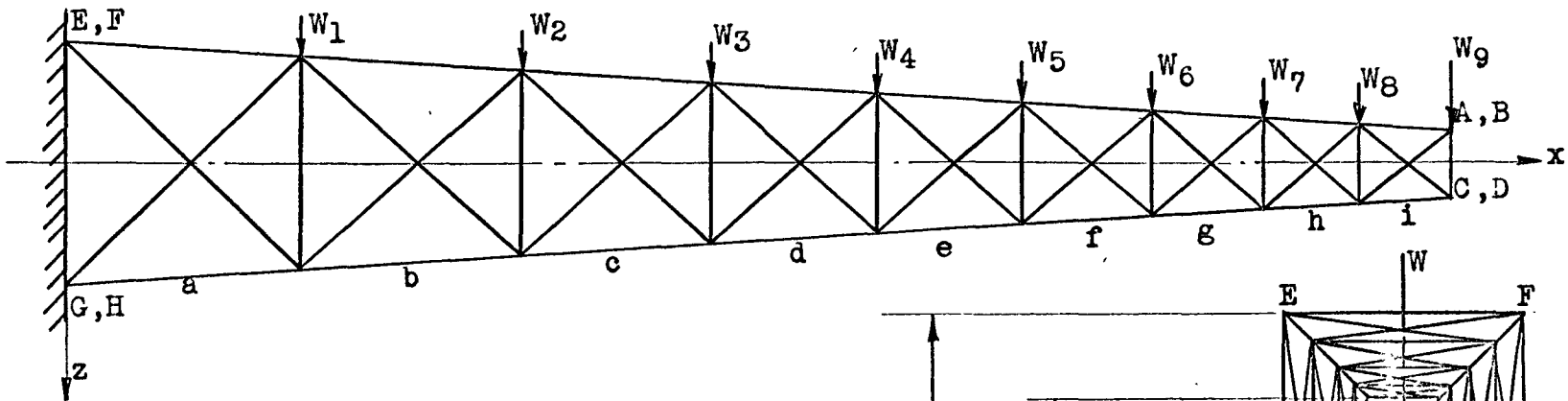
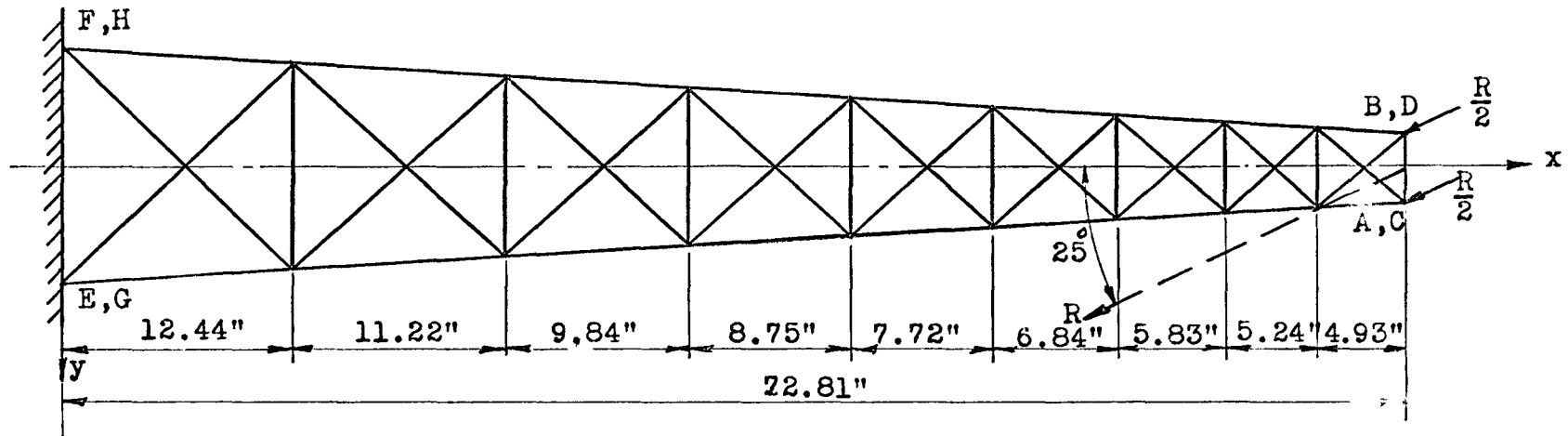


Figure 50 Indeterminate Lattice Tower Model, Showing Chordload (R) and Windloads (W) Applied

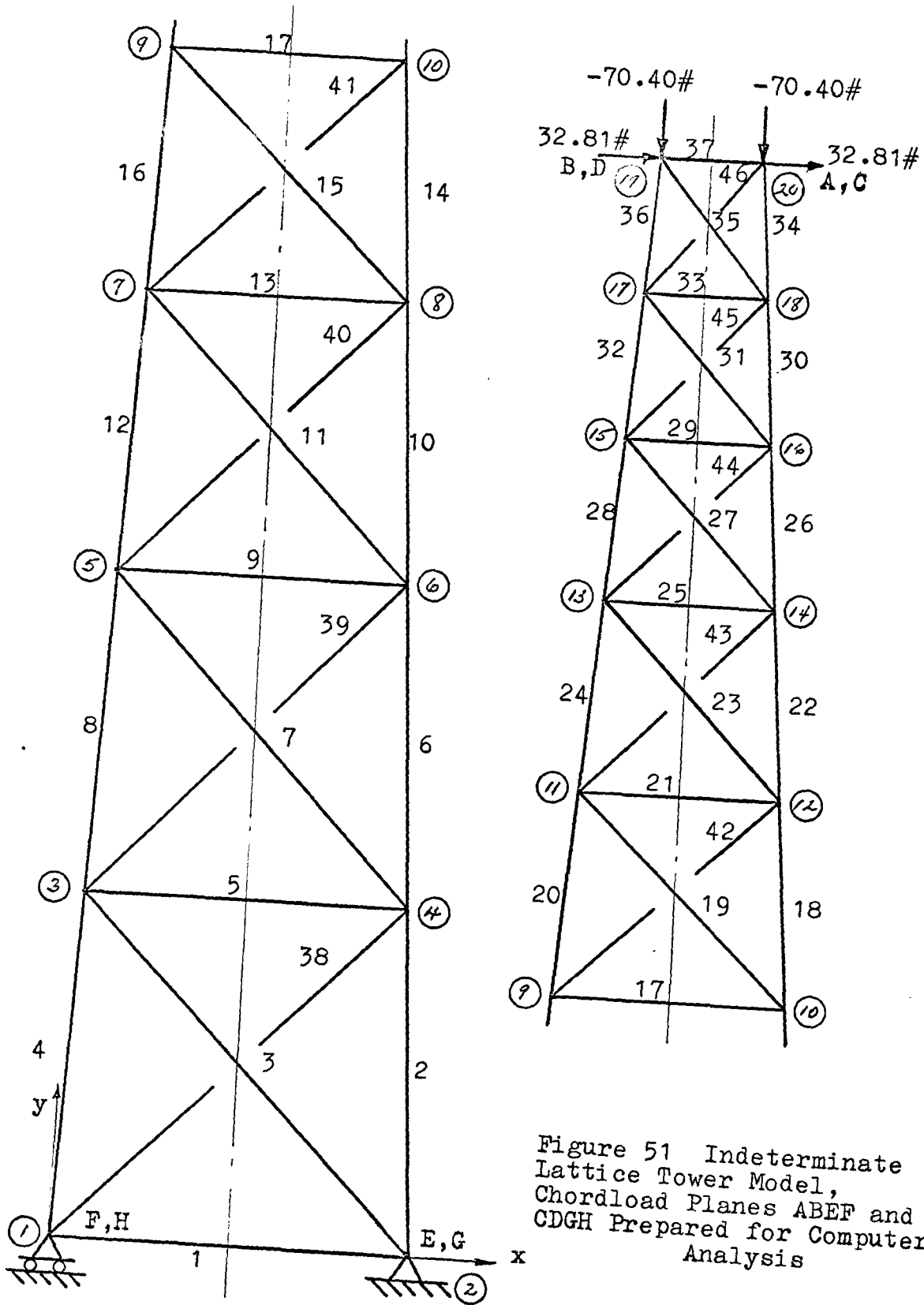


Figure 51 Indeterminate Lattice Tower Model, Chordload Planes AB EF and CD GH Prepared for Computer Analysis

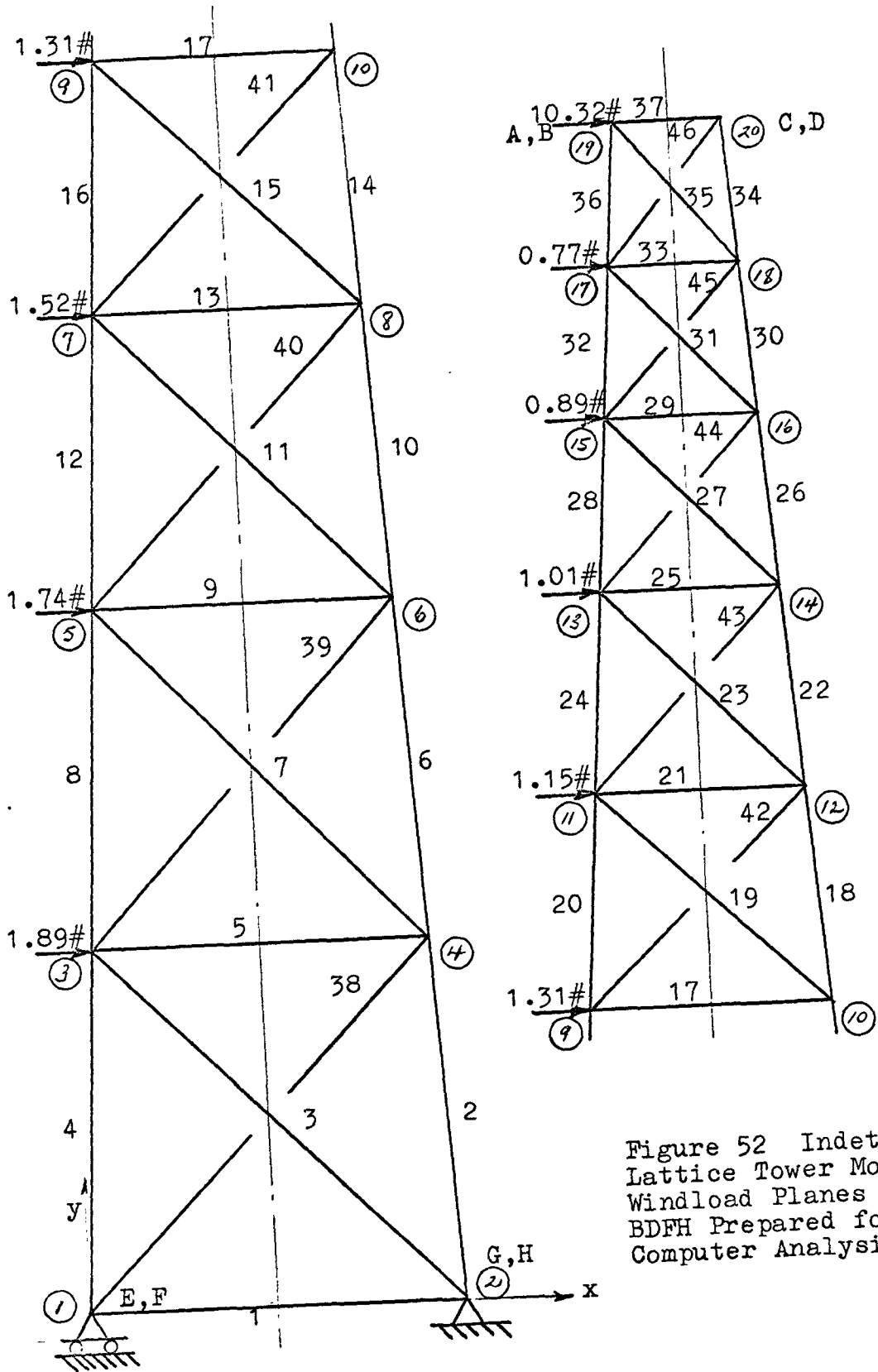


Figure 52 Indeterminate Lattice Tower Model, Windload Planes ACEG and BDFH Prepared for Computer Analysis

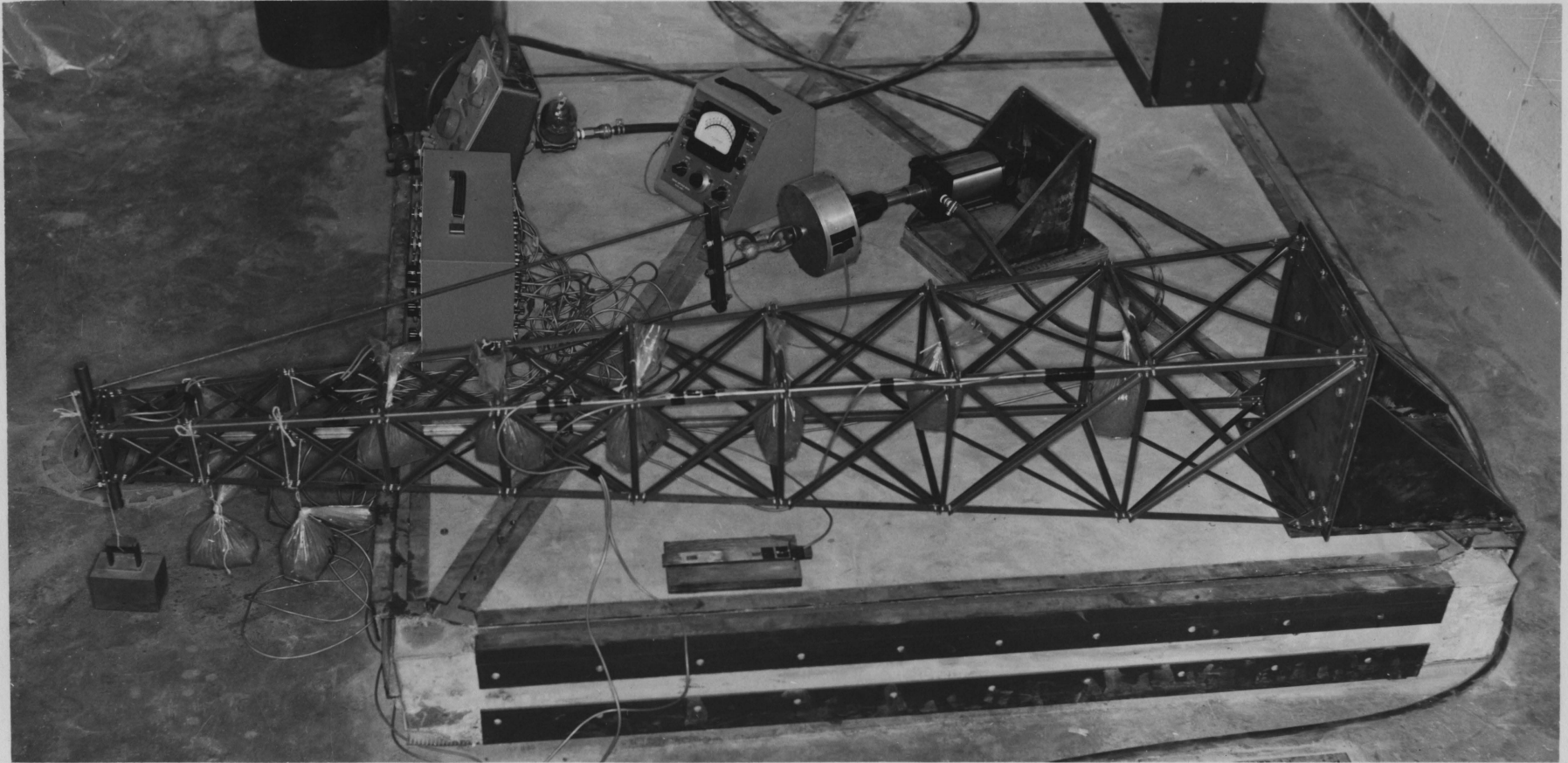
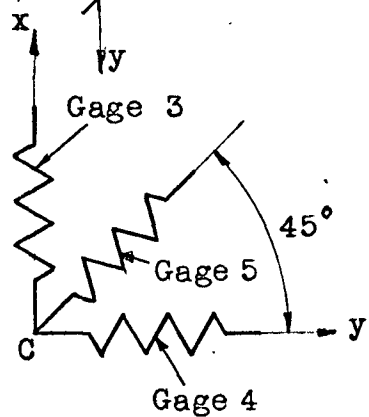
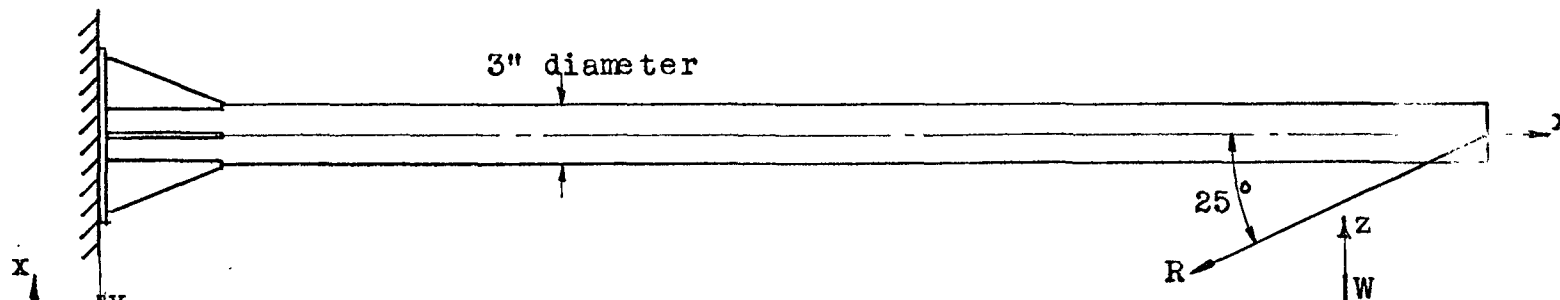
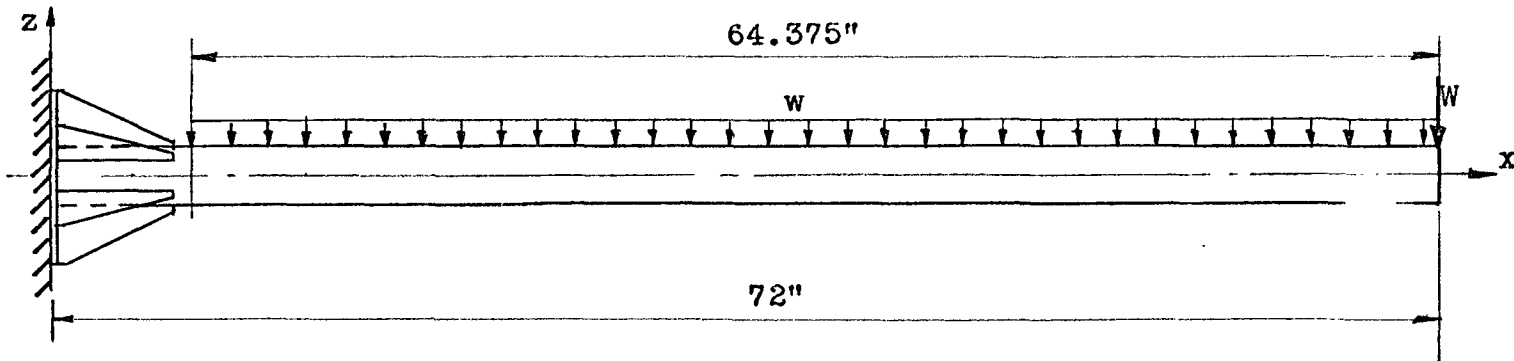


Figure 53 Indeterminate Lattice Tower Model
Showing Test Apparatus.



Strain gages at point C

Figure 54 Pipe Tower Model Showing Chordload (R) and Windloads (W) Applied

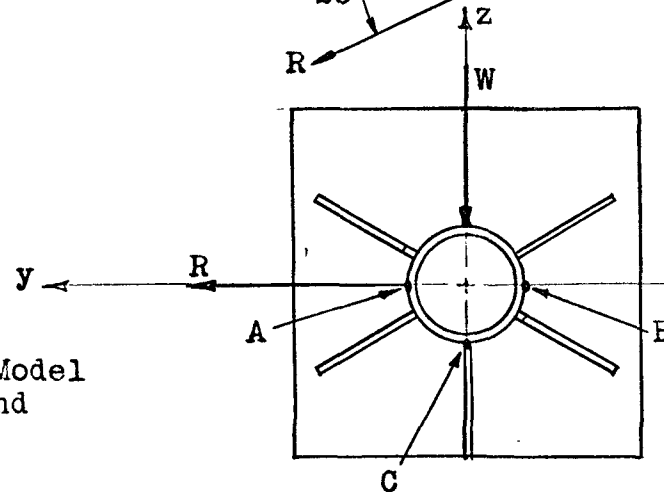




Figure 55 Pipe Tower Model Showing Test Apparatus

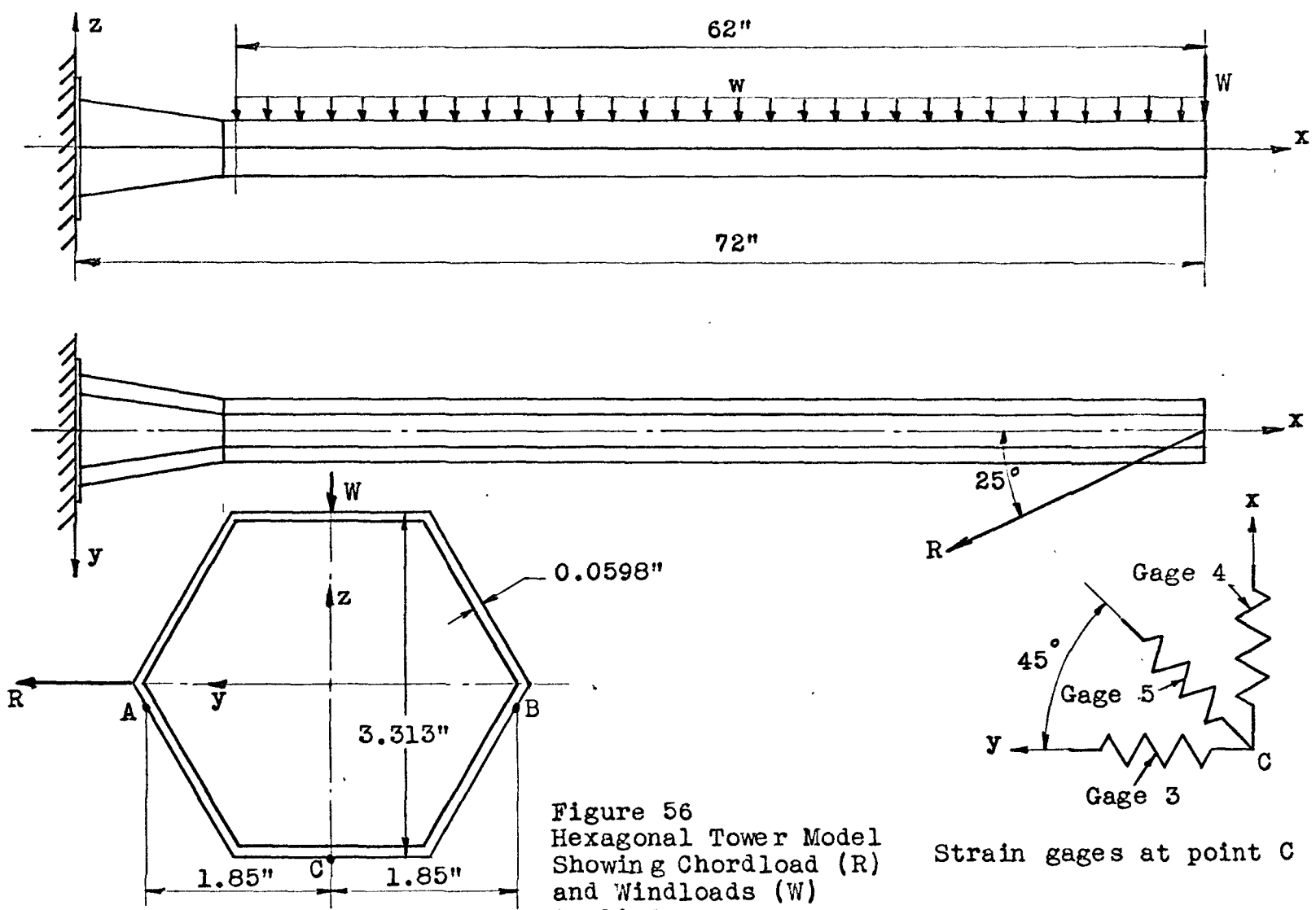


Figure 56
Hexagonal Tower Model
Showing Chordload (R)
and Windloads (W)
Applied.

Strain gages at point C

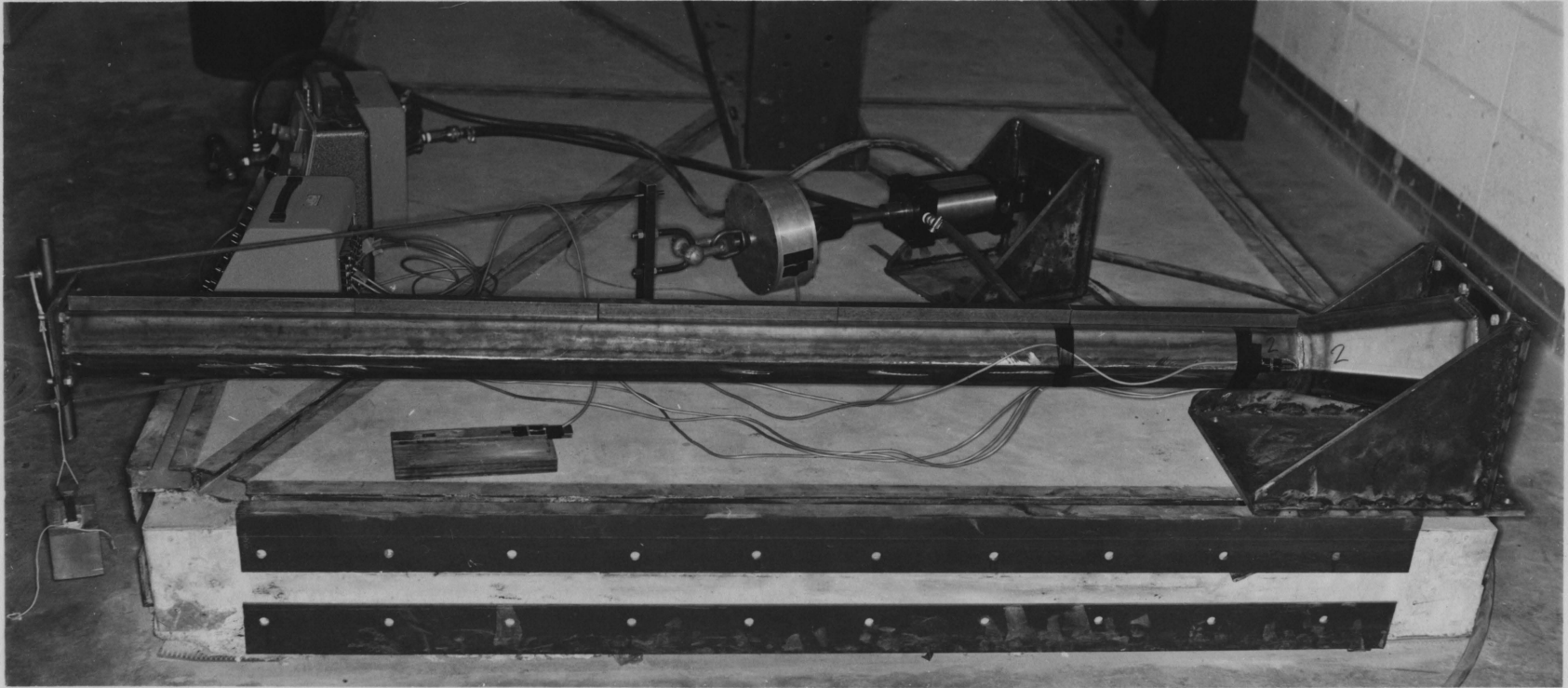
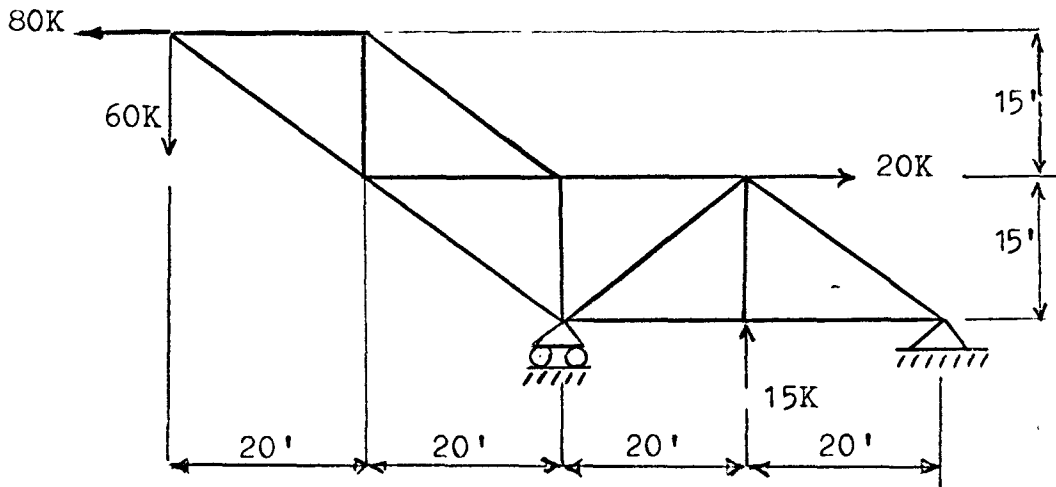
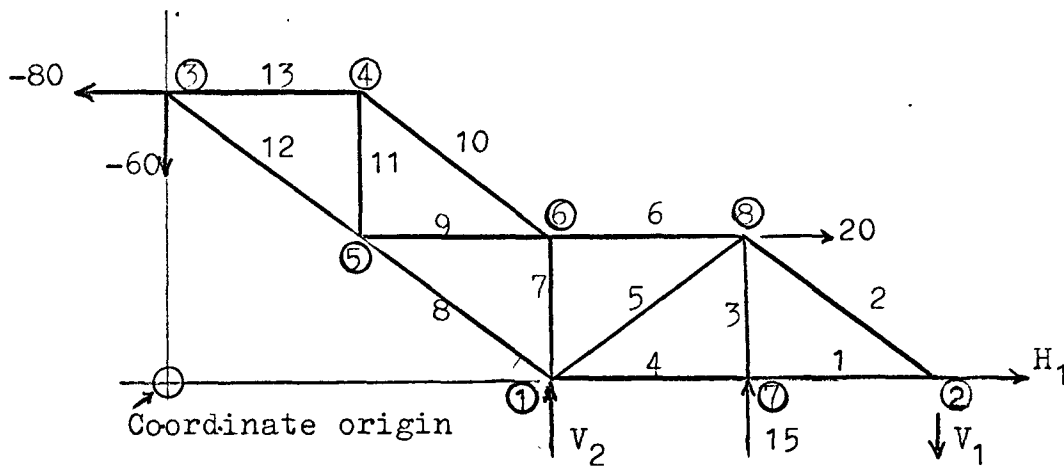


Figure 57 Hexagonal Tower Model Showing Test Apparatus



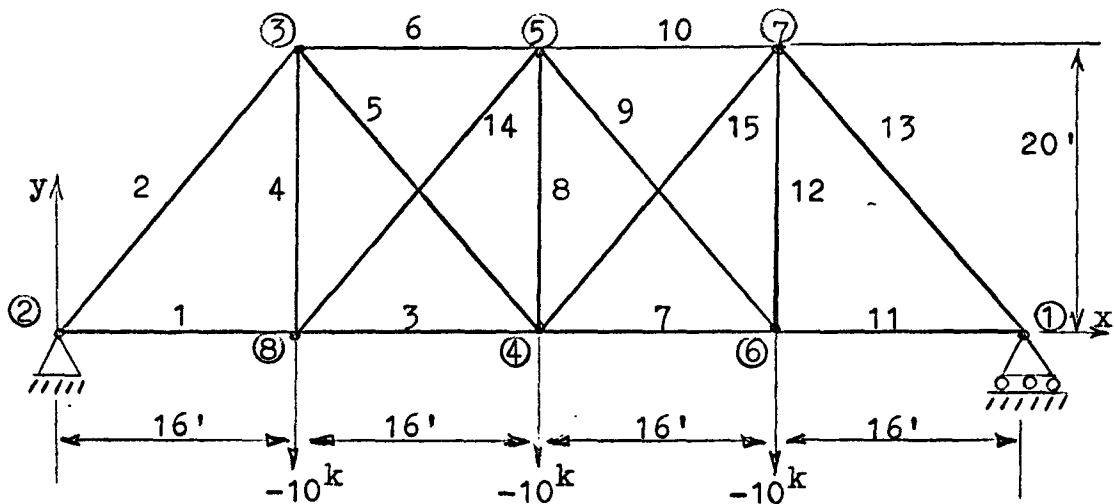
(a) Truss Dimensions with Applied Loads



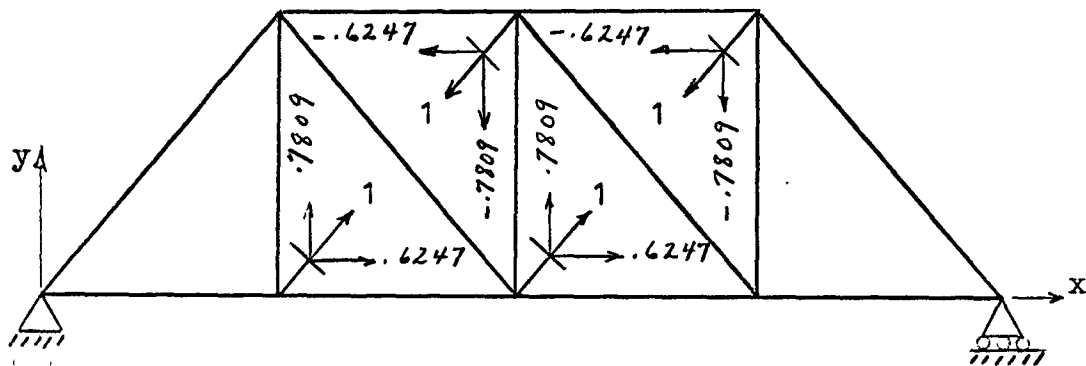
(b) Truss Prepared for Program Input

Figure 58 Sample Problem --
 Determinate Truss Analysis

Area of Members = 1.00 in.²



(a) Truss Prepared for Computer Analysis



(b) The primary structure with Unit Redundant Loads

Figure 59 Sample Problem,
Indeterminate Truss Analysis

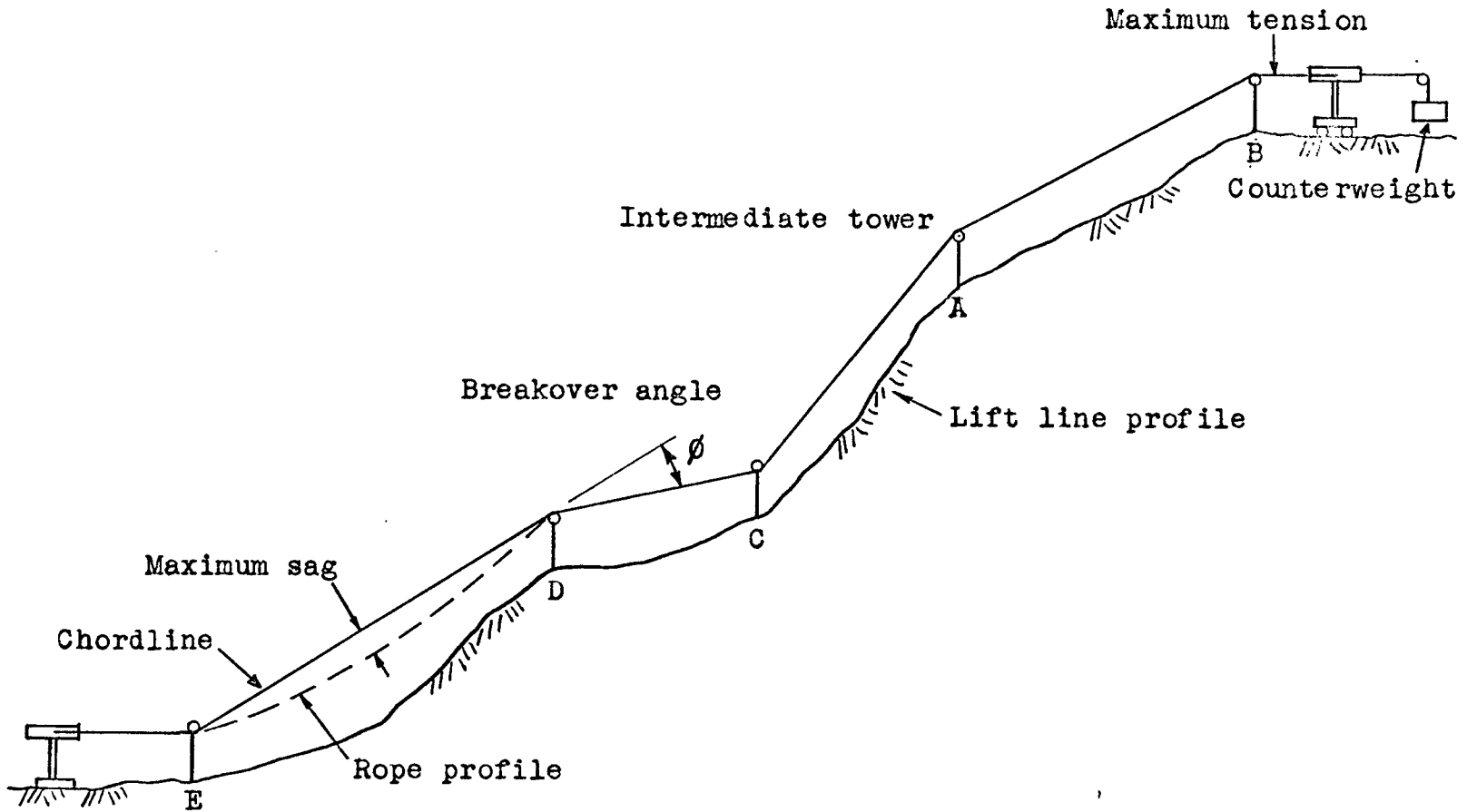


Figure 60 Chair Lift Profile Showing the Intermediate Tower Locations

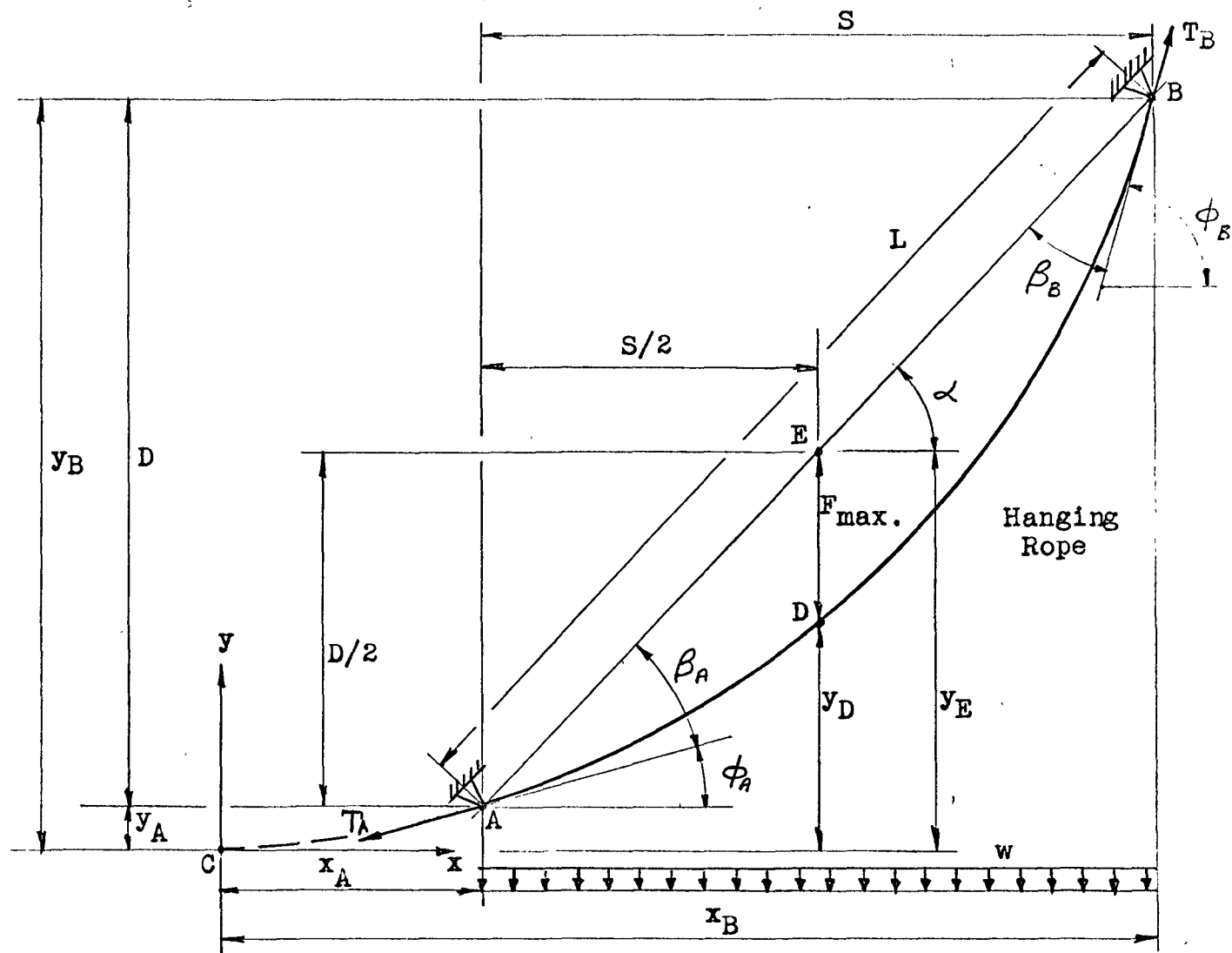


Figure 61 Hanging Rope Carrying a Horizontally Distributed Load

BIBLIOGRAPHY OUTLINE

Aerial Ropeways

- (A) General References
- (B) Mining Industry
 - (i) Descriptive Literature
 - (ii) Design Literature
- (C) Construction Industry
 - (i) Descriptive Literature
 - (ii) Design Literature
- (D) Logging Industry
 - (i) Descriptive Literature
 - (ii) Design Literature
- (E) Passenger Transport
 - (i) Descriptive Literature
 - (ii) Design Literature
- (F) General Design Literature
- (G) Intermediate Tower Design

Cableways

- (H) General References
- (I) Construction Industry
 - (i) Descriptive Literature
 - (ii) Design Literature

BIBLIOGRAPHY

Aerial Ropeways

(A) General References

1. Peele, R.: "Mining Engineers' Handbook", 3rd ed., John Wiley and Sons, New York, 1941, Vol. 2, section 26, Aerial Tramways and Cableways, pp. 26-01 to 26-51. Descriptive and some design.
2. Hudson, W. G.: "Conveyors and Related Equipment", 3rd ed., John Wiley and Sons, New York, 1954, Chapter 11, pp. 270-279. Descriptive.
3. Hay, W. M.: "An Introduction to Transportation Engineering", John Wiley and Sons, New York, 1961, pp. 211-214.
4. Zimmer, G. F.: "Mechanical Handling of Materials", D. Van Nostrand Co., New York, 1905, Chapter 16. Descriptive.
5. Czitary, E.: "Seilschwebbahnen", Springer-Verlag, Vienna, 1962, pp. 390. Probably the most modern general treatise of the design and operation of all types of ropeways. (German).
6. Stephan, P.: "Die Drahtseilbahnen", 4th ed., J. Springer, Berlin, 1926, pp. 572. Descriptive with some design, but outdated. (German).
7. Blyth, H.: "Modern Telepherage and Ropeways", Ernest Benn Limited, London, 1926. Descriptive of English practise.
8. Boltz, H. A. (editor): "Materials Handling Handbook", The Roland Press Co., New York, 1958, section 27, pp. 27.1 - 27.29. Descriptive with some design.

9. Koshkin, S. J.: "Modern Materials Handling", John Wiley and Sons, London, 1932, pp. 115-131. Descriptive.
10. Wallis-Taylor, A. J.: "Aerial or Wire Ropeways", Crosby Lockwood and Son, London, 1920, pp. 252. Descriptive with some design, but outdated.
11. Carstarphen, F. C.: "Aerial Tramways", Trans. Amer. Soc. Civil Engineers, 1929, Vol. 92, pp. 875-973. General treatise on ropeways with some design.
12. Gilmore, W.: "Aerial Ropeways", Mechanical Handling, (London, Eng.) Apr. 1954, Vol. 41, no. 4, pp. 187-191, and May 1954, Vol. 41, no. 4, pp. 243-250. Outlines the history and describes some installations.
13. Hutter, H. E.: "Aerial Ropeways", Mechanical World and Engineering Record, (Manchester, Eng.) June 25, 1948, Vol. 123, no. 3206, pp. 721-723. Describes the features of different types.
14. Anon: "British Ropeway Engineering Company Limited - Aerial Ropeways", British Ropeway Division, Vulcan, Ford-Smith Limited, Toronto, 1952, pp. 20. (mimeo.)
15. Metzger, I. O. H.: "Aerial Tramways in the Metal Mining Industry", U.S. Bureau of Mines, (Washington, D.C.), Information Circular no. 6948, Sept. 1937, pp. 32. Describes the features of different types.
16. Brillo, G.: "Mechanics of Aerial Ropeways", Mining Magazine, (London, Eng.), Jan. 1931, Vol. 44, no. 1, pp. 18-24, Feb. 1931, Vol. 44, no. 2, pp. 81-82.
17. Haynes, O. D.: "Materials Handling Equipment", Chilton Co., Philadelphia, 1957, pp. 491-496. Descriptive.

(B) Mining Industry(i) Descriptive Literature

1. Rislet, B. C.: "Aerial Tramway Construction in the Andes", Mining and Metallurgy, July, 1937.
2. Graham, W. L.: "World's Longest Bi-Cable Ropeway", Engineering and Mining Journal, July 1933, Vol. 134, pp. 287.
3. Pitt, D. L.: "Aerial Tramways", Trans. Canadian Inst. Mining and Metallurgy, 1930.
4. Morrison, M. P.: "Application of Aerial Tramways to Long and Short Hauls", Trans. ASME Mech. Handling Section, Jan.-Apr. 1930.
5. Morrison, M. P.: "One Man Aerial Tramway", Coal Age, Feb. 1929, pp. 88.
6. Anon: "Transporting Minerals by Aerial Ropeway", Mining Journal, (London, England), Mar. 16, 1962, Vol. 258, no. 6604, pp. 257-259.
7. Anon: "Brazil uses Ropeway Transport to Attack Giant Charcoal Forests", International Ropeway Review, Jan.-Mar. 1962, Vol. 4, no. 7, pp. 21-24.
8. Anon: "Silica Gets a Ski Lift at Central Silica Co.", Rock Products, Nov. 1964, pp. 80.
9. Anon: "Aerial Ropeways at Cologne", Engineer, Dec. 13, 1957, Vol. 204, pp. 876, 877.
10. Anon: "Algoma Ore Properties Limited; The Aerial Tramway", Canadian Mining Journal, Nov. 1956, Vol. 77, pp. 120.
11. Anon: "Transporting Minerals by Aerial Ropeway", Mining Journal, (London, England), Mar. 16, 1962, Vol. 258, no. 6604, pp. 257, 259.

Mining Industry(ii) Design Literature

12. Kill, J. D. and Johns, D. R.: "Aerial Ropeways", Colliery Engineering, Jan. 1963, Vol. 40, no. 467, pp. 8-12.
13. Carstarphen, F. C.: "Truck or Cableway? A Comparison of Costs", Engineering and Mining Journal, July 24, 1930, pp. 61.
14. Carstarphen, F. C.: "Ore Transport - Aerial Ropeway", Engineering and Mining Journal, Aug. 1941, Vol. 142, no. 8, pp. 110.
15. Carstarphen, F. C.: "Improving on Rope Tramway Location", Engineering and Mining Journal, Jan. 1930, Vol. 129, no. 2, pp. 59-62.

(C) Construction Industry

(i) Descriptive Literature

1. Grider, E. L.: "Operation and Maintenance of a 4-Mile Aerial Tramway at Conchas Dam", Western Construction News, Dec. 1938.
2. Ackerman, A. J.: "Madden Dam Aggregate Handling by Mile-Long Aerial Tramway", Construction Methods, Feb. 1933.
3. Anon: "Aerial Ropeway Serves Kemano Tunnels", Engineering News Record, Nov. 20, 1952, pp. 42-43.
4. Anon: "A Long Monocable Ropeway in the United States of South America", International Ropeway Review, Oct.-Dec. 1962, Vol. 4, no. 4, pp. 120-127.
5. Kluzer, C.: "Three Good Examples of Modern Bicable Ropeways", International Ropeway Review, Apr.-June 1963, Vol. 5, no. 2, pp. 60-65.
6. Walter, L.: "Aggregate for Aussie Dam Carried 12 Miles on Aerial Ropeway", Rock Products, Oct. 1958, Vol. 61, pp. 116.

Construction Industry(ii) Design Literature

7. Anon: "Telecommunications and Remote Control of the Banff-Sulphur Mountain Aerial Ropeway, Canada", International Ropeway Review, Jan.-Mar. 1960, Vol. 2, no. 1, pp. 15.

(D) Logging Industry

(i) Descriptive Literature

1. Bennett, W. D.: "Cableway Systems for Pulpwood Transport", Pulp and Paper Research Institute of Canada, Montreal, 1960, Technical Report Series 208, Woodlands Research Index No. 119, pp. 71. Descriptive with economic comparisons, limitations and productivity of this type of ropeway.
2. Anon: "Aerial Log Transportation", Lumberman, Nov. 1953, pp. 92, 114.
3. Anon: "Tramway Solved Log Transport Problem", Lumberman, Feb. 1952, pp. 50, 51.
4. Harris, K. F.: "The Wyssen Skyline Crane, a New Development in Pulpwood Logging," Canadian Pulp and Paper Industry, Mar. 1950, pp. 8-10, 24, 29.
5. Ross, C. G.: "Aerial Ropeways for Pulpwood Transportation", Canadian Woodlands Review, Jan. 1929, pp. 17-18.

Logging Industry(ii) Design Literature

6. Huggard, E. R.: "Foresters Engineering Handbook", W. Heffer and Sons Limited, Cambridge, 1958, Chapter 13.

(E) Passenger Transport(i) Descriptive Literature

1. Schmid, W.: "The Aerial Ropeway of the Arosa Weisshorn", Brown Boveri Review, (Baden, Switzerland), 1958, Vol. 45, no. 2, pp. 80-87.
2. Anon: "Aerial Ropeway Crosses the Turbulent Waters of Niagara Whirlpool", International Ropeway Review, July-Sept. 1963, Vol. 5, no. 3, pp. 74-78.
3. Sarbach, H.: "America's Largest Tramway", International Ropeway Review, July-Sept. 1963, Vol. 5, no. 3, pp. 91-95.
4. Anon: "Rope Transport in Military Warfare", International Ropeway Review, Apr.-June 1960, Vol. 2, no. 2, pp. 40-46.
5. Anon: "Description of a Ropeway for Military Transport, To and Fro Type", International Ropeway Review, Apr.-June 1960, Vol. 2, no. 2, pp. 69, 70.
6. Dumar, M.: "A New Four Seater Chairlift, Giovanola System", International Ropeway Review, Apr.-June, 1960, Vol. 2, no. 2, pp. 61-65.
7. Anon: "Austria's Youngest Ropeway at the Gates of Salzburg", International Ropeway Review, Oct.-Dec. 1963, Vol. 5, no. 4, pp. 122, 128.
8. Zuberbuhler, P.: "Chair and Cabin Lifts for Exhibitions, Fair and Amusement Parks", International Ropeway Review, Apr.-June, 1963, Vol. 5, no. 2, pp. 38-42.
9. Kravtchenko, M.: "The New Eibsee-Zugspitz Ropeway", International Ropeway Review, Jan.-Mar. 1964, Vol. 6, no. 1, pp. 2-4.
10. Hojo, F.: "The Mount Hakone Passenger Ropeway", International Ropeway Review, Jan.-Mar. 1964, Vol. 6, no. 1, pp. 8-12.

11. Schaler, R.: "The Trittkopf Ropeway", International Ropeway Review, Jan.-Mar. 1964, Vol. 6, no. 1, pp. 18-22.
12. Verges, F. S.: "A Chairlift in the Sierra Del Guadarrama - Spain", International Ropeway Review, Apr.-June 1964, Vol. 6, no. 2, pp. 41-45.
13. Miotti, A.: "Development of Touristic Installations in the Rhetic Alps", International Ropeway Review, Oct.-Dec. 1964, Vol. 6, no. 4, pp. 105-108.
14. Tudor, R. A.: "World's Largest Single Lift Tramway; Palm Springs Aerial Tramway", Civil Engineering, Nov. 1962, Vol. 32, pp. 62-65.
15. Anon: "Bavarian Cableway; New Passenger Cableway to the Top of Zugspitze", Engineer, Sept. 28, 1962, Vol. 214, pp. 564, 565.
16. Anon: "Swiss Cable Line Spans 3,300 Feet; Passenger Cableway Across the Lake of Zurich", Engineering News, May 19, 1960, Vol. 164, pp. 75-76.
17. Anon: "Cableway is Europe's Highest: Mount Pagnella, Italy", Engineering News, May 22, 1958, Vol. 160, pp. 65.
18. Anon: "Aerial Tramway Access to Winter Resort", Engineering News, Jan. 13, 1955, Vol. 154, pp. 43.
19. Anon: "Peak Project; Mountaintop Hotel will be Reached by Cableway North of Caracas, Venezuela", Engineering News, May 17, 1956, Vol. 156, pp. 92.
20. Anon: "World's Highest Ropeway, over 2 Miles Up; Being Built in the French Alps", Engineering News, Oct. 21, 1954, Vol. 153, pp.46
21. Browning, B.: "Big Mountain gets Lift", Pacific Builder and Engineer, June 1961, Vol. 67, no. 6, pp. 90-92.

22. Farwell, T.: "Tower Erection by Copter", Ski Area Management, Winter 1963, pp. 11-14.
23. Greco, G.: "Ropeway Systems - An Account of the Various Types of Passenger Carrying Ropeways", International Ropeway Review, Jan.-Mar. 1965, Vol. 7. no. 1, pp. 18-23.
24. Anon: "To and Fro Cabin Ropeways Built by Von Roll Ltd., Berne, Switzerland", International Ropeway Review, Apr.-June 1964, Vol. 6, no. 2, pp. 60-62.

Passenger Transport(ii) Design Literature

25. Anon: "Aerial Passenger Tramways", Canadian Standards Association, Draft CSA Standard Z98, October, 1964.
26. Anon: "The American Standard Safety Code for Aerial Passenger Tramways", American Standards Association Inc., No. B77.1, June 8, 1960.
27. Anon: "Technical Recommendations for the Construction of Continuous Movement Monocable Ropeways with Fixed Grips Intended for the Transportation of Passengers", International Ropeway Review, Jan.-Mar., 1962, Vol. 4, no. 7, pp. 25-31. (International Organization for Transportation by Rope).
28. Anon: "Technical Recommendations Concerning the Construction of To and From Bi-Cable Ropeways Intended for the Transportation of Passengers", International Ropeway Review, Oct.-Dec. 1962, Vol. 4, no. 4, pp. 134-140. (International Organization for Transportation by Rope).
29. Bakke, E.: "An Electro-Hydraulic Drive for Aerial Ropeways", International Ropeway Review, Oct.-Dec. 1962, Vol. 4, no. 4, pp. 108-111.
30. Klassen, H.: "South America Establishes Ropeway Passenger Links between Caracas and the Caribbean", International Ropeway Review, Oct.-Dec. 1962, Vol. 4, no. 4, pp. 114-119.
31. Anon: "Safety Equipment Preventing Derailment of Ropes of Ski-Lifts, Chairlifts and Monocable Ropeways", International Ropeway Review, Oct.-Dec. 1962, Vol. 4, no. 4, pp. 128-130.
32. Carlevaro, U.: "Chair Lift Grips, Recent Developments", International Ropeway Review, July-Sept. 1960, Vol. 1, no. 3, pp. 84-86.

33. Anon: "Travel in Space - the Rope Way", International Ropeway Review, July-Sept. 1960, Vol. 2, no. 3, pp. 87-93, 103.
34. Montuora, S. "A Suggestion to Reduce the Transversal Inclination of a Ropeway Cabin caused by the Pressure of Wind", International Ropeway Review, Apr.-June, 1964, Vol. 6, no. 2, pp. 46-48.
35. Stockhammer, G.: "Development and Limits of Passenger Ropeways", International Ropeway Review, July-Sept. 1964, Vol. 6, no. 3, pp. 97-98.
36. Kinney, R. E.: "Electricity First - Electric Motors for Ski Lift Drives", Ski Area Management, Spring 1965, pp. 26-31.
37. Kinney, R. E.: "Going Up - The Enclosed Lift", Ski Business, Spring 1965, pp. 192-195, 207.
38. Rose, H.: "The Internal Combustion Engine, is it Right for Your Lift?", Ski Area Management, Winter 1965, pp. 27-33.
39. Lutz, W.: "Roller Bearings for Aerial Ropeway Application", Ball and Roller Bearing Engineering, (Published by FAG Kugelfischer Georg Schafer and Co., Schweinfurt, Germany), No. 2, 1964, pp. 9-15.

(F) General Design Literature

1. Carstarphen, F. C.: "Simple Method of Computing Deflections of a Cable Span Carrying Multiple Loads Evenly Spaced", Trans. Amer. Soc. Civil Engineers, Vol. 83, pp. 1383-1408.
2. Anon: "Wire Rope Engineering Handbook", American Steel and Wire Co., New York, 1946, pp. 38-56. Stresses in suspended cables.
3. Michalos, F. and Birnstiel, C.: "Movements of a Cable due to Changes in Loading", Proc. Amer. Soc. Civil Engineers, Structural Div. Dec. 1960, Vol. 86, pp. 23-38.
4. Amstutz, E.: "Graphische Berechnung der Seile Mehrfeldriger Luftseilbahnen," Schweizerische Bauzeitung, (Zurich, Switzerland), February 14, 1942, Vol. 119, no. 7, pp. 75-77. Calculation of Rope Spans.
5. Czitary, E.: "Uber Schwingungen von Schwebebahenseilen", Bautechnik, (Berlin, Germany), Nov. 1, 1940, Vol. 18, no. 47/48, pp. 551-553. Vibration of ropeway cables.
6. Ando, S.: "Safety Factor of Wire Ropes used for Conveyance", International Ropeway Review, Jan.-Mar. 1964, Vol. 6, no. 1, pp. 29-33.
7. Kill, J. D. and Johns, D. R.: "Aerial Ropeways", Assoc. Electrical Industries, Engineering, (England), Dec. 1961, Vol. 1, no. 12, pp. 436-441. Good description of ropeway drives.
8. Pflueger, M. E.: "Electric Drives for Ropeways Carrying Goods", Brown Boveri Review, Apr. 1958, Vol. 45, no. 4, pp. 151-158.
9. Beisteiner, F.: "Versuche zur Ermittlung der Reibungszahl Zwischen Seil und Seilklemme bei Einseil-Schwebeliften und Schleppliften", VDI Zeitschrift (Dusseldorf, Germany), Nov. 11, 1960, Vol. 102, no. 32, pp. 1527-1534. Coefficient of friction between rope and clamp.

10. Azzaroli, G.: "The Braking Space on a Bi-Cable Ropeway", International Ropeway Review, Jan.-Mar. 1964, Vol. 6, no. 1, pp. 23-28.
11. Evans, T. H.: "Motion of a Suspended Mass with Practical Applications", Civil Engineering, Mar. 1939, Vol. 9, no. 3.
12. Anon: "Unique Engineering Problems Involved in the Design of an Aerial Tramway", Engineering and Contract Record, (Toronto) June 29, 1938, Vol. 51, no. 26, pp. 10-12.
13. Wright, A. H.: "Design and Construction of Aerial Ropeways", Mechanical Handling and Works Equipment, (London, England) Mar. 1933, Vol. 20, no. 3, pp. 87-89, April 1933, Vol. 20, no. 4, pp. 123-124.
14. Firmage, D. A.: "Fundamental Theory of Structures", John Wiley and Sons, 1963, pp. 247-267.
15. Au, Tung: "Elementary Structural Mechanics", Prentice-Hall, 1963, pp. 173-183.
16. Carpenter, S. T.: "Structural Mechanics", John Wiley and Sons, 1964, pp. 388-427.
17. Anon: "Wire Rope and Fittings", The B. Greening Wire Co. Limited, Hamilton, Canada, Catalogue WR-48, 159 pp.

(G) Intermediate Tower Design

1. Both, G. H.: "Design of Chairlift Trestles", International Ropeway Review, July-Sept. 1960, Vol. 2, no. 3, pp. 97-99.
2. Bittner, K.: "Aufgabe und Ausgestaltung von Seilbahnstuetzen von Personenseilscheebahnen", Stahlbau-Rundschau, (Vienna, Austria), 1961, no. 20, pp. 35-44.
3. Norris, C. H. and Wilbur, J. B.: "Elementary Structural Analysis", McGraw-Hill, 1960, pp. 256-273, 299, 300.
4. Sutherland, H. and Bowman, H.: "Structural Theory", John Wiley and Sons, 1956, pp. 383-389.
5. Morris, C. T. and Carpenter, S. T.: "Structural Frameworks", John Wiley and Sons, 1955, pp. 130-161.
6. Matheson, J. A.: "Hyperstatic Structures, Vol. 1", Butterworths Scientific Publications, 1959, pp. 166-169, 441, 442.
7. Charlton, T. M.: "Model Analysis of Structures", E. and F. N. Spon, 1954, 142 pp.
8. Borg, S. F. and Gennaro, J. J.: "Advanced Structural Analysis", D. Van Nostrand Co., 1964, 368 pp.
9. Bergstrom, R. N., Arena, F. and Kramer, J. M.: "Design of Self Supported Steel Transmission Towers", Proc. Amer. Soc. Civil Engineers, Journal of the Power Division, June 1960, pp. 55-88.
10. Roark, R. J.: "Formulas for Stress and Strain", McGraw-Hill, 1954, 381 pp.
11. Timoshenko, S. and Young, D. H.: "Theory of Structures," McGraw-Hill, 1945, pp. 171-212, 326-331.
12. Beedle, L. S. (editor): "Structural Steel Design", pp. 401-403.

13. Gennaro, J. J.: "Computer Methods in Solid Mechanics," The Macmillan Company, 1965, 291 pp.
14. Anon: "Structural Steel for Buildings", Canadian Institute of Steel Construction, book 3, 1964, 341 pp.
15. Heindel, D. S.: "Determinate Truss Analysis", IBM 1620 General Program Library, no. 1620 - 09.2.058, 15 pp.
16. Anon: "Steel Construction Manual", American Institute of Steel Construction, 1955, 341 pp.
17. Siddall, J. N.: "Strain Rosette Analysis", Lecture Notes, in Experimental Stress Analysis, 1965.

Cableways

(H) General References

1. Stubbs, F. W. (editor): "Handbook of Heavy Construction", McGraw Hill, 1959, Chapter 24, pp. 24-3 to 24-32. Probably the most modern treatment of cableways. Descriptive and some design.
2. Peele, R.: "Mining Engineers' Handbook", 3rd ed., John Wiley and Sons, New York, 1941, Volume 2, Section 26, Aerial Tramways and Cableways, pp. 26-01 to 26-51. Descriptive and some design.
3. Boltz, H. A. (editor): "Materials Handling Handbook", The Roland Press Co., New York, 1958, section 33, pp. 33.17-33.23. Descriptive.
4. Koshkin, S. J.: "Modern Materials Handling", John Wiley and Sons, London, 1932, pp. 132-142. Descriptive.
5. Carstarphen, F. C.: "Aerial Tramways", Trans. Amer. Soc. Civil Engineers, 1929, Vol. 92, pp. 881-882. Descriptive.

(I) Construction Industry(i) Descriptive Literature

1. Wise, L. L.: "Pine Flat Dam; Single Hi-Speed Cableway places 4,000 yards Daily", Construction Methods, Oct. 1951, Vol. 33, pp. 52-54.
2. Tripp, J. G.: "Will a Construction Cableway Fit Your Job?", Civil Engineering, Mar. 1951, Vol. 21, pp. 134-139.
3. Mackintosh, I. B.: "Cableways for Dam Construction", Water Power, (London, England), Sept. 1958, Vol. 10, no. 9, pp. 343-349.
4. Anon: "The Heavy Duty Aerial Ropeway for the Construction of the Albigna Dam", International Ropeway Review, Jan. to Mar. 1960, Vol. 2, no. 1, pp. 12-15.
5. Anon: "Aerial Cableway Speeds Dam Construction for Rhodesian Irrigation Project", International Ropeway Review, July-Sept. 1963, Vol. 5, no. 3, pp. 86, 87.
6. Nevrlly, V.: "Application of Cable Cranes in Water, Construction Schemes", International Ropeway Review, Apr.-June 1960, Vol. 2, no. 2, pp. 40-46.
7. Anon: "The Warragamba Dam", International Ropeway Review, Apr.-June 1963, Vol. 5, no. 2, pp. 44-49.
8. Anon: "Cableway used in the Construction of the Fehmarnsund Bridge", International Ropeway Review, Apr.-June 1963, Vol. 5, no. 2, pp. 54-58
9. Mansel, S. E.: "Russia's Ropeway Risk, Building of the Hydro Power Station at Stalingrad", International Ropeway Review, July-Sept. 1960, Vol. 2, no. 3, pp. 76-83.
10. Roewer, J.: "Twin Cableways for the Construction of the Kayna Dam in India", International Ropeway Review, Apr.-June, 1964, Vol. 6, no. 2, pp. 36-40.

11. Anon: "Soviet Crane for the Building Industry", International Ropeway Review, July-Sept. 1964, Vol. 6, no. 3, pp. 83.
12. Anon: "Cableway places Rockfill for Dutch Dam", Engineering News, Feb. 18, 1965, pp. 82.
13. Anon: "Cableways Erect Two Bridges", Engineering News, Mar. 1, 1962, Vol. 168, pp. 32
14. McIndoe, G. P.: "Mass-Concrete Operations in the Rocky Mountains," Trans. Amer. Soc. Civil Engineers, 1954, Vol. 119, pp. 899-909.

(ii) Design Literature

15. Sidler, J.: "Cable Cranes and their Drive Equipment", Brown Boveri Review, Oct. 1958 Vol. 45, no. 10, pp. 485-492.
16. Anon: "Design Factors for Cableway Towers," Trans. Amer. Soc. Civil Engineers, 1941, Vol. 106, No. 488, pp. 1498-1503.
17. Kravtchenko, M.: "Steel Tubes and Wire Ropes are used in the Construction of an Interesting Italian Cable Crane", International Ropeway Review, Jan. to Mar. 1960, Vol. 2, no. 1, pp. 6-11.
18. Kravtchenko, M. "Cruciani's New Cable Crane Shows its Versatility", International Ropeway Review, Jan.-Mar., 1962, Vol. 4, no. 7, pp. 2-5.
19. Nordstroms, A. B.: "Swedish Cableways with Circular Cylindrical Fixed Towers", International Ropeway Review, Oct.-Dec. 1963, Vol. 5, no. 4, pp. 118, 119.
20. Rothe, G.: "Bridge Cableway", International Ropeway Review, Apr.-June, 1964, Vol. 6, no. 2, pp. 50-56.
21. Hubbell, C. H. "Methods of Estimating Impact Factor in the Design of Tautline Cableways", Engineering and Contract Record, May, 1951, pp. 73-77.
22. Colburn, M., and Schmidt, L. A.: "Norris Dam Construction Cableways", Trans. Amer. Soc. Civil Engineers, 1941, Vol. 106, pp. 470-819.